

# Single Inverted Pendulum Validation for Bi-Pedal Quiet Standing in Healthy Controls and Persons with Parkinson's Disease

By

Camilo Giraldo

Submitted to the graduate program in Mechanical Engineering and the Graduate Faculty of the University of Kansas in partial fulfillment of the requirements for the degree of Master of Science

---

Chairperson Carl Luchies Ph.D.

---

Sara Wilson Ph.D.

---

Huazhen Fang Ph.D.

Date Defended: May 5, 2017

The Thesis Committee for Camilo Giraldo  
certifies that this is the approved version of the following thesis:

Single Inverted Pendulum Validation for Bi-Pedal Quiet Standing in Healthy Controls and Persons with  
Parkinson's Disease

---

Chairperson Carl Luchies Ph.D.

Date Approved: May 5, 2017

## Abstract

The goal of this study was to validate the SIP model for bi-pedal quiet standing on healthy old adults and people with PD by comparing the linear and nonlinear measures extracted from the COP that the SIP creates ( $COP_{SIP}$ ), and the ones extracted from the experimental COP ( $COP_{exp}$ ). In addition, this study intended to determine if the accuracy of the  $COP_{SIP}$  to replicate the  $COP_{exp}$  was sensitive to the current practice of assuming zero as initial conditions (ICs) in the differential equation (DEQ) of the SIP. It was also investigated if the accuracy of the  $COP_{SIP}$  was sensitive to the linearization of the DEQ that describes the motion of the SIP. Finally, this study investigated if it is appropriate to use a SIP model in unperturbed sway studies that analyze PD progression, since it is usually believed that people with PD sway like a SIP due to the increment of stiffness at the ankles.

This study showed that using zero, instead of optimized, ICs in the SIP DEQ is a practice that increases the error of the  $COP_{SIP}$  in terms of magnitude and shape of curve when compared to the  $COP_{exp}$ . In addition, this study determined that linearizing the DEQ around the vertical position of the SIP is a safe practice, since at worst, 3% of similarity would be lost when the linear DEQ is used, instead of the nonlinear DEQ. Regarding the optimized ICs, this study proposed to select as optimized ICs the set that maximizes the Cross Correlation between the  $COP_{SIP}$  (calculated using the linear DEQ) and the  $COP_{exp}$ .

This study also showed that the SIP is a valid model for unperturbed sway studies on healthy adults and people with PD, if an error of 30% or less is accepted in the linear and nonlinear measures extracted from the  $COP_{exp}$ , and the  $COP_{SIP}$  is calculated using the linear DEQ with optimized ICs. In fact, the  $COP_{SIP}$  has a 30% or less error only for certain linear and nonlinear measures (depending on the subject group); therefore, the SIP is a 70% (or more) valid model depending on the linear and nonlinear measures that want to be replicated from the  $COP_{exp}$ .

Finally, this study also showed that as PD progresses and ankle stiffness increases, the SIP becomes a less valid model. The increment of stiffness at the ankles reduces their motion, making the hips move more to maintain balance. This proposes that a double inverted pendulum could represent better the unperturbed sway of moderate to more severe PD subjects.

## Acknowledgements

I would like to thank Dr. Carl Luchies for his constant technical support and guidance through my work on this study. It would have not been possible for me to complete this work without his valuable comments and conversations that always made sure I was on the right track to success. I also would like to thank my research committee Dr. Sara Wilson and Dr. Huazhen Fang for being part of my graduate studies, and taking the time to make valuable comments about my work. I also want to thank Melanie Weilert and Logan Sidener for being great friends and labmates who were willing to give me technical help, or just time to talk.

I would like to extend my thanks to my parents (Oscar Giraldo and Amparo Grisales) who always encouraged me to pursue higher education, and chase my dreams even though they were thousands of miles away from them. Also, I want to thank my brother (Sebastian Giraldo) and his wife (Maria Clara Madrigal) who are two excellent engineers and role models in my professional life. Finally, I want to thank my father and mother in-law (Deron and Rhonda Soendlin) who always made me feel I was smart enough to complete this thesis.

Last but certainly not least, I want to thank my wife Katelyn Giraldo who has been so patient with my education. The completion of this work would have not been possible without her emotional support that kept me healthy and sane during the tough times.

# Table of Contents

<b>Abstract</b> .....	<b>iii</b>
<b>Acknowledgements</b> .....	<b>iv</b>
<b>Chapter One: Introduction</b> .....	<b>1</b>
1 Background and Motivation .....	1
2 Specific Aims .....	2
3 Thesis Content .....	2
<b>Chapter Two: Background</b> .....	<b>3</b>
1 Parkinson’s Disease.....	3
2 Postural Instability (PI).....	3
3 Postural Sway.....	4
3.1 Postural Sway Measures .....	5
3.1.1 Linear Measures.....	5
3.1.2 Nonlinear Measures.....	7
3.1.2.1 Detrended Fluctuation Analysis (DFA).....	8
3.1.2.2 Approximated Entropy (AE).....	9
3.1.2.3 Sample Entropy (SE).....	10
3.1.2.4 Largest Lyapunov Exponent (LLE) .....	11
4 Modeling Postural Sway.....	13
5 Single Inverted Pendulum (SIP).....	14
6 References .....	18
<b>Chapter Three: Single Inverted Pendulum Validation for Healthy and Parkinson’s Disease Subjects for Bi-Pedal Quiet Standing</b> .....	<b>25</b>
1 Abstract.....	25
2 Introduction .....	27
3 Methods.....	30
3.1 Participants .....	30
3.2 Experimental Protocol .....	31
3.3 Data Analysis.....	31
3.3.1 COP <sub>exp</sub> Calculation .....	31
3.3.2 COP <sub>SIP</sub> Calculation.....	32
3.3.2.1 Linear and Nonlinear SIP Model .....	32
3.3.2.2 COP <sub>SIP</sub> with Zero and Optimized ICs.....	33
3.3.3 COP <sub>SIP</sub> Sensitivity to ICs and Linearization of DEQ Determination.....	34
3.3.4 COP <sub>SIP</sub> Accuracy Determination and Further ICs Sensitivity Analysis.....	34
3.3.4.1 Linear Measures Analysis.....	35
3.3.4.2 Nonlinear Measures Analysis.....	36
3.3.4.3 Linear, Nonlinear and Overall Performance of SIP .....	36
3.4 Statistical Analysis.....	37
4 Results.....	38
4.1 COP <sub>SIP</sub> Sensitivity to ICs .....	38
4.2 COP <sub>SIP</sub> Sensitivity to Linearization of DEQ.....	39
4.3 COP <sub>SIP</sub> Linear Measures Performance .....	40
4.4 COP <sub>SIP</sub> Nonlinear Measures Performance.....	42

5	Discussion.....	44
6	Conclusions .....	49
7	Tables and Figures.....	51
8	References .....	70
<b>Chapter Four: Summary .....</b>		<b>74</b>
1	Summary of Study.....	74
2	Conclusions and Recommendations .....	75
3	Limitations and Future Work .....	75
<b>Appendices .....</b>		<b>77</b>
1	Appendix A: Equations.....	77
1.1	SIP Free Body Diagram: Kinetic Study of SIP.....	77
1.2	SIP Free Body Diagram: Kinetic Study of Stationary Foot.....	77
2	Appendix C: Selecting the Final Optimized ICs .....	78
3	Appendix B: Figures and Tables .....	81
3.1	SIP Linear Measure Accuracy between Subjects .....	81
3.2	SIP Nonlinear Measure Accuracy between Subjects .....	83

## List of Figures

Figure 1 - Wolf's Method to Calculate LLE (Nicholas Stergiou editor, 2016).....	12
Figure 2 - SIP Free Body Diagram: Kinetic Study of SIP.....	54
Figure 3 - SIP Free Body Diagram: Kinetic Study of Stationary Foot.....	54
Figure 4 - PD-Mi-Study (Sub 1013): ICs Optimization for Nonlinear/Linear Differential Equation .....	55
Figure 5 - PD-Mi-Study: Overall Comparison of Optimized and Zero ICs in EO and EC.....	55
Figure 6 - PD-Mo-Study: Overall Comparison of Optimized and Zero ICs in EO and EC.....	56
Figure 7 - PD-Mi-Study: Overall Comparison of Nonlinear/Linear Differential Equation.....	56
Figure 8 - PD-Mo-Study: Overall Comparison of Nonlinear/Linear Differential Equation.....	57
Figure 9 - PD-Mo-Study (Sub 4011): Comparison of $COP_{exp}$ and $COP_{SIP}$ with Optimized/Zero ICs .....	57
Figure 10 - SIP Linear Performance Based on Linear Measures on $COP_{Pos}$ .....	58
Figure 11 - SIP Linear Performance Based on Linear Measures on $COP_{Vel}$ .....	59
Figure 12 - SIP Linear Performance Based on Linear Measures on $COP_{Acc}$ .....	60
Figure 13 - SIP Linear Performance Based on Linear Measures on $COP_{Pos}$ , $COP_{Vel}$ and $COP_{Acc}$ .....	61
Figure 14 - SIP Nonlinear Performance Based on $\tau$ and EmbDim.....	62
Figure 15 - SIP Nonlinear Performance Based on LLE.....	63
Figure 16 - SIP Nonlinear Performance Based on DFA.....	64
Figure 17 - SIP Nonlinear Performance Based on SE .....	65
Figure 18 - SIP Nonlinear Performance Based on AE.....	66
Figure 19 - SIP Nonlinear Performance Based on All Nonlinear Measures .....	67
Figure 20 - SIP Nonlinear Performance Based on All Nonlinear Measures (Except $\tau$ , EmbDim, and LLE) ..	68
Figure 21 - SIP Linear and Nonlinear Overall Performance .....	69
Figure 22 - PD-Mi-Study: Overall Comparison of ICs between Similarity Measures for EO and EC .....	80
Figure 23 - PD-Mo-Study: Overall Comparison of ICs between Similarity Measures for EO and EC.....	80
Figure 24 - PD-Mi-Study: Linear Accuracy ( $\pm 15\%$ ) for SIP ( $R_2$ ) with Optimized ICs.....	81
Figure 25 - PD-Mi-Study: Linear Accuracy ( $\pm 15\%$ ) for SIP ( $R_2$ ) with Zero ICs .....	81
Figure 26 - PD-Mo-Study: Linear Accuracy ( $\pm 15\%$ ) for SIP ( $R_2$ ) with Optimized ICs.....	82
Figure 27 - PD-Mo-Study: Linear Accuracy ( $\pm 15\%$ ) for SIP ( $R_2$ ) with Zero ICs .....	82

Figure 28 - PD-Mi-Study (HS): Nonlinear Accuracy ( $\pm 15\%$ ) for SIP ( $R_2$ ) with Optimized ICs .....	83
Figure 29 - PD-Mi-Study (PD-Mi): Nonlinear Accuracy ( $\pm 15\%$ ) for SIP ( $R_2$ ) with Optimized ICs .....	83
Figure 30 - PD-Mi-Study (HS): Nonlinear Accuracy ( $\pm 15\%$ ) for SIP ( $R_2$ ) with Zero ICs.....	84
Figure 31 - PD-Mi-Study (PD-Mi): Nonlinear Accuracy ( $\pm 15\%$ ) for SIP ( $R_2$ ) with Zero ICs.....	84
Figure 32 - PD-Mo-Study (HS): Nonlinear Accuracy ( $\pm 15\%$ ) for SIP ( $R_2$ ) with Optimized ICs .....	85
Figure 33 - PD-Mo-Study (PD-Mo): Nonlinear Accuracy ( $\pm 15\%$ ) for SIP ( $R_2$ ) with Optimized ICs .....	85
Figure 34 - PD-Mo-Study (HS): Nonlinear Accuracy ( $\pm 15\%$ ) for SIP ( $R_2$ ) with Zero ICs .....	86
Figure 35 - PD-Mo-Study (PD-Mo): Nonlinear Accuracy ( $\pm 15\%$ ) for SIP ( $R_2$ ) with Zero ICs.....	86

## List of Tables

Table 1 - Linear Measures for Bi-Pedal Quiet Standing Studies in PD and Healthy Subjects .....	5
Table 2 - DFA log-log Slope Range Description .....	8
Table 3 - HS from PD-Mi-Study .....	51
Table 4 - PD-Mi from PD-Mi-Study .....	51
Table 5 - HS from PD-Mo-Study .....	52
Table 6 - PD-Mo from PD-Mo-Study .....	52
Table 7 - Anthropometric Equations for the SIP Model Constants.....	52
Table 8 - Average Percent between Trials of Linear and Nonlinear Measures within Defined Error for COP <sub>SIP</sub> with Optimized ICs .....	53
Table 9 - Average Percent between Trials of Linear and Nonlinear Measures with Error Applied for COP <sub>SIP</sub> with Optimized ICs .....	53

## Chapter One: Introduction

### 1 Background and Motivation

Parkinson's disease (PD) is a neurodegenerative disorder for which there is currently no cure, and it is the second most common neurological disease in the world. PD has chemical and physiological consequences in the people who have it. The dopamine level in the basal ganglia is reduced to 50% or less when compared to healthy people, and therefore, daily living activities become more difficult. The most common symptoms that cause this reduction on quality of life are tremor, bradykinesia, and rigidity, which usually results in Postural Instability (PI) as the disease progresses. PI results in an increase in fall risk and actual falls for the person with PD, and since falls can lead to death or other health complications, assessment of PI is currently a significant unmet need.

Clinical methods such as the Unified Parkinson's Disease Rating Scale (UPDRS), Schwab & England Scale, and Hoehn & Yahr Scale (H&Y) are being used in hospitals and clinics to assess PI. However, it has been determined that they do not predict future falls. Therefore, PI assessment is being researched using signal processing and mechanical modeling techniques applied to activities of the daily living such as standing, walking, sitting, etc. done in controlled research laboratory settings that offer advanced measurement technologies. For the quiet standing task, signal processing (or posturographic) methods consist on analyzing through linear and nonlinear measures the postural sway or center of pressure (COP) time series of the subjects as they stand on a force plate. On the other hand, mechanical modeling consists on developing a mechanical system that can replicate the linear and nonlinear measures extracted from the experimental COP. Mechanical models of the human biomechanical system can be categorized by the number of rigid bodies that are used to model the human body while standing, and what type of controller is used to model the central nervous system.

The single inverted pendulum (SIP) is the most common mechanical model used to represent the human body during quiet bi-pedal standing. Because of this, over the last decades of research, multiple theories and mechanical systems for human sway have been proposed. They have helped to understand the motor control system of the body while standing, and have added insight into the problem of PI. However, recently it has been claimed that the SIP is not an accurate model for the postural sway task. In order to defend the theories and mechanical systems created around the SIP, authors have started to validate the SIP for certain ages, diseases and experimental conditions. The SIP has not been validated for the postural sway task in people with PD, which represents a gap in our knowledge, since multiple

mechanical systems and theories are based on the SIP. The main motivation of this study is to determine how accurate the SIP is for sway studies on people with PD, so that informed decisions can be made regarding the application of the theories and mechanical systems proposed up to this point (and in the future) to the PD population within the context of the modeling limitations.

## 2 Specific Aims

The goal of this study is to validate the SIP model for healthy old adults and people with PD using a novel validation approach. To date, the primary method used to validate the SIP model consists of comparing the whole body center of mass (COM) time series when it is calculated using kinematic and kinetic data. On the other hand, the approach proposed in the current study consists of comparing the COP obtained experimentally with the COP resulting from the SIP model which uses its dynamics and mathematical equations. It is hypothesized that the accuracy of the SIP is sensitive to the initial conditions (ICs) used in the differential equation (DEQ) that describes the SIP; but not sensitive to the linearization of this DEQ. In addition, it is hypothesized that the SIP can describe at least 70% of the experimental COP in healthy subjects, and that as PD progresses, people with PD behave more like a SIP due to their increased stiffness at the ankles.

## 3 Thesis Content

This document contains four chapters. Chapter One consists of an introduction and motivation to the work done in this study. Chapter Two consists of an extensive background survey of relevant literature published. Chapter Three consists of the validation study of the SIP model for healthy older adults and people with PD for bi-pedal quiet standing. Finally, Chapter Four consists of a summary of the work done in this study, its conclusions and future work.

## Chapter Two: Background

### 1 Parkinson's Disease

Parkinson's disease (PD) is a neurological disease that is present in 0.3% of the population of industrialized countries, and in 1% of the population older than 60 years old (de Lau and Breteler, 2006). According to the World Health Organization, PD can become the second most common cause of death, overtaking cancer by 2040 (World Health Organization, 2008). In addition, PD increases the falls and fall risk in people (Grimbergen et al., 2004; Wood et al., 2002), which leads to reduced quality of life, depression, and possibly mortality (Bloem et al., 2004). Falls in general are not only catastrophic for the patient; but as well for the economy of a country. In a study performed in the United States of America in 2006, it was found that in 2000, 0.2 billion dollars and 19 billion dollars were used to treat fatal and non-fatal falls cases in old adults ( $\geq 65$  years old) (Stevens et al., 2006).

In terms of physiological characteristics, PD is reflected as the loss of dopamine cells in the basal ganglia (below 50% of the common content in healthy subjects) (Lauk et al., 1999; Rektorova et al., 2012), which is reflected in changes of the motor cortex (Centonze et al., 1999). The most common symptoms observed in PD are bradykinesia, tremor, rigidity (Carpenter et al., 2004; Horak et al., 1996), and postural instability (PI) (Centonze et al., 1999); which are shown in the ability of PD patients to keep their balance while standing quietly or under perturbations. Currently, there is no cure for PD; however, multiple treatments to control the disease's symptoms are available. These treatments vary from pharmaceutical treatments like Levodopa (Mancini et al., 2008; Salat and Tolosa, 2013), to novel treatments such as electroacupuncture therapy (Toosizadeh et al., 2015), to more conventional treatments like exercise (boxing, or cycling) (Combs et al., 2011; Hazamy et al., 2017), and to more invasive treatments like deep brain stimulation (Colnat-Coulbois et al., 2005; Maurer et al., 2003).

### 2 Postural Instability (PI)

As PD progresses, the ability of the subject to keep a stable stance is reduced, as well as the ability to perform other daily-living tasks such as walking, reaching, sitting, standing up, etc. This phenomenon, referred as PI, is the most common factor for falls and risk of falling in PD patients (Qutubuddin et al., 2007; Smania et al., 2010). This creates a need in PD clinics to measure the PI of the patients, as well as the physiological and chemical parameters of the body. Currently, there are 3 standardized rating scales to measure PI: Unified Parkinson's Disease Rating Scale (UPDRS), Schwab & England Scale, and Hoehn & Yahr (H&Y) (Pahwa et al., 2003). Regardless of the worldwide use and success of these standardized

rating scales, it is recognized by the literature that the outcomes of these scales are subjective to the PD patients and doctors, creating the need of more objective measures (Adkin et al., 2005; Visser et al., 2008). That is why gait, quiet standing, perturbed standing, and sitting/standing tests (among others) are being investigated by biomechanical engineers.

### 3 Postural Sway

For quiet standing tests (which is one of the many tests to measure PI), postural sway is the measurement that is obtained from each subject. Postural sway has been used extensively over the last two decades in PD research since it allows scientists to analyze the combined performance of the visual, vestibular and somatosensory feedback systems during quiet or perturbed standing (Winter, 1995). This combination of feedback systems during quiet standing is a complex relationship that involves the peripheral and central nervous structures of the brain (Schoneburg et al., 2013), which if understood correctly, it can help the diagnosis and stage identification of PD (Hoehn and Yahr, 1967). In fact, it has been determined that postural sway is a more accurate measure for PI than regular clinical neurological examinations (Adkin et al., 2005; Visser et al., 2008).

Postural sway is commonly measured using a force plate attached to the ground. The readings of the force plate (foot/floor force and moment reactions) are used to calculate the location of the Center of Pressure (COP) time series. The COP represents the location of the resultant force exerted on the force plate by the subject when standing on it in the Anterior-Posterior (AP) and Medial-Lateral (ML) directions, and it can be calculated using the following equations (Winter, 1990):

$$COP_{AP} = -\frac{M_y + F_x \cdot d_z}{F_z}$$

$$COP_{ML} = \frac{M_x - F_y \cdot d_z}{F_z}$$

for a reference system where the x-axis is pointing to the anterior of the body ( $\uparrow$ ), the y-axis is pointing to the lateral right of the body ( $\rightarrow$ ), and the z-axis is pointing to the inferior of the body, as well as where M and F are the moments and forces read by the force plate. Finally,  $d_z$  represents the distance below the force plate surface and the origin of the coordinate system, which is given by the manufacturer of the force plate.

When postural sway is not obtained using a force plate, there are alternative methods such as Inertial Measurement Unit technology (Mancini et al., 2012b; Whitney et al., 2011). Both methods have its

advantages and disadvantages depending on the dedicated use. However, it has been proved that measures obtained through Inertial Measurement Units are reliable and consistent with the ones obtained using a force plate during quiet standing tests (Whitney et al., 2011). Another method to obtain postural sway, that has already been validated with an COP average error of  $\pm 2$  mm when compared to force plate measures is Markerless Motion Capture (Corazza and Andriacchi, 2009).

### 3.1 Postural Sway Measures

Postural sway or COP, which is a time series, is normally characterized by a set of measures. These measures could be extracted from the time series using linear or nonlinear analysis, depending on the approach of the scientists. The most popular linear and nonlinear measures, as well as the conclusions driven from them, used recently in research studies are summarized below.

#### 3.1.1 Linear Measures

The latest linear measures used in COP time series for quiet standing PD studies that have shown significant differences between Healthy Subjects (HS) and PD subjects, as well as the conclusions driven from them, are:

*Table 1 - Linear Measures for Bi-Pedal Quiet Standing Studies in PD and Healthy Subjects*

Measure	Time Series	Conclusion
Mean	$\frac{d^3}{dt^3} COP$	<ul style="list-style-type: none"> <li>• PD subjects showed larger and significant mean COP jerk (AP and ML) when compared to HS; however, difference in the ML was more significant than AP (Mancini et al., 2012a).</li> <li>• Mean COP jerk in the resultant direction is one of the most distinguishable measures between PD subjects and HS (Mancini et al., 2012b), and between PD subjects (Din et al., 2016).</li> </ul>
	$\frac{d}{dt} COP$	<ul style="list-style-type: none"> <li>• PD subjects showed larger and significant mean COP velocity (AP and ML) when compared to HS (Adkin et al., 2005; Mancini et al., 2012a; Maurer et al., 2003; Schlenstedt et al., 2016).</li> <li>• Mean COP velocity is one of the best measures to differentiate between PD subjects and HS (Mancini et al., 2012b), and between PD subjects (Ni et al., 2016).</li> <li>• PD subjects showed significant reduction of mean COP velocity, which is considered improvement of stability, when Levodopa is consumed (Maurer et al., 2004).</li> </ul>
	$COP$	<ul style="list-style-type: none"> <li>• PD subjects showed significant differences in mean COP when compared to HS (Adkin et al., 2005; Schlenstedt et al., 2016), as well as when compared between PD subjects (Ni et al., 2016).</li> <li>• Mean COP (AP) is one of the best measures to differentiate PD subjects and HS (Błaszczuk et al., 2007).</li> </ul>

Standard Deviation (SD)	<i>COP</i>	<ul style="list-style-type: none"> <li>• PD subjects showed significant and larger SD COP (AP) than HS (Colnat-Coulbois et al., 2011; Mancini et al., 2012a).</li> <li>• SD COP (AP and ML) is significant larger in PD subjects than in HS; however, this is inconclusive due the nonstationary behavior of the COP (Schmit et al., 2006).</li> <li>• PD subjects can be differentiated between each other using SD COP (Ni et al., 2016).</li> </ul>
Root Mean Square (RMS)	$\frac{d^2}{dt^2} COP$	<ul style="list-style-type: none"> <li>• RMS COP acceleration in the resultant direction is one of the best measures to differentiate PD subjects and HS (Mancini et al., 2012b)</li> </ul>
	<i>COP</i>	<ul style="list-style-type: none"> <li>• PD subjects showed significant and larger RMS COP (AP and ML) when compared to HS (Mitchell et al., 1995; Morrison et al., 2008; Schlenstedt et al., 2016).</li> <li>• RMS COP does not reflect improvement of stability in PD subjects based on UPDRS scores (Maurer et al., 2004).</li> </ul>
Frequency at 95% of Power Spectrum Density	<i>COP</i>	<ul style="list-style-type: none"> <li>• PD subjects showed significant differences in COP frequency (AP and ML) when compared to HS (Adkin et al., 2005).</li> <li>• COP frequency (AP and ML) is one of the best measures to differentiate PD subjects and HS (Mancini et al., 2012b).</li> </ul>
95% Ellipsis	$\frac{d^2}{dt^2} COP$	<ul style="list-style-type: none"> <li>• PD subjects showed significant and larger COP acceleration area than HS (Colnat-Coulbois et al., 2011; Doná et al., 2016; Morrison et al., 2008).</li> <li>• 95% Ellipsis on PD subjects shows a relationship with confidence on stability (Lee et al., 2016).</li> </ul>
Radial Area	<i>COP</i>	<ul style="list-style-type: none"> <li>• PD subjects showed a significant and larger radial area when compared to HS (Mitchell et al., 1995; Stylianou et al., 2011).</li> </ul>
Curve Length	<i>COP</i>	<ul style="list-style-type: none"> <li>• COP curve length (AP and ML) is not a good differentiator between PD subjects and HS (Horak, 1997).</li> <li>• COP curve length in the resultant direction is one of the best measures to differentiate PD subjects and HS (Błaszczuk et al., 2007; Colnat-Coulbois et al., 2011); as well as in the AP and ML directions (Morrison et al., 2008; Park et al., 2015; Stylianou et al., 2011)</li> </ul>
Range	<i>COP</i>	<ul style="list-style-type: none"> <li>• COP range (ML) is one of the best measures that can differentiate PD subjects and HS (Błaszczuk et al., 2007).</li> <li>• PD subjects showed be significant different to young and age-matched HS in terms of COP range (AP and ML) (Stylianou et al., 2011)</li> </ul>

As it can be seen in Table 1, there is no clear understanding on how PD affects the stability of a patient when he/she is tested using bi-pedal quiet standing experiments, and is analyzed with linear measures. This observation has been made by multiple authors (Błaszczuk et al., 2007; Schmit et al., 2006) since they observed that up to the point of their work, quiet standing experiments that were analyzed using linear measures were contradictory between authors, or inconclusive. In fact, a recent study could not differentiate between HS and PD subjects using linear measures when the participants were asked to

stand “still” (Sciadas et al., 2016), meaning that it was possible that the HS and PD subjects used standing strategies for which linear measures were not sensitive. However, there are researchers who still believe that it is possible to differentiate PD subjects from HS, and even to evaluate the evolution of PD, using linear measures. For example, Rocchi et al conducted quiet standing tests on PD subjects and HS, and through a principal component analysis of linear measures it was concluded that the RMS COP, mean COP velocity, SD COP, and frequency of the COP time series were sufficient to differentiate between PD subjects in ON and OFF states of Levodopa, as well between PD subjects and HS (Rocchi et al., 2006). But, other authors like Gervasoni et al, claim that linear measures of the COP velocity, plus non-posturographic tests are the best predictors of falls and differentiators in PD subjects (Gervasoni et al., 2015).

### 3.1.2 Nonlinear Measures

In addition to the linear measures, nonlinear analysis has started to be used since it has been determined that COP is a nonlinear and time-dependent signal (Winters and Stark, 1985), which is completely opposite to the assumptions made when linear measures are used (time invariant and stationary signal). For example, it has been found that COP changes mostly in the first 30 seconds of quiet standing, and that it changes at different rates for HS and PD subjects (Din et al., 2016). It was also determined in this study that after 30 seconds into a standing trial, quiet standing becomes more stationary. In addition, a recent study on machine learning for HS during multiple tasks while standing, showed that linear measures perform better when used as nonlinear (polynomials) classifiers than when they are used as linear classifiers (Saripalle et al., 2014). Even when the human body is modeled as a single inverted pendulum (SIP), it is possible to observe nonlinear features such as stable states (limit cycles) and bifurcation points (Creath et al., 2005). This idea of viewing the COP coming from a chaotic nonlinear dynamical system, have allowed authors to hypothesize that diseases such as PD can be detected when the COP becomes less complex and more deterministic (Schmit et al., 2006; Stergiou and Decker, 2011), which are qualities that can be observed through nonlinear measures. With that said, the latest nonlinear measures used in COP time series for bi-pedal quiet standing on PD studies that have shown significant differences between HS and PD subjects, as well as the conclusions driven from them, are summarized next.

### 3.1.2.1 Detrended Fluctuation Analysis (DFA)

Detrended Fluctuation Analysis (DFA) was first proposed by Peng et al in the analysis of DNA structures (Peng et al., 1994), with the purpose of analyzing how a time series fluctuated when it was observed using different scales in time. The equation to calculate this measure is:

$$F(n) = \sqrt{\frac{1}{N} \sum_{k=1}^N [y(k) - y_n(k)]^2}$$

where  $n$  is the number of equal divisions of the time series in time,  $N$  is the total number of elements of the time series,  $y$  is the time series in the division defined by  $n$ , and  $y_n$  is the linear trend of  $y$ . In other words, DFA is an improvement of the RMS, since it does not assume that the time series is stationary and time-invariant. After calculating the fluctuations ( $F$ ) as a function of the number of equal intervals in the time series ( $n$ ), they are plotted against each other ( $F$  vs.  $n$ ) where both axis are scaled using a  $\log_{10}$ . The slope ( $\alpha$ ) of the log-log plot is calculated since it describes the behavior of the signal (Delignières et al., 2011; Peng et al., 1995):

Table 2 - DFA log-log Slope Range Description

Range	Description
$0 < \alpha < 0.5$	Anti-correlated and anti-persistent
$\alpha \approx 0.5$	Uncorrelated (White Noise)
$0.5 < \alpha < 1$	Correlated and persistent
$\alpha \approx 1$	1/f-noise (Pink Noise)
$1 < \alpha < 1.5$	Non-stationary, unbounded and anti-persistent
$\alpha \approx 1.5$	(Brown Noise)
$\alpha > 1.5$	Non-stationary, unbounded and persistent

One of the most important factors when calculating the slope of the DFA log-log plot is the minimum and maximum number of  $n$ . A final decision on this aspect has not been made; however, according to the literature, they range around  $8 \leq n_{\min} \leq 10$  samples (sampling frequency 40 Hz), and  $N/10 \leq n_{\max} \leq N/2$  (Delignières et al., 2011; Hu et al., 2001; Teresa Blázquez et al., 2009).

DFA analysis was introduced in COP studies by Collins and De Luca (Collins and De Luca, 1994), and it has then been applied to PD bi-pedal quiet standing studies by authors like Mitchell et al (Mitchell et al., 1995). In these last two studies, DFA analysis was not explicitly performed; Stabilogram Diffusion Analysis was done instead. But, in a later study (Delignières et al., 2011), it was proven that the DFA of the COP velocity was equivalent to the Stabilogram Diffusion Analysis of the COP position. Multiple

authors (Collins and De Luca, 1994; Delignières et al., 2011; Mitchell et al., 1995; Teresa Blázquez et al., 2009), agree that in bi-pedal quiet standing tests it is possible to notice a breaking point in the log-log plot which creates the need of the calculation of two slopes. For example, authors have found that HS and PD subjects significantly differ in the slopes before this breaking point, as well as in the slopes of the entire log-log plot for both AP and ML directions (Mitchell et al., 1995; Stylianou et al., 2011). In fact, it was observed that the slopes before the breaking point were larger in PD subjects than in HS. It was also observed in the same study that the slope after the breaking point in the ML direction has a possible relationship with the history of falls in PD subjects.

### 3.1.2.2 Approximated Entropy (AE)

Approximated Entropy (AE) was developed as an approximation of the real entropy of a system (defined by differential equations) (Pincus, 1991). The equations to calculate the AE from a time series  $x(N)$  are:

$$AE(m, r, N) = \Phi^m(r) - \Phi^{m+1}(r)$$

$$\Phi^m(r) = (N - m + 1)^{-1} \sum_{i=1}^{N-m+1} \ln C_i^m(r)$$

$$\Phi^{m+1}(r) = (N - m)^{-1} \sum_{i=1}^{N-m} \ln C_i^{m+1}(r)$$

$$C_i^m(r) = \sum_{i=1}^{N-m+1} \frac{\text{number of times } d[x_m(i), x_m(j)] \leq r}{N - m + 1}$$

$$C_i^{m+1}(r) = \sum_{i=1}^{N-m} \frac{\text{number of times } d[x_m(i), x_m(j)] \leq r}{N - m}$$

$$d[x(i), x(j)] = \max_{k=1,2,\dots,m} |u(i+k-1) - u(j+k-1)|$$

$$x(i) = [u(i), u(i+1), \dots, u(i+m-1)]$$

where  $N$  is the number of elements in the time series,  $m$  is the dimension of the vectors  $x(i)$  and  $x(j)$ , and  $r$  is the maximum distance (number of SD) between vectors  $x(i)$  and  $x(j)$  that counts them as similar vectors. AE is sometimes scaled by dividing it by the length of data points  $N$  (Nicholas Stergiou editor, 2016). The value of AE indicates the level of complexity or how predictable the time series is. A high value of AE means that the time series is very complex and has low predictability, and vice versa. Finally, choosing the parameters  $m$ ,  $r$ , and  $N$  is an important part of this calculation since they have a significant

effect on the result of AE. A final decision for AE's parameters in sway data has not been made yet; however it is advised that the time series has a  $N > 200$ , that  $m$  represents a biological characteristic, and that after calculating AE with the chosen  $m$  and  $r$ , the study is repeated around the chosen values to make sure the result is consistent (Yentes et al., 2013).

Regarding COP, it is hypothesized that when the body creates a COP that has low levels of complexity (low value of AE), any small perturbation can take the body out of balance; while a body with higher levels of complexity (high value of AE) can withstand those small perturbations and still be in balance (Morrison et al., 2008). In addition in this last study and others (Karimi et al., 2015; Park et al., 2015), it was found that AE can detect differences between PD subjects and HS, as well as when PD subjects were ON and OFF from Levodopa. It was also observed that the significant differences between PD subjects come from larger AE in both AP and ML directions as PD progressed. These increments of AE in PD subjects support the theory that the healthy level of complexity is dependent on the task being performed (Vaillancourt and Newell, 2002), not meaning that higher complexity means automatically healthier and better balance (Goldberger et al., 2002).

### 3.1.2.3 Sample Entropy (SE)

Sample Entropy (SE) was developed by Richman and Moorman, and it was intended to improve the AE (Richman and Moorman, 2000); however, after using these two parameters in biomechanics research, there is no wide spread agreement regarding which one is better, since it all depends on the analysis that is being performed. The equations to calculate SE are:

$$SE(m, r, N) = -\ln \frac{A^m(r)}{B^m(r)}$$

$$B^m(r) = (N - m)^{-1} \sum_{i=1}^{N-m} \ln B_i^m(r)$$

$$A^m(r) = (N - m)^{-1} \sum_{i=1}^{N-m} \ln A_i^m(r)$$

$$B_i^m(r) = \sum_{j=1}^{N-m} \frac{\text{number of times } d[x_m(i), x_m(j)] \leq r}{N - m - 1}$$

$$A_i^m(r) = \sum_{j=1}^{N-m} \frac{\text{number of times } d[x_{m+1}(i), x_{m+1}(j)] \leq r}{N - m - 1}$$

$$d[x(i), x(j)] = \max_{k=1,2,\dots,m} |u(i+k-1) - u(j+k-1)| \quad \text{with } i \neq j$$

$$x(i) = [u(i), u(i+1), \dots, u(i+m-1)]$$

Where the parameters  $m$ ,  $r$ , and  $N$  have the same meaning as in AE; however, SE is not scaled by being divided by the length of the time series  $N$ . In addition, the value of SE has the same interpretation as in AE; the higher the value, the more complex and less predictable the time series is, and vice versa.

Finally, as mentioned in the AE explanation, selection of  $m$ ,  $r$ , and  $N$  have a significant effect on the value of SE. With that said, it has been recommended that in biomechanical signals the time series has a  $N > 200$ , that  $m$  represents a biological characteristic, and that after calculating SE with the chosen  $m$  and  $r$ , the study should be repeated around the chosen values of  $m$  and  $r$  to make sure the result is consistent (Yentes et al., 2013). In addition, a study that consisted on studying the sensitivity of SE in COP in terms of  $m$ , and  $r$  found that SE converges when  $m \geq 3$ , and that the highest confidence of estimation from SE to the real entropy value of the time series is obtained around  $r = 0.3$  (Ramdani et al., 2009). It needs to be mentioned that this last study had a sampling frequency of 40 Hz. Finally, a similar study to the last one was conducted on PD subjects' COP time series. This study (Pelykh et al., 2015) recommends using a sampling frequency of 100 Hz to record the COP time series, and use  $m = 2$  and  $r = 0.1, 0.2$  to calculate the SE. It needs to be mentioned that the methods from the last two studies to select  $r$  were the same one, which consisted on maximizing the confidence of estimation of the SE.

Regarding PD bi-pedal quiet standing studies, it has been observed that SE can differentiate between diseases such as PD, Multiple Sclerosis, and Strokes; however, it could not differentiate between eyes open (EO) and eyes closed (EC) (Cattaneo et al., 2016). In addition, when it comes to comparing PD subjects and HS, SE ( $r = 0.2$  and  $m = 2$ , in a 100 Hz study) can differentiate PD subjects (with and without freezing of gait) from HS (Pelykh et al., 2015; Schlenstedt et al., 2016).

#### 3.1.2.4 Largest Lyapunov Exponent (LLE)

The Largest Lyapunov Exponent (LLE) is a nonlinear measure that indicates if the time series is sensitive to initial conditions which is one of the most accepted qualities of chaotic time series (Steven H Strogatz, 2015). Multiple numerical methods to calculate the LLE have been proposed; however the two most common methods in biomechanics research are Wolf's (Wolf et al., 1985) and Rosenstein's (Rosenstein et al., 1993) algorithms which are available online. Rosenstein's algorithm was developed as an improvement of Wolf's calculation; however, multiple authors have concluded that both methods have their disadvantages and advantages depending on the experiment being conducted (Nicholas Stergiou

editor, 2016). Regardless of the method used to calculate the LLE, the obtained value has the same interpretation which is: if  $LLE < 0$ , it means that the system converges which is not an indication of sensitivity to initial conditions; if  $LLE > 0$ , it means that the system diverges which is an indication of sensitivity to initial conditions; and finally, if  $LLE = 0$ , it means that the system does not diverge or converge which is an indication of a limit cycle.

Since there is not an absolute answer on which method is the best to calculate the LLE, the method used in this thesis will be Wolf's which is defined by the following equations:

$$LLE = \frac{1}{M} \sum_{i=1}^M Z_i$$

$$Z_i = \frac{\log_2 \frac{L'(t_i)}{L(t_0)}}{\Delta t \cdot n}$$

where  $L$  is the distance travelled by a state after being evolved,  $\Delta t$  is the sampling time in the time series,  $n$  is the number of evolutions, and  $M$  is the number of exponents  $Z$  that are calculated. In other words, the LLE is calculated by choosing a trajectory in the time series (normally the trajectory starting at its initial point is chosen), find the nearest neighbor within a specified distance and angle, let those two states evolve  $n$  times, calculate the distances travelled, calculate  $Z_i$ , and repeat the process until the time series allows it. This calculation is graphically explained in this image:

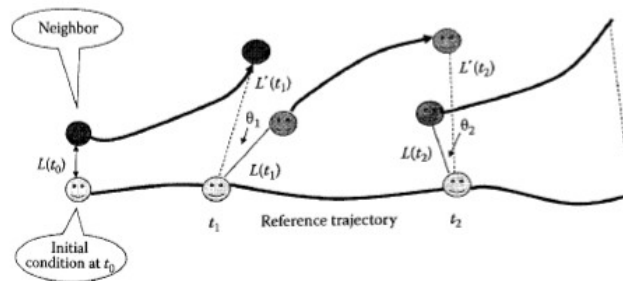


Figure 1 - Wolf's Method to Calculate LLE (Nicholas Stergiou editor, 2016)

It needs to be acknowledged that before calculating the LLE, the time series must be reconstructed in its state-space form, meaning that the embedding dimension (EmbDim) and time delay ( $\tau$ ) need to be calculated previous to the LLE. Different methods to calculate these two parameters exist; however, the chosen method to calculate  $\tau$  in this thesis is through mutual information (MI) (Fraser and Swinney,

1986), which bins the time series based on the optimal bin size (Scott, 1979), and the chosen method to calculate the EmbDim is through Euclidian distances (Kennel et al., 1992).

Regarding PD bi-pedal quiet standing studies on the COP time series, the LLE has been used to see if the postural sway time series in subjects is chaotic or not. For example, Pascolo et al found that the LLE indicates that both HS and PD subjects have chaotic COP time series; however, it was not possible to differentiate the LLE between PD subjects and HS (Pascolo et al., 2006, 2005).

## 4 Modeling Postural Sway

Modeling the human body during quiet stance using a mechanical system has been a common research in the last two decades (Crétual, 2015), especially in PD (Boonstra et al., 2013; Chagdes et al., 2016a; Maurer et al., 2004; Park et al., 2004). Linear and nonlinear measures of the COP time series (most common research in PD assessment for PI) have limitations when it comes to describing how the central nervous system (CNS) is performing while the subject is standing. In other words, based on our current understanding of the linear and nonlinear measures, they are a binning tool for PD; while a mechanical model represents an opportunity for a diagnostic tool. When linear and nonlinear measures of the COP are determined from a PD subjects, it is possible to correlate them with UPDRS and H&Y scores, or number of falls, etc., and then see where the subject stands when compared to other PD subjects and HS. However, they cannot explicitly tell how the CNS system is working in the PD subjects during the performed test (Visser et al., 2008). That is why if a mechanical model could reproduce the measures extracted from the experimental COP of the PD subjects by tuning the model's parameters, that have physiological meaning, it potentially could provide a level of diagnosis about his/her CNS. If needed, this diagnosis can then be further developed through more expensive diagnosis tools such as brain scanning techniques. As stated by multiple researchers, developing a mechanical model for bi-pedal quiet standing would allow the understanding of the changes in linear and nonlinear measures extracted from the COP time series (Chagdes et al., 2016b), how the human body interacts with the environment (Park et al., 2004), how the muscles are activated (Pang and Mak, 2012), among others.

There are many mechanical models for bi-pedal quiet standing and they differ on the type of controller chosen and the number of links that it contains. In more recent publications, it has been discussed how many members or links the model needs to have to represent the body accurately. The most common way to represent the human body during bi-pedal quiet standing is by modeling the body as a SIP.

## 5 Single Inverted Pendulum (SIP)

Modeling the human body stance in general cannot be done using a SIP since not all balance corrections are controlled by the ankles (Bloem et al., 2000); in fact, it has been observed that the human body performs different muscles and body segments synergies depending on the perturbation that is applied (Allum et al., 1993, 1989; Horak and Kuo, 2000), as well as where the body was located before the perturbation (Tokuno et al., 2006). However, during bi-pedal quiet stance ( $<0.5$  Hz) or small body perturbations, the SIP is believed to be an accurate representation of the human body (Fujisawa et al., 2005; Horak and Nashner, 1986; McCollum and Leen, 1989; Nashner, 1976), as well as when the body is not close to its limits of stability in either the AP or ML directions (Mancini et al., 2008). This hypothesis was tested by Clifford and Holder-Powell by making healthy subjects stand using one leg (dominant and non-dominant) (Clifford and Holder-Powell, 2010). It was observed that the SIP could model the kinematics of the subject, if his/her motion was not large enough to trigger the motion of the other joints (knee and hip). This was proven when the triple inverted pendulum (TIP) (shank, quad and head-arm-torso (HAT)) and the SIP predicted similar locations for the Center of Mass (COM) of the whole body.

The validation of the SIP during stance experiments has become a needed step since lately multiple authors have claimed that human quiet stance on two feet cannot be modeled using a SIP (Freitas et al., 2009; Günther et al., 2011, 2009; Kato et al., 2014; Sasagawa et al., 2009; Yamamoto et al., 2015). Conclusions to believe that the SIP is not an accurate representation of bi-pedal quiet standing has been tested by using invasive testing such as strapping the knee, hips, and torso with casts to see if the body is represented by a SIP (Freitas et al., 2009), to non-invasive testing. From these non-invasive experiments, the main argument is that when the motion of the ankle and hip are correlated, the value is not equal to 1 which is the value that the SIP would produce (Günther et al., 2011; Kato et al., 2014; Sasagawa et al., 2009). However, they have also found that the motion of the knee correlates differently with the hip and ankles, meaning that instead of using a double inverted pendulum (DIP) to simulate quiet standing, a TIP should be used (Günther et al., 2009; Yamamoto et al., 2015). Following the need for the DIP or TIP to model quiet standing, it was shown (Wang et al., 2014) that during bi-pedal quiet standing the neck moves as well, and that the coherences (or correlations) between the motion of shank, quad, torso and neck change as function of the frequency (0.0167 – 0.8016 Hz) of the COP. However, in the same study it was found that the coherence of COP and COM remained almost constant for all frequencies and its value was always bigger than 0.8; not like the coherences between

body links which were around 0.5 in average for all frequencies. This means that it is acknowledged that bi-pedal quiet standing requires the motion of multiple body parts; however, the most constant relation in this dynamic behavior is the one between the COP and COM (Wang et al., 2014), which has been also identified in the SIP models (Gage et al., 2004).

Looking that SIP models can analyze the relationship between the COP and COM, which is considered an important collective variable in bi-pedal quiet standing (Kilby et al., 2016; Mani et al., 2015; Wang et al., 2014), validation of the SIP as representation of the human body during bi-pedal quiet stance has been a common research over last decade. This work started by performing bi-pedal quiet standing tests with eyes open in 11 healthy university students (Age =  $26.5 \pm 3.9$ ) while gathering kinematic and kinetic data using 3D cameras and force plate respectively (Gage et al., 2004). The kinematic data was used to calculate the COM of the entire body, as well as the COM of the different parts of the body; while the kinetic data was used to calculate the COP. The results and conclusions that supported the SIP as a valid model for bi-pedal quiet standing were: (1) the strong correlation between the acceleration of the COM of the body and the difference COP – COM ( $R_{AP} = -0.954 \pm 0.020$ ,  $R_{ML} = -0.840 \pm 0.054$ ), which is a derived relationship when the human body is modeled as a SIP, and (2) the strong correlation between the amount of motion (RMS) of each body part's COM in the AP and ML directions, and their height from the ankle ( $R^2 > 0.9$  for AP and ML). These strong and almost perfect correlations allowed Gage et al to claim that the body does not only consist on ankle motion; however, it is mostly described by ankle motion. Other studies have agreed with these conclusions. For example, a study of 26 healthy young adults (Mean age = 26) obtained  $R^2$  values bigger than 0.8 when the amount of motion of the body parts was plotted vs. the height of them from the ankles (Winter et al., 1997), which agrees with the second conclusion; while a study of bi-pedal quiet standing on young and post-stroke subjects found that for both subject groups, the acceleration of the body COM has a strong linear correlation with the difference COP – COM ( $R > 0.9$ ) (Yu et al., 2008), which agrees with the first conclusion. Another study (Masani et al., 2007) compared the acceleration of the COM of the body calculated from the 3D cameras (kinematic data), and the one calculated from the force plate (kinetic data) which assumed that the body was a SIP. Their subject population was 15 healthy old adults (Mean age = 72) and 11 healthy young adults (Mean age = 29), and the test consisted on EO and EC bi-pedal quiet standing. Their main result was the comparison of the body COM accelerations (EO and EC) in the AP direction when calculated from the kinematic and kinetic data, which for the young adults was  $\ddot{C}O\ddot{M}_{FP} = -0.21 + 1.14 \cdot \ddot{C}O\ddot{M}_{3D}$  ( $R = 0.973$ ), and  $\ddot{C}O\ddot{M}_{FP} = -0.04 + 1.01 \cdot \ddot{C}O\ddot{M}_{3D}$  ( $R = 0.976$ ) for the old adults. Using those equations, the authors of the study concluded that the SIP is an appropriate method for EO and EC

bi-pedal quiet standing since the slope of the equations, and fitting coefficients were very close to 1. Finally, a study on 29 young adults (16 male of age =  $24.6 \pm 3.2$ , 13 female of age =  $23.3 \pm 2.9$ ) for quiet standing (bi-pedal, tandem and single leg) with EO showed through principal component analysis that during bi-pedal quiet stance 71.7% of the sway in the AP direction can be explained by the motion of the ankles (Federolf et al., 2013). From this same study, it was also concluded that in bi-pedal quiet stance, ankle motion was always the most significant motion for all subjects during sway in the AP direction, which was not the case on the tandem and single-leg stances.

Other studies have not focused on validating the SIP for bi-pedal quiet stance, but have obtained results that support the model. For example, an experiment that consisted on analyzing the correlation between the body COM and the shank COM before and after the lumbar region was fatigued (Madigan et al., 2006), found that there were not significant differences due to fatigue ( $R_{\text{before}} = 0.8 \pm 0.18$ ,  $R_{\text{after}} = 0.79 \pm 0.17$ ). Similar to the last study, an experiment that consisted on analyzing the motion of the ankles, knees and hip before and after the fatigue of the ankle region (Boyas et al., 2013), found that only during bi-pedal quiet standing with EC, differences were found in all the motions. These two results support the SIP since the ankle strategy was present before and after fatigue, which is the strategy assumed in the SIP models. Also, two studies that consisted on modifying the mass ( $m$ ) and mass moment of inertia ( $J$ ) of the subjects during bi-pedal quiet stance (Costello et al., 2012; Rosker et al., 2011), obtained the results that a SIP model of the body would have predicted (regarding amplitude of sway). Finally, validating the SIP model in general is not the ideal case for biomechanics research since diseases can change the behavior of the human body. With that said, validation of the SIP model for certain human conditions and/or disease is being done. For example, the SIP model has been successfully validated for bi-pedal quiet standing tests on transtibial prosthesis users (Rusaw and Ramstrand, 2016), and partially successful for post-stroke subjects (Yu et al., 2008).

Besides the validity of the SIP in mechanical modeling studies, the way its differential equation (DEQ) is used differs between authors. For example, the SIP DEQ (Refer to Figure 2, Table 7 and Appendix A: Equations – Section 1.1) that relates the angular position of the pendulum and the torque applied at the ankles:

$$\ddot{\theta} = \frac{1}{J_{SIP}} (F_z COP_{exp} - m_{SIP} g h_{SIP} \sin \theta - m_{feet} g COM_{feet} - F_x h_{ank})$$

can be linearized ( $\sin \theta \cong \theta$ ) around the vertical orientation of the pendulum. Turning this nonlinear differential equation (N-DEQ) into a linear differential equation (L-DEQ).

$$\ddot{\theta} = \frac{1}{J_{SIP}} (F_z COP_{exp} - m_{SIP} g h_{SIP} \theta - m_{feet} g COM_{feet} - F_x h_{ank})$$

The L-DEQ is currently the most popular practice (Asai et al., 2009; Bottaro et al., 2008; Kooij et al., 1999; Loram and Lakie, 2002; Maurer et al., 2004, p. 2; Peterka, 2002; Vette et al., 2010); however, some authors prefer to use the N-DEQ (Chagdes et al., 2016a, 2016b). The advantage of using the nonlinear differential equation is the improved accuracy of the model when large sways occur; however, authors who use the L-DEQ claim that the magnitude of unperturbed sway of humans is small enough to be represented by the linear differential equation. Regardless of the chosen DEQ (linear vs. nonlinear), most of the mechanical modeling studies use initial conditions equal to zero for simplicity (Initial angle  $\theta_0 = 0$ , and initial angular velocity  $\dot{\theta}_0 = 0$ ). However, it has been observed in experimental studies that the initial position of the body changes significantly the sway in humans (Tokuno et al., 2006).

Finally, all validations listed previously for the SIP have used the strategy of comparing the COM obtained through kinematic and kinetic data. However, the SIP has not been validated using the COP that it creates when its dynamics and mathematical equations are used. In fact, the COP that the SIP creates when the feet are assumed to be stationary in an inverse dynamics study, is described by the following equation (Refer to Figure 3 and Appendix A: Equations – Section 1.2):

$$COP_{SIP} = \frac{1}{GRF_z} (T + m_{feet} g COM_{feet} + GRF_x h_{ank})$$

which requires the solution of either the L-DEQ or N-DEQ using initial conditions equal to zero, or non-zero.

## 6 References

- Adkin, A.L., Bloem, B.R., Allum, J.H.J., 2005. Trunk sway measurements during stance and gait tasks in Parkinson's disease. *Gait Posture* 22, 240–249. doi:10.1016/j.gaitpost.2004.09.009
- Allum, J.H., Honegger, F., Pfaltz, C.R., 1989. The role of stretch and vestibulo-spinal reflexes in the generation of human equilibrating reactions. *Prog. Brain Res.* 80, 399–409; discussion 395–397.
- Allum, J.H., Honegger, F., Schicks, H., 1993. Vestibular and proprioceptive modulation of postural synergies in normal subjects. *J. Vestib. Res. Equilib. Orientat.* 3, 59–85.
- Asai, Y., Tasaka, Y., Nomura, K., Nomura, T., Casadio, M., Morasso, P., 2009. A model of postural control in quiet standing: robust compensation of delay-induced instability using intermittent activation of feedback control. *PLoS One* 4, e6169. doi:10.1371/journal.pone.0006169
- Błaszczyk, J.W., Orawiec, R., Duda-Kłodowska, D., Opala, G., 2007. Assessment of postural instability in patients with Parkinson's disease. *Exp. Brain Res.* 183, 107–114. doi:10.1007/s00221-007-1024-y
- Bloem, B.R., Allum, J.H.J., Carpenter, M.G., Honegger, F., 2000. Is lower leg proprioception essential for triggering human automatic postural responses? *Exp. Brain Res.* 130, 375–391. doi:10.1007/s002219900259
- Bloem, B.R., Hausdorff, J.M., Visser, J.E., Giladi, N., 2004. Falls and freezing of gait in Parkinson's disease: a review of two interconnected, episodic phenomena. *Mov. Disord. Off. J. Mov. Disord. Soc.* 19, 871–884. doi:10.1002/mds.20115
- Boonstra, T.A., Schouten, A.C., Van der Kooij, H., 2013. Identification of the contribution of the ankle and hip joints to multi-segmental balance control. *J. NeuroEngineering Rehabil. JNER* 10, 1–18. doi:10.1186/1743-0003-10-23
- Bottaro, A., Yasutake, Y., Nomura, T., Casadio, M., Morasso, P., 2008. Bounded stability of the quiet standing posture: An intermittent control model. *Hum. Mov. Sci.* 27, 473–495. doi:10.1016/j.humov.2007.11.005
- Boyas, S., Hajj, M., Bilodeau, M., 2013. Influence of ankle plantarflexor fatigue on postural sway, lower limb articular angles, and postural strategies during unipedal quiet standing. *Gait Posture* 37, 547–551. doi:10.1016/j.gaitpost.2012.09.014
- Carpenter, M.G., Allum, J.H.J., Honegger, F., Adkin, A.L., Bloem, B.R., 2004. Postural abnormalities to multidirectional stance perturbations in Parkinson's disease. *J. Neurol. Neurosurg. Psychiatry* 75, 1245–1254. doi:10.1136/jnnp.2003.021147
- Cattaneo, D., Carpinella, I., Aprile, I., Prosperini, L., Montesano, A., Jonsdottir, J., 2016. Comparison of upright balance in stroke, Parkinson and multiple sclerosis. *Acta Neurol. Scand.* 133, 346–354. doi:10.1111/ane.12466
- Centonze, D., Calabresi, P., Giacomini, P., Bernardi, G., 1999. Neurophysiology of Parkinson's disease: from basic research to clinical correlates. *Clin. Neurophysiol. Off. J. Int. Fed. Clin. Neurophysiol.* 110, 2006–2013.
- Chagdes, J.R., Huber, J.E., Saletta, M., Darling-White, M., Raman, A., Rietdyk, S., Zelaznik, H.N., Haddad, J.M., 2016a. The relationship between intermittent limit cycles and postural instability associated with Parkinson's disease. *J. Sport Health Sci.* 5, 14–24. doi:10.1016/j.jshs.2016.01.005
- Chagdes, J.R., Rietdyk, S., Haddad, J.M., Zelaznik, H.N., Cinelli, M.E., Denomme, L.T., Powers, K.C., Raman, A., 2016b. Limit cycle oscillations in standing human posture. *J. Biomech.* 49, 1170–1179. doi:10.1016/j.jbiomech.2016.03.005
- Clifford, A.M., Holder-Powell, H., 2010. Postural control in healthy individuals. *Clin. Biomech.* 25, 546–551. doi:10.1016/j.clinbiomech.2010.03.005
- Collins, J.J., De Luca, C.J., 1994. Random Walking during Quiet Standing. *Phys. Rev. Lett.* 73, 764–767. doi:10.1103/PhysRevLett.73.764

- Colnat-Coulbois, S., Gauchard, G., Maillard, L., Barroche, G., Vespignani, H., Auque, J., Perrin, P., 2005. Bilateral subthalamic nucleus stimulation improves balance control in Parkinson's disease. *J. Neurol. Neurosurg. Psychiatry* 76, 780–787. doi:10.1136/jnnp.2004.047829
- Colnat-Coulbois, S., Gauchard, G.C., Maillard, L., Barroche, G., Vespignani, H., Auque, J., Perrin, P.P., 2011. Management of postural sensory conflict and dynamic balance control in late-stage Parkinson's disease. *Neuroscience* 193, 363–369. doi:10.1016/j.neuroscience.2011.04.043
- Combs, S.A., Diehl, M.D., Staples, W.H., Conn, L., Davis, K., Lewis, N., Schaneman, K., 2011. Boxing Training for Patients With Parkinson Disease: A Case Series. *Phys. Ther. Wash.* 91, 132–42.
- Corazza, S., Andriacchi, T.P., 2009. Posturographic analysis through markerless motion capture without ground reaction forces measurement. *J. Biomech.* 42, 370–374. doi:10.1016/j.jbiomech.2008.11.019
- Costello, K.E., Matrangola, S.L., Madigan, M.L., 2012. Independent effects of adding weight and inertia on balance during quiet standing. *Biomed. Eng. Online* 11, 20. doi:10.1186/1475-925X-11-20
- Creath, R., Kiemel, T., Horak, F., Peterka, R., Jeka, J., 2005. A unified view of quiet and perturbed stance: simultaneous co-existing excitable modes. *Neurosci. Lett.* 377, 75–80. doi:10.1016/j.neulet.2004.11.071
- Crétual, A., 2015. Which biomechanical models are currently used in standing posture analysis? *Neurophysiol. Clin. Clin. Neurophysiol.* 45, 285–295. doi:10.1016/j.neucli.2015.07.004
- de Lau, L.M.L., Breteler, M.M.B., 2006. Epidemiology of Parkinson's disease. *Lancet Neurol.* 5, 525–535. doi:10.1016/S1474-4422(06)70471-9
- Delignières, D., Torre, K., Bernard, P.-L., 2011. Transition from Persistent to Anti-Persistent Correlations in Postural Sway Indicates Velocity-Based Control. *PLoS Comput. Biol.* 7, 1–10. doi:10.1371/journal.pcbi.1001089
- Din, S.D., Godfrey, A., Coleman, S., Galna, B., Lord, S., Rochester, L., 2016. Time-dependent changes in postural control in early Parkinson's disease: what are we missing? *Med. Biol. Eng. Comput.* 54, 401–410. doi:10.1007/s11517-015-1324-5
- Doná, F., Aquino, C.C., Gazzola, J.M., Borges, V., Silva, S.M.C.A., Ganança, F.F., Caovilla, H.H., Ferraz, H.B., 2016. Changes in postural control in patients with Parkinson's disease: a posturographic study. *Physiotherapy* 102, 272–279. doi:10.1016/j.physio.2015.08.009
- Federolf, P., Roos, L., Nigg, B.M., 2013. Analysis of the multi-segmental postural movement strategies utilized in bipedal, tandem and one-leg stance as quantified by a principal component decomposition of marker coordinates. *J. Biomech.* 46, 2626–2633. doi:10.1016/j.jbiomech.2013.08.008
- Fraser, null, Swinney, null, 1986. Independent coordinates for strange attractors from mutual information. *Phys. Rev. Gen. Phys.* 33, 1134–1140.
- Freitas, P.B. de, Freitas, S.M.S.F., Duarte, M., Latash, M.L., Zatsiorsky, V.M., 2009. Effects of joint immobilization on standing balance. *Hum. Mov. Sci.* 28, 515–528. doi:10.1016/j.humov.2009.02.001
- Fujisawa, N., Masuda, T., Inaoka, H., Fukuoka, Y., Ishida, A., Minamitani, H., 2005. Human standing posture control system depending on adopted strategies. *Med. Biol. Eng. Comput.* 43, 107–114. doi:10.1007/BF02345130
- Gage, W.H., Winter, D.A., Frank, J.S., Adkin, A.L., 2004. Kinematic and kinetic validity of the inverted pendulum model in quiet standing. *Gait Posture* 19, 124–132. doi:10.1016/S0966-6362(03)00037-7
- Gervasoni, E., Cattaneo, D., Messina, P., Casati, E., Montesano, A., Bianchi, E., Beghi, E., 2015. Clinical and stabilometric measures predicting falls in Parkinson disease/parkinsonisms. *Acta Neurol. Scand.* 132, 235–241. doi:10.1111/ane.12388

- Goldberger, A.L., Peng, C.-K., Lipsitz, L.A., 2002. What is physiologic complexity and how does it change with aging and disease? *Neurobiol. Aging* 23, 23–26.
- Grimbergen, Y.A.M., Munneke, M., Bloem, B.R., 2004. Falls in Parkinson's disease. *Curr. Opin. Neurol.* 17, 405–415.
- Günther, M., Grimmer, S., Siebert, T., Blickhan, R., 2009. All leg joints contribute to quiet human stance: A mechanical analysis. *J. Biomech.* 42, 2739–2746. doi:10.1016/j.jbiomech.2009.08.014
- Günther, M., Müller, O., Blickhan, R., 2011. Watching quiet human stance to shake off its straitjacket. *Arch. Appl. Mech.* 81, 283–302. doi:10.1007/s00419-010-0414-y
- Hazamy, A.A., Altmann, L.J.P., Stegemöller, E., Bowers, D., Lee, H.K., Wilson, J., Okun, M.S., Hass, C.J., 2017. Improved cognition while cycling in Parkinson's disease patients and healthy adults. *Brain Cogn.* 113, 23–31. doi:10.1016/j.bandc.2017.01.002
- Hoehn, M.M., Yahr, M.D., 1967. Parkinsonism: onset, progression and mortality. *Neurology* 17, 427–442.
- Horak, F., Kuo, A., 2000. Postural Adaptation for Altered Environments, Tasks, and Intentions, in: Winters, J.M., Crago, P.E. (Eds.), *Biomechanics and Neural Control of Posture and Movement*. Springer New York, pp. 267–281. doi:10.1007/978-1-4612-2104-3\_19
- Horak, F.B., 1997. Clinical assessment of balance disorders. *Gait Posture* 6, 76–84. doi:10.1016/S0966-6362(97)00018-0
- Horak, F.B., Frank, J., Nutt, J., 1996. Effects of dopamine on postural control in parkinsonian subjects: scaling, set, and tone. *J. Neurophysiol.* 75, 2380–2396.
- Horak, F.B., Nashner, L.M., 1986. Central programming of postural movements: adaptation to altered support-surface configurations. *J. Neurophysiol.* 55, 1369–1381.
- Hu, K., Ivanov, P.C., Chen, Z., Carpena, P., Stanley, H.E., 2001. Effect of Trends on Detrended Fluctuation Analysis. *Phys. Rev. E* 64. doi:10.1103/PhysRevE.64.011114
- Karimi, M., Sadeghisani, M., Omar, A., Kouchaki, E., Mirahmadi, M., Fatoye, F., 2015. STABILITY ANALYSIS IN PATIENTS WITH NEUROLOGICAL AND MUSCULOSKELETAL DISORDERS USING LINEAR AND NON-LINEAR APPROACHES. *J. Mech. Med. Biol.* 15. doi:10.1142/S0219519415300045
- Kato, T., Yamamoto, S., Miyoshi, T., Nakazawa, K., Masani, K., Nozaki, D., 2014. Anti-phase action between the angular accelerations of trunk and leg is reduced in the elderly. *Gait Posture* 40, 107–112. doi:10.1016/j.gaitpost.2014.03.006
- Kennel, M.B., Brown, R., Abarbanel, H.D.I., 1992. Determining embedding dimension for phase-space reconstruction using a geometrical construction. *Phys. Rev. A* 45, 3403–3411. doi:10.1103/PhysRevA.45.3403
- Kilby, M.C., Slobounov, S.M., Newell, K.M., 2016. Augmented feedback of COM and COP modulates the regulation of quiet human standing relative to the stability boundary. *Gait Posture* 47, 18–23. doi:10.1016/j.gaitpost.2016.03.021
- Kooij, H. van der, Jacobs, R., Koopman, B., Grootenboer, H., 1999. A multisensory integration model of human stance control. *Biol. Cybern.* 80, 299–308. doi:10.1007/s004220050527
- Lauk, M., Köster, B., Timmer, J., Guschlbauer, B., Deuschl, G., Lüking, C.H., 1999. Side-to-side correlation of muscle activity in physiological and pathological human tremors. *Clin. Neurophysiol. Off. J. Int. Fed. Clin. Neurophysiol.* 110, 1774–1783.
- Lee, H.K., Altmann, L.J.P., McFarland, N., Hass, C.J., 2016. The relationship between balance confidence and control in individuals with Parkinson's disease. *Parkinsonism Relat. Disord.* 26, 24–28. doi:10.1016/j.parkreldis.2016.02.015
- Loram, I.D., Lakie, M., 2002. Human balancing of an inverted pendulum: position control by small, ballistic-like, throw and catch movements. *J. Physiol.* 540, 1111–1124. doi:10.1113/jphysiol.2001.013077

- Madigan, M.L., Davidson, B.S., Nussbaum, M.A., 2006. Postural sway and joint kinematics during quiet standing are affected by lumbar extensor fatigue. *Hum. Mov. Sci.* 25, 788–799. doi:10.1016/j.humov.2006.04.004
- Mancini, M., Carlson-Kuhta, P., Zampieri, C., Nutt, J.G., Chiari, L., Horak, F.B., 2012a. Postural sway as a marker of progression in Parkinson’s disease: A pilot longitudinal study. *Gait Posture* 36, 471–476. doi:10.1016/j.gaitpost.2012.04.010
- Mancini, M., Rocchi, L., Horak, F.B., Chiari, L., 2008. Effects of Parkinson’s disease and levodopa on functional limits of stability. *Clin. Biomech. Bristol Avon* 23, 450–458. doi:10.1016/j.clinbiomech.2007.11.007
- Mancini, M., Salarian, A., Carlson-Kuhta, P., Zampieri, C., King, L., Chiari, L., Horak, F.B., 2012b. ISway: a sensitive, valid and reliable measure of postural control. *J. NeuroEngineering Rehabil. JNER* 9, 59–66. doi:10.1186/1743-0003-9-59
- Mani, H., Hsiao, S.-F., Takeda, K., Hasegawa, N., Tozuka, M., Tsuda, A., Ohashi, T., Suwahara, T., Ito, K., Asaka, T., 2015. Age-related changes in distance from center of mass to center of pressure during one-leg standing. *J. Mot. Behav.* 47, 282–290. doi:10.1080/00222895.2014.979756
- Masani, K., Vette, A.H., Kouzaki, M., Kanehisa, H., Fukunaga, T., Popovic, M.R., 2007. Larger center of pressure minus center of gravity in the elderly induces larger body acceleration during quiet standing. *Neurosci. Lett.* 422, 202–206. doi:10.1016/j.neulet.2007.06.019
- Maurer, C., Mergner, T., Peterka, R.J., 2004. Abnormal resonance behavior of the postural control loop in Parkinson’s disease. *Exp. Brain Res.* 157, 369–376. doi:10.1007/s00221-004-1852-y
- Maurer, C., Mergner, T., Xie, J., Faist, M., Pollak, P., Lücking, C.H., 2003. Effect of chronic bilateral subthalamic nucleus (STN) stimulation on postural control in Parkinson’s disease. *Brain* 126, 1146–1163. doi:10.1093/brain/awg100
- McCollum, G., Leen, T.K., 1989. Form and exploration of mechanical stability limits in erect stance. *J. Mot. Behav.* 21, 225–244.
- Mitchell, S.L., Collins, J.J., De Luca, C.J., Burrows, A., Lipsitz, L.A., 1995. Open-loop and closed-loop postural control mechanisms in Parkinson’s disease: increased mediolateral activity during quiet standing. *Neurosci. Lett.* 197, 133–136.
- Morrison, S., Kerr, G., Newell, K.M., Silburn, P.A., 2008. Differential time- and frequency-dependent structure of postural sway and finger tremor in Parkinson’s disease. *Neurosci. Lett.* 443, 123–128. doi:10.1016/j.neulet.2008.07.071
- Nashner, L.M., 1976. Adapting reflexes controlling the human posture. *Exp. Brain Res.* 26, 59–72.
- Ni, M., Signorile, J.F., Mooney, K., Balachandran, A., Potiaumpai, M., Luca, C., Moore, J.G., Kuenze, C.M., Eltoukhy, M., Perry, A.C., 2016. Comparative Effect of Power Training and High-Speed Yoga on Motor Function in Older Patients With Parkinson Disease. *Arch. Phys. Med. Rehabil.* 97, 345–354.e15. doi:10.1016/j.apmr.2015.10.095
- Nicholas Stergiou editor, 2016. *Nonlinear analysis for human movement variability*. Taylor & Francis, CRC Press, Boca Raton.
- Pahwa, R., Lyons, K.E., William C. Koller, 2003. *Handbook of Parkinson’s disease*, 3rd ed.. ed, Neurological disease and therapy ; v. 59. Dekker, New York.
- Pang, M.Y., Mak, M.K., 2012. Influence of contraction type, speed, and joint angle on ankle muscle weakness in Parkinson’s disease: implications for rehabilitation. *Arch. Phys. Med. Rehabil.* 93, 2352–2359. doi:10.1016/j.apmr.2012.06.004
- Park, J.-H., Youm, S., Jeon, Y., Park, S.-H., 2015. Development of a balance analysis system for early diagnosis of Parkinson’s disease. *Int. J. Ind. Ergon.* 48, 139–148. doi:10.1016/j.ergon.2015.05.005
- Park, S., Horak, F.B., Kuo, A.D., 2004. Postural feedback responses scale with biomechanical constraints in human standing. *Exp. Brain Res.* 154, 417–427. doi:10.1007/s00221-003-1674-3

- Pascolo, P., Barazza, F., Carniel, R., 2006. Considerations on the application of the chaos paradigm to describe the postural sway. *Chaos Solitons Fractals* 27, 1339–1346.  
doi:10.1016/j.chaos.2005.04.111
- Pascolo, P.B., Marini, A., Carniel, R., Barazza, F., 2005. Posture as a chaotic system and an application to the Parkinson's disease. *Chaos Solitons Fractals* 24, 1343–1346.  
doi:10.1016/j.chaos.2004.09.062
- Pelykh, O., Klein, A.-M., Bötzel, K., Kosutzka, Z., Ilmberger, J., 2015. Dynamics of postural control in Parkinson patients with and without symptoms of freezing of gait. *Gait Posture* 42, 246–250.  
doi:10.1016/j.gaitpost.2014.09.021
- Peng, C.-K., Buldyrev, S.V., Havlin, S., Simons, M., Stanley, H.E., Goldberger, A.L., 1994. Mosaic organization of DNA nucleotides. *Phys. Rev. E* 49, 1685–1689. doi:10.1103/PhysRevE.49.1685
- Peng, C.K., Havlin, S., Stanley, H.E., Goldberger, A.L., 1995. Quantification of scaling exponents and crossover phenomena in nonstationary heartbeat time series. *Chaos Woodbury N* 5, 82–87.  
doi:10.1063/1.166141
- Peterka, R.J., 2002. Sensorimotor Integration in Human Postural Control. *J. Neurophysiol.* 88, 1097–1118.
- Pincus, S.M., 1991. Approximate entropy as a measure of system complexity. *Proc. Natl. Acad. Sci. U. S. A.* 88, 2297–2301.
- Qutubuddin, A.A., Cifu, D.X., Armistead-Jehle, P., Carne, W., Mcguirk, T.E., Baron, M.S., 2007. A comparison of computerized dynamic posturography therapy to standard balance physical therapy in individuals with Parkinson's disease: A pilot study. *NeuroRehabilitation* 22, 261–265.
- Ramdani, S., Seigle, B., Lagarde, J., Bouchara, F., Bernard, P.L., 2009. On the use of sample entropy to analyze human postural sway data. *Med. Eng. Phys.* 31, 1023–1031.  
doi:10.1016/j.medengphy.2009.06.004
- Rektorova, I., Mikl, M., Barrett, J., Marecek, R., Rektor, I., Paus, T., 2012. Functional neuroanatomy of vocalization in patients with Parkinson's disease. *J. Neurol. Sci.* 313, 7–12.  
doi:10.1016/j.jns.2011.10.020
- Richman, J.S., Moorman, J.R., 2000. Physiological time-series analysis using approximate entropy and sample entropy. *Am. J. Physiol. - Heart Circ. Physiol.* 278, H2039–H2049.
- Rocchi, L., Chiari, L., Cappello, A., Horak, F.B., 2006. Identification of distinct characteristics of postural sway in Parkinson's disease: A feature selection procedure based on principal component analysis. *Neurosci. Lett.* 394, 140–145. doi:10.1016/j.neulet.2005.10.020
- Rosenstein, M.T., Collins, J.J., Luca, C.J.D., 1993. A practical method for calculating largest Lyapunov exponents from small data sets. *Phys. D* 65, 117–134.
- Rosker, J., Markovic, G., Sarabon, N., 2011. Effects of vertical center of mass redistribution on body sway parameters during quiet standing. *Gait Posture* 33, 452–456. doi:10.1016/j.gaitpost.2010.12.023
- Rusaw, D.F., Ramstrand, S., 2016. Validation of the Inverted Pendulum Model in standing for transtibial prosthesis users. *Clin. Biomech.* 31, 100–106. doi:10.1016/j.clinbiomech.2015.09.014
- Salat, D., Tolosa, E., 2013. Levodopa in the treatment of Parkinson's disease: current status and new developments. *J. Park. Dis.* 3, 255–269. doi:10.3233/JPD-130186
- Saripalle, S.K., Paiva, G.C., Cliett III, T.C., Derakhshani, R.R., King, G.W., Lovelace, C.T., 2014. Classification of body movements based on posturographic data. *Hum. Mov. Sci.* 33, 238–250.  
doi:10.1016/j.humov.2013.09.004
- Sasagawa, S., Ushiyama, J., Kouzaki, M., Kanehisa, H., 2009. Effect of the hip motion on the body kinematics in the sagittal plane during human quiet standing. *Neurosci. Lett.* 450, 27–31.  
doi:10.1016/j.neulet.2008.11.027

- Schlenstedt, C., Muthuraman, M., Witt, K., Weisser, B., Fasano, A., Deuschl, G., 2016. Postural control and freezing of gait in Parkinson's disease. *Parkinsonism Relat. Disord.* 24, 107–112. doi:10.1016/j.parkreldis.2015.12.011
- Schmit, J.M., Riley, M.A., Dalvi, A., Sahay, A., Shear, P.K., Shockley, K.D., Pun, R.Y.K., 2006. Deterministic center of pressure patterns characterize postural instability in Parkinson's disease. *Exp. Brain Res.* 168, 357–367. doi:10.1007/s00221-005-0094-y
- Schoneburg, B., Mancini, M., Horak, F., Nutt, J.G., 2013. Framework for Understanding Balance Dysfunction in Parkinson's Disease. *Mov. Disord. Off. J. Mov. Disord. Soc.* 28, 1474–1482. doi:10.1002/mds.25613
- Sciadas, R., Dalton, C., Nantel, J., 2016. Effort to reduce postural sway affects both cognitive and motor performances in individuals with Parkinson's disease. *Hum. Mov. Sci.* 47, 135–140. doi:10.1016/j.humov.2016.03.003
- Scott, D.W., 1979. On Optimal and Data-Based Histograms. *Biometrika* 66, 605–610. doi:10.2307/2335182
- Smania, N., Corato, E., Tinazzi, M., Stanzani, C., Fiaschi, A., Girardi, P., Gandolfi, M., 2010. Effect of Balance Training on Postural Instability in Patients With Idiopathic Parkinson's Disease. *Neurorehabil. Neural Repair* 24, 826–834. doi:10.1177/1545968310376057
- Stergiou, N., Decker, L.M., 2011. Human movement variability, nonlinear dynamics, and pathology: is there a connection? *Hum. Mov. Sci.* 30, 869–888. doi:10.1016/j.humov.2011.06.002
- Steven H Strogatz, author, 2015. *Nonlinear dynamics and chaos: with applications to physics, biology, chemistry, and engineering*, Second edition.. ed. Westview Press, a member of the Perseus Books Group, Boulder, CO.
- Stevens, J.A., Corso, P.S., Finkelstein, E.A., Miller, T.R., 2006. The costs of fatal and non-fatal falls among older adults. *Inj. Prev. J. Int. Soc. Child Adolesc. Inj. Prev.* 12, 290–295. doi:10.1136/ip.2005.011015
- Stylianou, A.P., McVey, M.A., Lyons, K.E., Pahwa, R., Luchies, C.W., 2011. Postural Sway in Patients with Mild to Moderate Parkinson's Disease. *Int. J. Neurosci.* 121, 614–621. doi:10.3109/00207454.2011.602807
- Teresa Blázquez, M., Anguiano, M., de Saavedra, F.A., Lallena, A.M., Carpena, P., 2009. Study of the human postural control system during quiet standing using detrended fluctuation analysis. *Phys. Stat. Mech. Its Appl.* 388, 1857–1866. doi:10.1016/j.physa.2009.01.001
- Tokuno, C.D., Carpenter, M.G., Thorstensson, A., Cresswell, A.G., 2006. The influence of natural body sway on neuromuscular responses to an unpredictable surface translation. *Exp. Brain Res.* 174, 19–28. doi:10.1007/s00221-006-0414-x
- Toosizadeh, N., Lei, H., Schwenk, M., Sherman, S.J., Sternberg, E., Mohler, J., Najafi, B., 2015. Does integrative medicine enhance balance in aging adults? Proof of concept for the benefit of electroacupuncture therapy in Parkinson's disease. *Gerontology* 61, 3–14. doi:10.1159/000363442
- Vaillancourt, D.E., Newell, K.M., 2002. Changing complexity in human behavior and physiology through aging and disease. *Neurobiol. Aging* 23, 1–11.
- Vette, A.H., Masani, K., Nakazawa, K., Popovic, M.R., 2010. Neural-Mechanical Feedback Control Scheme Generates Physiological Ankle Torque Fluctuation During Quiet Stance. *IEEE Trans. Neural Syst. Rehabil. Eng.* 18, 86–95. doi:10.1109/TNSRE.2009.2037891
- Visser, J.E., Carpenter, M.G., van der Kooij, H., Bloem, B.R., 2008. The clinical utility of posturography. *Clin. Neurophysiol.* 119, 2424–2436. doi:10.1016/j.clinph.2008.07.220
- Wang, Z., Ko, J.H., Challis, J.H., Newell, K.M., 2014. The Degrees of Freedom Problem in Human Standing Posture: Collective and Component Dynamics: e85414. *PLoS One San Franc.* 9, e85414. doi:http://dx.doi.org/10.1371/journal.pone.0085414

- Whitney, S.L., Roche, J.L., Marchetti, G.F., Lin, C.-C., Steed, D.P., Furman, G.R., Musolino, M.C., Redfern, M.S., 2011. A comparison of accelerometry and center of pressure measures during computerized dynamic posturography: A measure of balance. *Gait Posture* 33, 594–599. doi:10.1016/j.gaitpost.2011.01.015
- Winter, D., 1995. Human balance and posture control during standing and walking. *Gait Posture* 3, 193–214. doi:10.1016/0966-6362(96)82849-9
- Winter, D.A., 1990. *Biomechanics and motor control of human movement*, 2nd ed.. ed. Wiley, New York.
- Winter, D.A., Prince, F., Patla, A., 1997. Validity of the inverted pendulum model of balance in quiet standing. *Gait Posture* 5, 153–154. doi:10.1016/S0966-6362(97)83376-0
- Winters, J.M., Stark, L., 1985. Analysis of fundamental human movement patterns through the use of in-depth antagonistic muscle models. *IEEE Trans. Biomed. Eng.* 32, 826–839. doi:10.1109/TBME.1985.325498
- Wolf, A., Swift, J.B., Swinney, H.L., Vastano, J.A., 1985. Determining Lyapunov exponents from a time series. *Phys. Nonlinear Phenom.* 16, 285–317. doi:10.1016/0167-2789(85)90011-9
- Wood, B.H., Bilclough, J.A., Bowron, A., Walker, R.W., 2002. Incidence and prediction of falls in Parkinson's disease: a prospective multidisciplinary study. *J. Neurol. Neurosurg. Psychiatry* 72, 721–725.
- World Health Organization, 2008. *The world health report 2008 primary health care: now more than ever*. World Health Organization, Geneva.
- Yamamoto, A., Sasagawa, S., Oba, N., Nakazawa, K., 2015. Behavioral effect of knee joint motion on body's center of mass during human quiet standing. *Gait Posture* 41, 291–294. doi:10.1016/j.gaitpost.2014.08.016
- Yentes, J.M., Hunt, N., Schmid, K.K., Kaipust, J.P., McGrath, D., Stergiou, N., 2013. The appropriate use of approximate entropy and sample entropy with short data sets. *Ann. Biomed. Eng.* 41, 349–365. doi:10.1007/s10439-012-0668-3
- Yu, E., Abe, M., Masani, K., Kawashima, N., Eto, F., Haga, N., Nakazawa, K., 2008. Evaluation of postural control in quiet standing using center of mass acceleration: comparison among the young, the elderly, and people with stroke. *Arch. Phys. Med. Rehabil.* 89, 1133–1139. doi:10.1016/j.apmr.2007.10.047

## Chapter Three: Single Inverted Pendulum Validation for Healthy and Parkinson's Disease Subjects for Bi-Pedal Quiet Standing

### 1 Abstract

**Background:** Assessment of postural instability (PI) in people with Parkinson's disease (PD) is a significant unmet need. Analyzing the center of pressure (COP) time series calculated using force plate measures during bi-pedal quiet standing task can be done by utilizing a mechanical model that represents the human biomechanical system. The single inverted pendulum (SIP) is the most common mechanical model used to analyze the quiet standing task; however, recently this modeling approach has received criticism. In this study, we validated the SIP model for healthy older adults and people with mild (H&Y 2) and moderate (H&Y 3) PD, by comparing the linear and nonlinear measures extracted from the COP time series obtained experimentally ( $COP_{exp}$ ), and the COP time series obtained from the SIP model ( $COP_{SIP}$ ). In addition, it was investigated if assuming zero as initial conditions (ICs) on the SIP differential equation (DEQ), and linearization around its vertical position had effect on the  $COP_{SIP}$ 's ability to represent the  $COP_{exp}$ . Finally, it was also investigated if it is appropriate to assume that as PD progresses, people with PD sway more like a SIP due to increment of stiffness at their ankles.

**Methods:** Foot-floor reactions were obtained from two different quiet standing studies: 1) Healthy Controls (n = 12) vs. PD Mild (n = 12); 2) Healthy Controls (n = 9) vs. PD moderate (n = 10), for eyes open (EO) and eyes closed (EC) conditions. In the Anterior-Posterior (AP) direction, the  $COP_{exp}$  time series was calculated, as well as the  $COP_{SIP}$  using anthropometric equations and the SIP DEQ in its linear and nonlinear form with zero, or optimized ICs. Using time series similarity measures (Goodness of Fit, Sum Squared Errors, Mutual Information and Cross Correlation), it was determined how similar was the  $COP_{SIP}$  to the  $COP_{exp}$ . Finally, it was determined for each group of subjects if the errors between the  $COP_{SIP}$  and  $COP_{exp}$  based on the extracted linear and nonlinear measure were within a  $\pm 5\%$ ,  $\pm 10\%$ ,  $\pm 15\%$ , and  $\pm 20\%$ .

**Results:** When the  $COP_{SIP}$  is calculated using zero as ICs in the SIP DEQ, instead of optimized ICs, a significant error in magnitude and shape of curve (10% to 35%) is added to the time series. In addition, its ability to replicate linear and nonlinear measures is reduced when zero as ICs are used, instead of optimized ICs. On the other hand, when the  $COP_{SIP}$  is calculated using the Linear SIP DEQ does not significantly affect the accuracy of the  $COP_{SIP}$ ; i.e. at the most 3% in shape of curve is lost when the Linear DEQ is used, instead of the Nonlinear DEQ. Finally, the SIP is a valid model for unperturbed sway studies on healthy older adults and mild and moderate PD patients, when an error of 30% or less is

allowed in certain group of linear and nonlinear measures. However, the SIP model losses accuracy as PD progresses.

**Conclusions:** Assuming zero as ICs in the SIP model for unperturbed sway studies, significantly decreases the accuracy of the model. However, linearizing the DEQ around its vertical location does not. Finally, the SIP is valid model for healthy old adults and people with PD (H&Y 2 and 3) when its COP is calculated using the linear DEQ, and ICs that are determined based on the Cross Correlation between the  $COP_{SIP}$  and  $COP_{exp}$ . The validity of the SIP is contingent for each group of subjects if an error of 30% is accepted for certain groups of linear and nonlinear measures. Finally, as PD progresses the SIP losses accuracy, suggesting the use of a double inverted pendulum to represent the sway of people with moderate or more severe PD.

## 2 Introduction

Parkinson's Disease (PD) is a neurological disease that affects around 1% of the population in industrialized countries (de Lau and Breteler, 2006), and it is predicted to become the second most common cause of death by 2040 (World Health Organization, 2008). PD has negative physiological effects such as tremor, bradykinesia, and rigidity. It has been determined that as PD progresses, the stiffness at the ankles increases (Carpenter et al., 2004; Horak et al., 1996). But in terms of the impact on the activities of daily living, postural instability (PI) is the most significant and common effect and is directly related to the problem of increased fall risk (Smania et al., 2010). Due to the increased incidence of falls and fall risk, PI assessment on people with PD has become a high priority since falls lead to lower quality of life, injury, and even death (Bloem et al., 2004). PI in PD patients has been assessed using standardized clinical tests such as the United Parkinson's Disease Rating Scale (UPDRS), Schwab & England Scale, and the Hoehn and Yahr (H&Y) (Pahwa et al., 2003), or through human performance tests such as the analysis of postural sway during bi-pedal quiet stance. The postural sway task consists of the participant standing relaxed on one or two force plates, which measure the foot-floor reaction forces and moments over a period of time. The foot-floor reactions are used to calculate the location of center of pressure (COP) time series, which is the location in space of the whole body resultant force as a function of time (Winter, 1990). Previous studies that have investigated the effect of PD on the COP time series can be divided in posturographic analysis and mechanical modeling.

Posturographic analysis of the COP time series in PD studies has been done by extracting characteristics of the time series using both linear and nonlinear measures. Linear measures, which focus on the amount or the magnitude of the signal, consist of the mean, standard deviation (SD), root mean square (RMS), frequency, or areas (among others) of the COP time series and/or its respective derivatives with respect to time (Błaszczuk et al., 2007; Gervasoni et al., 2015; Mancini et al., 2012; Rocchi et al., 2006). Nonlinear measures, which focus on the temporal structure or organization of the signal, consist of detrended fluctuation analysis (DFA) (Mitchell et al., 1995; Stylianou et al., 2011), approximated entropy (AE) (Karimi et al., 2015; Park et al., 2015), sample entropy (SE) (Pelykh et al., 2015; Schlenstedt et al., 2016), or the largest Lyapunov exponent (LLE) (Pascolo et al., 2006, 2005) (among others) of the COP time series. Both linear and nonlinear methods have produced successful results regarding the goal of assessing PI in people with PD, and have gained acceptance in the literature over the last couple of decades.

The modeling strategy in PD studies consists of developing a dynamical model, based on the appropriate physics, mathematics, and control principles, that represents the physical system and can be used to analyze and predict the system dynamics (Boonstra et al., 2013; Chagdes et al., 2016a; Maurer et al., 2004; Park et al., 2004). Authors have proposed multiple models for bi-pedal quiet stance in humans, which can be categorized by the number of included rigid bodies (single, double, triple, etc.) and by the type of controller (linear, nonlinear, stochastic, intermittent, etc.) included in the model (Asai et al., 2009; Bottaro et al., 2008; Chagdes et al., 2016b; Kooij et al., 1999; Loram and Lakie, 2002; Peterka, 2002; Suzuki et al., 2012; Vette et al., 2010). A common approach for modeling postural sway is to represent the human body as a single inverted pendulum (SIP) (Crétual, 2015). Although a widely utilized model, the SIP approach has received some criticism with limitations observed (Günther et al., 2009; Sasagawa et al., 2009; Yamamoto et al., 2015). The criticism often results from observed motion in other articulations besides the ankles during the quiet standing task. In response to the criticism of the SIP approach, several studies have attempted to validate the SIP for bi-pedal postural sway (Gage et al., 2004; Masani et al., 2007; Winter et al., 1997; Yu et al., 2008). Also, other studies (Boyas et al., 2013; Costello et al., 2012; Federolf et al., 2013) on bi-pedal quiet stance inadvertently produced results that added additional support to the validation of the SIP model approach for standing quietly. Boyas et al tested the ankle strategy dominance, before and after ankle muscle fatigue was induced on 13 young healthy subjects (Age = 21.4 ± 4.6), and found that the ankle strategy (SIP) was the dominant postural strategy both before and after fatigue. Costello et al analyzed how increasing weight and inertia on 16 young healthy subjects (Age = 22.1 ± 1.7) affected their sway and found that the magnitude of the sway in their subjects changed in accordance to the SIP model. Federolf et al using PCA, quantified how much of the sway of 29 young adults (Age = 23.9 ± 3) can be explained by the motion of the ankles and found that 71.7% of the sway with eyes open in the AP direction can be explained by the motion of the ankles.

The original method to validate the SIP was proposed in (Gage et al., 2004) using 11 healthy young subjects (Age = 26.5 ± 3.9), which consisted on analyzing  $\frac{d^2}{dt^2} COM \propto COP - COM$  (where COM is the estimation of the total body center of mass location based on body segment kinematic measures using 3D cameras, and COP is the center of pressure location calculated based on force plate measurements) which is a fundamental relationship on the SIP model, as well as analyzing the relationship between the amount of motion of the body segments (RMS) and their height with respect to the ankles  $RMS(COM_{body\ part}) \propto Height_{body\ part/ankle}$ . Gage et al obtained very high linear correlations for both observations  $R_{AP} = -0.954 \pm 0.020$ ,  $R_{ML} = -0.840 \pm 0.054$ , and  $R^2 > 0.9$  respectively, allowing the conclusion

that, although the SIP model cannot completely replicate the human body dynamics during sway, it can be mostly described by the SIP. To support Gage et al conclusions, the first conclusion was supported by Yu et al using 12 post-stroke and 22 healthy controls ( $R > 0.9$ , Age =  $66.5 \pm 4.9$ ) (Yu et al., 2008), while the second conclusion was supported by Winter et al using 26 healthy subjects ( $R^2 > 0.8$ , Mean Age = 26). However, the method used by Gage et al is not the only accepted method to validate the SIP model. For example, Masani et al (Masani et al., 2007) compared the  $\frac{d^2}{dt^2} COM$  term calculated using two different methods: 1) body segment kinematics measured using 3D cameras and 2) force plates. Masani et al results were  $C\ddot{O}M_{FP} = -0.21 + 1.14 \cdot C\ddot{O}M_{3D}$  ( $R = 0.973$ ) for 11 healthy young adults (Mean Age = 29), and  $C\ddot{O}M_{FP} = -0.04 + 1.01 \cdot C\ddot{O}M_{3D}$  ( $R = 0.976$ ) for the 15 healthy old adults (Mean Age = 72). Since a perfect validation is represented with an intercept equal to 0 and slope equal to 1, Masani et al concluded that the SIP can represent the majority of the sway in healthy subjects.

Validation of the SIP during sway studies cannot be generalized. It is not only task specific (e.g. perturbed, eyes open/closed, etc.), but also population specific (e.g. age, disease, etc.). For example, in the presence of a balance perturbation during bi-pedal quiet stance, the SIP has been shown not to be valid (Horak and Nashner, 1986; McCollum and Leen, 1989). In addition, the SIP model for bi-pedal quiet standing has been validated for certain conditions such as prosthesis users (Rusaw and Ramstrand, 2016), through the method proposed by Gage et al (Gage et al., 2004) and other calculations, and partially validated for post-stroke subjects (Yu et al., 2008). However, the SIP has not been validated for participants who have been diagnosed with PD, or as PD progresses.

The current use of the SIP in mechanical modeling studies differ from author to author. For example, the differential equation that relates the angular position of the pendulum and the torque applied at the ankles is normally linearized ( $\sin \theta \cong \theta$ ) around the vertical orientation of the pendulum (Asai et al., 2009; Bottaro et al., 2008; Kooij et al., 1999; Loram and Lakie, 2002; Maurer et al., 2004, p. 2; Peterka, 2002; Vette et al., 2010); however, sometimes it is not linearized (Chagdes et al., 2016a, 2016b). The advantage of using the nonlinear differential equation is the improved accuracy of the model when large sways occur; however, authors who use the linear differential equation claim that the magnitude of unperturbed sway of humans is small enough to be represented by the linear differential equation. Regardless of the chosen differential equation (linear vs. nonlinear), most of the mechanical modeling studies use initial conditions (ICs) equal to zero for simplicity (Initial angle  $\theta_0 = 0$ , and initial angular velocity  $\dot{\theta}_0 = 0$ ). However, it has been observed that the initial position of the body changes

significantly the sway in humans (Tokuno et al., 2006). A sensitivity study of linear vs. nonlinear and ICs equal to zero. vs non-equal to zero have not been done for the SIP.

The purpose of the current study is to validate the SIP model using a novel approach. All validations listed above have used the strategy of comparing the body COM obtained through kinematic and kinetic data. However, the SIP has not been validated using the COP that it creates when its dynamic and mathematical equations are used in all forms (linear/nonlinear and ICs equal to zero/non-zero). Model validation is done based on the bi-pedal quiet standing in the Anterior-Posterior (AP) direction, using two visual feedback conditions (eyes open (EO) and closed (EC)) and three participant groups (healthy subjects (HS), mild PD (PD-Mi), and moderate PD (PD-Mo)). The parameters used for validation included both linear and nonlinear measures extracted from two COP time series: 1) obtained from the force plates directly ( $COP_{exp}$ ) and 2) predicted from the SIP inverse dynamics model ( $COP_{SIP}$ ). It is hypothesized: (1) The SIP model accuracy is sensitive to whether or not the ICs are set equal to zero or appropriate values are derived (zero vs optimized ICs); (2) The SIP model accuracy is not sensitive to linearizing the differential equation of motion (linear vs nonlinear); (3) The SIP model can represent at least 70% of the sway in HS in both EO and EC conditions; and (4) As PD progresses the human body behaves more like a SIP in the AP direction due to increased rigidity at the ankles associated with PD progression.

### 3 Methods

#### 3.1 Participants

Subjects for this study were obtained from two separate PD sway studies: 1) a Healthy Control vs. Mild PD study (PD-Mi-Study) and 2) a Healthy Control vs. PD Moderate study (PD-Mo-Study). The studies were conducted in the Human Performance Laboratory at the University of Kansas Medical Center and the Biodynamics Laboratory at The University of Kansas, respectively (Barnds, 2015; Stylianou et al., 2011). The PD-Mi-Study consisted on 12 HS (7 female, Age =  $66.4 \pm 9.2$ , Height =  $165.8 \pm 9.6$  cm, Weight =  $68.9 \pm 9.5$  Kg), and 12 PD-Mi (H&Y 2, 6 female, Age =  $61.5 \pm 8.0$ , Height =  $167.4 \pm 7.0$  cm, Weight =  $74.4 \pm 11.3$  Kg); while the PD-Mo-Study consisted on 9 HS (2 female, Age =  $67.7 \pm 5.0$ , Height =  $174.5 \pm 5.4$ , Weight =  $73.7 \pm 11.8$  Kg), and 10 PD-Mo (H&Y 3, 1 female, Age =  $67.4 \pm 3.4$ , Height =  $175.0 \pm 8.7$  cm, Weight =  $92 \pm 12.6$  Kg). All individuals gave written consent as approved by The University's Institutional Review Board. In addition, PD-Mi had no postural deficits, while PD-Mo subjects were all diagnosed with

PI. However, all subjects could stand and walk without assistance. Finally, HS had no significant cognitive, musculoskeletal or neurological issues. Details on the subjects can be found in Table 3Table 6.

## 3.2 Experimental Protocol

Details on the experimental protocols for the postural sway tests during quiet standing can be found in (Barnds, 2015; Stylianou et al., 2011); however, a brief description of the protocols is provided here. The participant was instructed to stand on two force plates (one under each foot) using standardized shoes, with arms relaxed at their sides, with feet at a self-selected and comfortable width, and with their feet's medial malleolus aligned with the coordinate system of the force plates. The selected position for their feet was recorded, marked and used for all trials. Three 30-second trials were collected using two conditions: EO and EC, with 1-minute break between trials. The order of the trials was randomized for each participant, and for the EO trials, participants were asked to look at a stationary image placed directly in front of them. Finally, participants with PD were tested during the "on period" of their usual medication, and the time between the test and their last intake of medication was approximately 1 hour. The 6 trials for each participant were collected in a single session, and before each session, multiple measures of the participant's body were taken. The measures used for the current study included: body mass ( $M$ ), body height ( $H$ ), length of the thigh ( $l_{thigh}$ ), length of the calf ( $l_{calf}$ ), length of the foot ( $l_{foot}$ ), and height from the ground to the ankle ( $h_{ank}$ ).

The kinetic data (foot-floor force and moment reactions) collected from the force plates (AMTI, Watertown, MA, USA) were recorded at 1080 Hz and 1000 Hz for the PD-Mi-Study and PD-Mo-Study, respectively using a 16-bit A/D acquisition system and LabVIEW (NI, Austin, TX, USA). Finally, all data and statistical analyses were done using MATLAB (Mathworks, Natick, MA, USA).

## 3.3 Data Analysis

### 3.3.1 $COP_{exp}$ Calculation

The center of pressure location based on experimental measures ( $COP_{exp}$ ) was calculated based on the raw measured foot-floor kinetic data from the force plates using standardized equations (Winter, 1990) in the AP direction.

$$COP_{AP} = -\frac{M_y + F_x \cdot d_z}{F_z} \quad (1)$$

The  $COP_{exp}$  was then downsampled to 40 Hz, which falls within the range of frequencies previously used in published sway studies (10 Hz – 100 Hz), and has been proven to be an adequate frequency for nonlinear measures in sway studies (Delignières et al., 2011; Ramdani et al., 2009).

### 3.3.2 $COP_{SIP}$ Calculation

The center of pressure location based on the SIP model results ( $COP_{SIP}$ ) was calculated based on the SIP model, which used anthropometric data and a differential equation (DEQ) as the equation of motion. The human body (i.e. without feet) was modeled as a single rigid body with a fixed revolute joint at the ankles (SIP) using the following anthropometric equations (Winter, 1990):

$$m_{SIP} = 0.971M \quad (2)$$

$$h_{SIP} = \frac{m_{calf}COM_{calf} + m_{thigh}(l_{calf} + COM_{thigh}) + m_{HAT}(l_{calf} + l_{thigh} + COM_{HAT})}{m_{SIP}} \quad (3)$$

$$J_{SIP} = J_{calfs} + J_{thighs} + J_{HAT} \quad (4)$$

where  $m_{SIP}$  is the mass of the human body without feet when simulated as a SIP,  $h_{SIP}$  is the distance from the ankles to the COM of the  $m_{SIP}$ , and  $J_{SIP}$  is the mass moment of inertia of the  $m_{SIP}$  with respect to the ankles. The equations to derive the constants of equations (2) through (4) are provided in Table 7.

#### 3.3.2.1 Linear and Nonlinear SIP Model

A kinetic study was performed to obtain a DEQ that determines the angular position, velocity and acceleration of the SIP in the AP direction. Using the calculated anthropometric values for the SIP, and assuming that the feet are rigid bodies and stationary, the DEQ for SIP in the AP direction is (Refer to Figure 2 and Appendix A: Equations – Section 1.1):

$$\ddot{\theta} = \frac{1}{J_{SIP}} (F_z COP_{exp} - m_{SIP}gh_{SIP} \sin \theta - m_{feet}gCOM_{feet} - F_x h_{ank}) \quad (5)$$

which uses the  $COP_{exp}$  and foot-floor reactions after being downsampled, making  $COP_{exp}$  and  $COP_{SIP}$  time series of equal length and sampling time. Equation (5) is a second order nonlinear differential equation (N-DEQ), which was used for the nonlinear SIP model. This N-DEQ can be linearized using the small angle assumption, i.e. it is assumed that  $\sin \theta \cong \theta$ . The resultant linearized equation is:

$$\ddot{\theta} = \frac{1}{J_{SIP}} (F_z COP_{exp} - m_{SIP}gh_{SIP}\theta - m_{feet}gCOM_{feet} - F_x h_{ank}) \quad (6)$$

Equation (6) is a second order linear DEQ (L-DEQ), which was used for the linear SIP model.

### 3.3.2.2 $COP_{SIP}$ with Zero and Optimized ICs

To calculate the  $COP_{SIP}$  (Equation (7)), Refer to Figure 3 and Appendix A: Equations – Section 1.2), the N-DEQ (5) and L-DEQ (6) had to be solved first since the angular position, velocity, and acceleration of the SIP are required.

$$COP_{SIP} = \frac{1}{GRF_z} (T + m_{feet} g COM_{feet} + GRF_x h_{ank}) \quad (7)$$

To solve the N-DEQ (5) and L-DEQ (6), the ICs  $\theta_0$  and  $\dot{\theta}_0$  are required. Two different methods were used to select the ICs: 1) zero as ICs ( $\theta_0 = 0, \dot{\theta}_0 = 0$ ), and 2) optimized ICs. The method used to select the optimized ICs involved comparing the time series  $COP_{SIP}$  and  $COP_{exp}$ . The method included maximizing the Goodness of Fit (GOF, Equation (8)), Mutual Information (MI, Equation (10)), and Cross Correlation (CrossCorr, Equation (11)), or minimizing the Sum of Squared Errors (SSE, Equation (9)) between the  $COP_{SIP}$  and  $COP_{exp}$ , using the following equations.

$$GOF [\%] = 100 \cdot \left( 1 - \frac{1}{N} \sum_{i=1}^N \left| \frac{COP_{exp_i} - COP_{SIP_i}}{COP_{exp_i}} \right| \right) \quad (8)$$

$$SSE [m^2] = \sum_{i=1}^N (COP_{exp_i} - COP_{SIP_i})^2 \quad (9)$$

$$MI [ ] = \frac{\sum_{i=1}^N P(COP_{exp_i}, COP_{SIP_i}) \log_2 \frac{P(COP_{exp_i}, COP_{SIP_i})}{P(COP_{exp_i})P(COP_{SIP_i})}}{\sum_{i=1}^N P(COP_{exp_i}, COP_{exp_i}) \log_2 \frac{P(COP_{exp_i}, COP_{exp_i})}{P(COP_{exp_i})P(COP_{exp_i})}} \quad (10)$$

$$CrossCorr [ ] = (N - 1) \frac{\sum_{i=1}^N (COP_{SIP_i} - \overline{COP_{SIP}})(COP_{exp_i} - \overline{COP_{exp}})}{\sum_{i=1}^N (COP_{SIP_i} - \overline{COP_{SIP}})^2 \cdot \sum_{i=1}^N (COP_{exp_i} - \overline{COP_{exp}})^2} \quad (11)$$

The process used to select the optimized ICs consisted on using all the possible combinations in  $-0.5 \text{ rad} \leq \theta_0 \leq 0.5 \text{ rad} \cap -1 \frac{\text{rad}}{\text{s}} \leq \dot{\theta}_0 \leq 1 \frac{\text{rad}}{\text{s}}$  using  $\Delta\theta_0 = 0.01 \text{ rad} \cap \Delta\dot{\theta}_0 = 0.02 \frac{\text{rad}}{\text{s}}$  as ICs to solve equations (5) and (6), calculate the  $COP_{SIP}$  using equation (7), and then calculate the different similarity measures between  $COP_{SIP}$  and  $COP_{exp}$  (Equations (8) to (11)). Each set of ICs that maximized GOF, MI and CrossCorr, or minimized SSE was recorded as a set of optimized ICs, i.e. 8 sets of optimized ICs were calculated (4 based on GOF, SSE, MI and CrossCorr for equations (5) and (6)) per trial on a subject. An example of the outcome of this optimization process using all similarity measures and equations (5) and (6) is found in Figure 4.

### 3.3.3 COP<sub>SIP</sub> Sensitivity to ICs and Linearization of DEQ Determination

To investigate how sensitive the COP<sub>SIP</sub> was to the ICs and linearization of the DEQ of motion for all trials in each group of subjects, the similarity measures (GOF, SSE, MI and CrossCorr) between COP<sub>exp</sub> and COP<sub>SIP</sub> were calculated when the COP<sub>SIP</sub> was calculated using zero and optimized ICs, as well as the N-DEQ (5) and L-DEQ (6).

For the sensitivity to ICs, the difference of each similarity measure in each subject when the COP<sub>SIP</sub> was calculated using optimized and zero ICs was determined. Finally, the differences were separated between the conditions EO and EC, and the average between all trials in each group of subjects per condition was calculated. In other words, for all trials the difference  $\text{Similarity Measure}_{\text{ICs: Optimized}} - \text{Similarity Measure}_{\text{ICs: Zero}}$  was performed for all permutations of HS<sub>PD-Mi-Study</sub>/PD-Mi/HS<sub>PD-Mo-Study</sub>/PD-Mo  $\cap$  EO/EC  $\cap$  N-DEQ/L-DEQ, and the average of all trials per condition in each group of subjects was calculated.

For the sensitivity to the linearization of the DEQ of motion, the difference of each similarity measure in each subject when the COP<sub>SIP</sub> was calculated using the N-DEQ (5) and L-DEQ (6) was determined. Finally, the differences were separated between the conditions EO and EC, and the average between all trials in each group of subjects per condition was calculated. In other words, for all trials the difference  $\text{Similarity Measure}_{\text{N-DEQ}} - \text{Similarity Measure}_{\text{L-DEQ}}$  was performed for all permutations of HS<sub>PD-Mi-Study</sub>/PD-Mi/HS<sub>PD-Mo-Study</sub>/PD-Mo  $\cap$  EO/EC  $\cap$  Optimized ICs/Zero ICs, and the average of all trials per condition in each group of subjects was calculated.

### 3.3.4 COP<sub>SIP</sub> Accuracy Determination and Further ICs Sensitivity Analysis

Up to this point there were 8 ways to calculate the COP<sub>SIP</sub> using optimized ICs (optimization based on GOF, SSE, MI, or CrossCorr using equation (5) or (6)), and 2 ways to calculate the COP<sub>SIP</sub> using zero as ICs (using equation (5) or (6)). Based on the results regarding the sensitivity of COP<sub>SIP</sub> to the linearization of the DEQ of motion (Section 4.2), it was decided to not use the N-DEQ (5) further in this study. The differences observed in the COP<sub>SIP</sub> when using equations (5) and (6) were in average less than 2% when optimized ICs were used, and less than 3% when zero ICs were used. In addition, to decide the method that selects the final optimized ICs, a comparison between optimized ICs based on each similarity measure using optimized ICs was performed. Details on this analysis are in Appendix C: Selecting the Final Optimized ICs. The final method used to select the optimized ICs was to calculate the CrossCorr between COP<sub>SIP</sub> and COP<sub>exp</sub>, with the COP<sub>SIP</sub> based on the L-DEQ (6) and multiple sets of ICs, and finding the ICs that maximized this similarity measure. Therefore, from this point forward in the study, the

$COP_{SIP}$  calculated with optimized ICs ( $COP_{SIP(CC)}$ ) was determined using the L-DEQ (6), and ICs that are found through the optimization of CrossCorr; while the  $COP_{SIP}$  calculated with zero ICs ( $COP_{SIP(0,0)}$ ) was determined using the L-DEQ (6), and ICs that are equal to zero.

An example of how the  $COP_{exp}$ ,  $COP_{SIP(CC)}$ , and  $COP_{SIP(0,0)}$  compared visually to each other is demonstrated in Figure 9. However, to investigate truly how well the  $COP_{SIP}$  time series ( $COP_{SIP(0,0)}$  and  $COP_{SIP(CC)}$ ) represented the  $COP_{exp}$  time series, two methods were used: 1) Linear analysis parameter extraction, and 2) nonlinear analysis parameter extraction. Within each measure extracted in subject and trial, two absolute percent errors were calculated. ERROR 1: based on the difference between that measure derived from the  $COP_{exp}$  and  $COP_{SIP(CC)}$  time series. ERROR 2: based on the difference between that measure derived from the  $COP_{exp}$  and  $COP_{SIP(0,0)}$  time series. In both errors for each measure, an error of zero suggested that for that measure, no difference existed between  $COP_{exp}$  and  $COP_{SIP(CC)}$  or  $COP_{SIP(0,0)}$ . For both methods, the EO and EC trials were organized from best-to-worst fit for each subject based on the CrossCorr between  $COP_{exp}$  and  $COP_{SIP(CC)}$  ( $R_1$ ,  $R_2$ ,  $R_3$ ).

#### 3.3.4.1 Linear Measures Analysis

Linear measures were extracted from the  $COP_{exp}$ ,  $COP_{SIP(CC)}$  and  $COP_{SIP(0,0)}$  time series. The parameters extracted from each COP time series included: mean, SD, RMS, 95% power spectrum frequency ( $f_{95\%}$ ), median frequency ( $f_{med}$ ), curve length, range, and maximum magnitude ( $|Max|$ ) (Doná et al., 2016; Mancini et al., 2012; Ni et al., 2016; Park et al., 2015; Schlenstedt et al., 2016). These linear measures were calculated on the unfiltered COP time series ( $COP_{Pos}$ ), and in the first and second derivatives of the  $COP_{Pos}$  ( $COP_{Vel}$  and  $COP_{Acc}$ ). The  $COP_{Pos}$  was filtered using a second order low pass Butterworth filter with a cutoff frequency of 5 Hz prior to the numerical differentiation. For each linear measure extracted in subject and trial, ERROR 1 and 2 were calculated. Also, for each subject, EO and EC trials were organized using  $R_1$ ,  $R_2$ , and  $R_3$ . Next, the averages of both error types on each linear measure and trial were calculated between the subjects of each group. In other words, the means of errors for each linear measure were determined for trial numbers ( $R_1$ ,  $R_2$ , and  $R_3$ ), condition (EO and EC), and group of subjects ( $HS_{PD-Mi-Study}$ , PD-Mi,  $HS_{PD-Mo-Study}$ , and PD-Mo). Finally, it was determined if these means of errors were within a  $\pm 5\%$ ,  $\pm 10\%$ ,  $\pm 15\%$ , and  $\pm 20\%$  error, and the ones that had a p-value less or equal than 0.05 were identified (white \* in Figure 24-Figure 27). This operation was further analyzed when filters of CrossCorr were applied; i.e. this operation was done for the errors that had a CrossCorr between  $COP_{exp}$  and  $COP_{SIP(CC)}/COP_{SIP(0,0)}$  larger than 0, 0.90, 0.95, and 0.99. In summary, it was identified if the means of linear measure errors 1 and 2 between subjects in a group were within a  $\pm 5\%$ ,  $\pm 10\%$ ,  $\pm 15\%$ , and  $\pm 20\%$

error for all permutations of Linear Measure  $\cap R_1/R_2/R_3 \cap EO/EC \cap HS_{PD-Mi-Study}/PD-Mi/HS_{PD-Mo-Study}/PD-Mo \cap CrossCorr > 0, 0.90, 0.95, 0.99$ .

#### 3.3.4.2 *Nonlinear Measures Analysis*

Nonlinear measures were extracted from the  $COP_{exp}$ ,  $COP_{SIP(CC)}$  and  $COP_{SIP(0,0)}$  time series. The parameters extracted from each COP time series included:

- Time lag ( $\tau$ ) was determined through the analysis of MI as the time lag increases (Fraser and Swinney, 1986)
- Embedding dimension (EmbDim) was determined by using Euclidian distance method using  $Rtol = 15$ ,  $Atol = 2$ , and  $Rtol \cap Atol$  (Kennel et al., 1992).
- DFA's (Peng et al., 1994) slopes ( $\alpha$ ) and coefficients of determination ( $R^2$ ) at small and large window sizes using (Teresa Blázquez et al., 2009) method, due to the observed breaking point in the log-log plot (Collins and De Luca, 1994; Delignières et al., 2011; Mitchell et al., 1995). The minimum and maximum window sizes were  $t_{min} = 0.1$  seconds and  $t_{max} = 4.5$  seconds at a sampling frequency of 40 Hz (Delignières et al., 2011; Hu et al., 2001; Teresa Blázquez et al., 2009).
- SE (Richman and Moorman, 2000) and AE (Pincus, 1991) using  $2 \leq m \leq 5$  ( $\Delta m = 1$ ) and  $0.1 \leq r \leq 0.6$  ( $\Delta r = 0.1$ ) at a frequency of 40 Hz, which agrees with the recommendations of entropy analysis on sway studies (Pelykh et al., 2015; Ramdani et al., 2009; Yentes et al., 2013).
- LLE (Wolf et al., 1985) using the minimum and maximum distance for nearest neighbor respectively as  $10^{-3}$  and  $10^{-1}$  of the range of the time series. In addition, the evolve number of points in the time series were 1 to 5 ( $\Delta = 1$ ) times the calculated time lag.

These nonlinear measures were calculated only on the unfiltered COP time series. Also, a parallel analysis was done on the nonlinear analysis parameters as was done on the linear analysis parameters.

#### 3.3.4.3 *Linear, Nonlinear and Overall Performance of SIP*

Once the linear and nonlinear measures were identified that had errors 1 and 2 that had an average between subjects in a group within a  $\pm 5\%$ ,  $\pm 10\%$ ,  $\pm 15\%$ , and  $\pm 20\%$ , it was decided to group them. The linear measures were grouped based on the time series used:  $COP_{Pos}$ ,  $COP_{Vel}$ , and  $COP_{Acc}$ , and as all the linear measures; while the nonlinear measures of the  $COP_{Pos}$  were grouped in: State-Space Reconstruction ( $\tau$  and EmbDim), LLE, SE, AE, all nonlinear measures, and all nonlinear measures except  $\tau$ , EmbDim and LLE. Next, it was determined for each group the percentage of the errors that were

successfully within the analyzed error boundaries. In other words, the number of white \* in each group were counted, divided by the number of measures in each group, and multiplied by 100. This count was done for the permutations of Measure Group  $\cap$  HS<sub>PD-Mi-Study</sub>/PD-Mi/HS<sub>PD-Mo-Study</sub>/PD-Mo  $\cap$  COP<sub>SIP (CC)</sub>/COP<sub>SIP (0,0)</sub>  $\cap$  R<sub>1</sub>/R<sub>2</sub>/R<sub>3</sub> based on the permutations of EO/EC  $\cap$  Error of  $\pm 5\%$ ,  $\pm 10\%$ ,  $\pm 15\%$ , and  $\pm 20\%$   $\cap$  CrossCorr > 0.00, 0.90, 0.95, 0.99. Referring to Figure 10-Figure 20, heat maps for each measure group were used to visualize the linear and nonlinear performance of the SIP, where the y-axes were HS<sub>PD-Mi-Study</sub>/PD-Mi/HS<sub>PD-Mo-Study</sub>/PD-Mo  $\cap$  COP<sub>SIP (CC)</sub>/COP<sub>SIP (0,0)</sub>  $\cap$  R<sub>1</sub>/R<sub>2</sub>/R<sub>3</sub>, and the x-axes were EO/EC  $\cap$  Error of  $\pm 5\%$ ,  $\pm 10\%$ ,  $\pm 15\%$ , and  $\pm 20\%$   $\cap$  CrossCorr > 0.00, 0.90, 0.95, 0.99.

A final heat map (Figure 21) that shows the overall performance of the SIP was created (State-Space Reconstruction and LLE were omitted). It consisted of averaging the percentages determined in previous heat maps between trials (R<sub>1</sub>, R<sub>2</sub>, R<sub>3</sub>), and not restricting the percentages based on CrossCorr (CrossCorr > 0). The final heat map had a re-arrangement that consisted of making the y-axes HS<sub>PD-Mi-Study</sub>/PD-Mi/HS<sub>PD-Mo-Study</sub>/PD-Mo  $\cap$  COP<sub>SIP (CC)</sub>/COP<sub>SIP (0,0)</sub>, and the x-axes Measure Group  $\cap$  EO/EC  $\cap$  Error of  $\pm 5\%$ ,  $\pm 10\%$ ,  $\pm 15\%$ , and  $\pm 20\%$ . The means of the percentages between trials were identified by the color outside the circle or square using the color bar on the left. On the other hand, the color inside the circle or square indicated the SD of the percentages between trials using the color bar on the right. Also, the shape that enclosed the SD declared if the variability was less than  $\pm 5\%$  (circle), or larger (square).

Finally, in all heat maps, the HS listed on top of the PD-Mi came from the PD-Mi-Study; while the HS listed on top of the PD-Mo came from the PD-Mo-Study.

### 3.4 Statistical Analysis

All statistical analysis was performed in MATLAB (Mathworks, Natick, MA, USA) with significance defined using  $\alpha = 0.05$ . The comparison between COP<sub>exp</sub> and COP<sub>SIP</sub> using similarity measures when the ICs were optimized and equal to zero, as well as the comparison between similarity measures when the COP<sub>SIP</sub> was calculated using equations (5) and (6), were performed using a two-tail one-sample t-test with  $\alpha = 0.05$  and  $H_0 = 0$  (Section 3.3.3).

Determining if the mean of the linear and nonlinear measures errors between subjects were within a  $\pm 5\%$ ,  $\pm 10\%$ ,  $\pm 15\%$ , and  $\pm 20\%$  error, was done using a left-tail one-sample t-test with  $\alpha = 0.05$  and  $H_0 \geq 0.05, 0.10, 0.15,$  and  $0.20$  respectively (Determination of white \* in Sections 3.3.4.1 and 3.3.4.2). Due to the large number of linear measures (24) and nonlinear measures (61), multiple comparisons (Bonferroni) correction was applied on this step (Benjamini and Hochberg, 1995). The correction

number used for the linear measures was 8 since they were grouped in  $COP_{Pos}$ ,  $COP_{Vel}$ , and  $COP_{Acc}$ , and each of them had 8 linear measures. Therefore, the significance on these statistical analyses became  $\alpha = 0.00625$ . On the other hand, the correction number for the nonlinear measures was based on the number of measures of each group. This strategy was decided because each group expresses different qualitative information about the COP time series. Therefore, the correction numbers and significance on these statistical analyses were: 4 and  $\alpha = 0.0125$ , 4 and  $\alpha = 0.0125$ , 5 and  $\alpha = 0.01$ , 24 and  $\alpha = 0.00208$ , and 24 and  $\alpha = 0.00208$ , for State-Space Reconstruction, DFA, LLE, SE, and AE respectively.

Finally, the linear and nonlinear errors were averaged between trials (Section 3.3.4.3), and to determine if the means between trials were within 5%, a left-tail one-sample t-test with  $\alpha = 0.05$  and  $H_0 \geq 0.05$  was performed.

## 4 Results

### 4.1 $COP_{SIP}$ Sensitivity to ICs

The effect of ICs (zero vs optimized) was initially determined by calculating the difference in similarity measures between  $COP_{exp}$  and  $COP_{SIP}$ , when the  $COP_{SIP}$  was calculated using optimized and zero ICs (Section 3.3.3). The difference  $\text{Similarity Measure}_{ICs: Optimized} - \text{Similarity Measure}_{ICs: Zero}$  was calculated for all permutations of  $HS_{PD-Mi-Study}/PD-Mi/HS_{PD-Mo-Study}/PD-Mo \cap EO/EC \cap N-DEQ/L-DEQ$ , and the average of all trials per condition (EO and EC) in each group of subjects was calculated. A significant difference (two-tail one-sample t-test,  $H_0 = 0$ ,  $\alpha = 0.05$ ) meant that the difference in similarity measures was different than zero (95% confidence) when the  $COP_{SIP}$  was calculated using optimized and zero ICs. Results from these comparisons are in Figure 5-Figure 6, in which the p-value of each comparison is displayed; red font meaning  $p \leq 0.05$ .

Results showed that the  $COP_{SIP}$ 's accuracy depended strongly on the ICs when similarity between  $COP_{SIP}$  and  $COP_{exp}$  was measured using GOF, SSE, MI and CrossCorr. In both sets of results (using L-DEQ (6) and N-DEQ (5)), most of the similarity measures were significantly different than zero. In addition, it was noticed that both sets of results did not differ from a visual point of view when the L-DEQ and N-DEQ were used.

In the PD-Mi-Study, 3 out of 8 (EO GOF, EC GOF, EC CrossCorr) and 2 out of 8 (EO GOF, EC GOF) similarity measures did not show significant difference for HS and PD-Mi respectively, when the  $COP_{SIP}$  was calculated using equations (5) and (6). Acknowledging that the GOF was not significant different in the PD-Mi-Study, HS and PD-Mi showed an approximate loss of 10% in GOF with EO, as well as a loss of

approximately 20% with EC when the ICs were not optimized. Also, acknowledging that CrossCorr was not significantly different for HS with EC, in terms of MI and CrossCorr, losses of approximately 20% and 10% respectively for HS and PD-Mi are expected when ICs are assumed to be zero for EO and EC. Finally, acknowledging that SSE was not significantly different for PD-Mi with EO when their  $COP_{SIP}$  was calculated using equation (5), in terms of SSE, a negative difference was always obtained.

In the PD-Mo-Study, 3 out of 8 (EO GOF, EC GOF, EC CrossCorr) and 2 out of 8 (EO GOF, EC GOF) similarity measures did not show a significant difference for PD-Mo using equations (5) and (6) respectively. Acknowledging that the GOF was not significantly different for PD-Mo, GOF did not show large losses of accuracy for HS and PD-Mo; respectively in average 2% and 2.5%. However, acknowledging that CrossCorr was not significant for PD-Mo with EC when their  $COP_{SIP}$  was calculated using equation (6), approximate losses of 30% and 20% for HS, and 25% and 10% for PD-Mo are expected according to MI and CrossCorr respectively (EO and EC). Finally, in terms of SSE (significant in all cases), a negative difference was always obtained.

#### 4.2 $COP_{SIP}$ Sensitivity to Linearization of DEQ

The effect of linearizing the DEQ (N-DEQ (5) vs L-DEQ (6)) was determined by calculating the difference in similarity measures between  $COP_{exp}$  and  $COP_{SIP}$ , when the  $COP_{SIP}$  was calculated using the N-DEQ and L-DEQ (Section 3.3.3). The difference  $Similarity\ Measure_{N-DEQ} - Similarity\ Measure_{L-DEQ}$  was calculated for all permutations of  $HS_{PD-Mi-Study}/PD-Mi/HS_{PD-Mo-Study}/PD-Mo \cap EO/EC \cap Optimized\ ICs/Zero\ ICs$ , and the average of all trials per condition (EO and EC) in each group of subjects was calculated. A significant difference (two-tail, one-sample t-test,  $H_0 = 0$ ,  $\alpha = 0.05$ ) meant that the difference in time series similarity was different than zero (95% confidence) when the  $COP_{SIP}$  was calculated using equations (5) and (6). Results from these comparisons are in Figure 7-Figure 8, in which the p-value of each comparison is displayed; red font meaning  $p \leq 0.05$ .

Results showed that the  $COP_{SIP}$ 's accuracy when calculated using equations (5) and (6) was very similar. Even though the majority of the similarity measures proved to be significantly different when optimized ICs were used, the largest difference was found in MI with EC for PD-Mo, which was approximate -1.7%. When the  $COP_{SIP}$  was calculated using zero as ICs, it was possible to notice that there were less significant measures present (due to more variability in results) when compared to the other set of results (Optimized ICs). In addition, regardless if the similarity measure was significant, the largest difference was found in CrossCorr with EO for HS, which was approximate -3%. Since results from

Section 4.1 showed that optimizing ICs allowed stronger similarity between  $COP_{SIP}$  and  $COP_{exp}$ , further results of this sub-section were only based on the  $COP_{SIP}$  that used optimized ICs.

In the PD-Mi-Study, the  $COP_{SIP}$ 's accuracy for HS according to GOF (EO) and MI (EO and EC) proved to be significantly different; while for PD-Mi, GOF (EO and EC), SSE (EO) and MI (EO) proved to be significantly different. Even though some of the similarity measures in the PD-Mi-Study were significantly different in accuracy when the  $COP_{SIP}$  was calculated using equations (5) and (6) and optimized ICs, the largest difference (magnitude) in accuracy was approximately -0.5%. In addition, regardless if SSE proved to be significantly different, the sign of the means of SSE between subjects in each group was always positive.

In the PD-Mo-Study, the  $COP_{SIP}$ 's accuracy for HS and PD-Mo according to GOF, SSE and MI (EO and EC) proved to be significantly different. Even though the majority of the similarity measures in the PD-Mo-Study were significantly different in accuracy when the  $COP_{SIP}$  was calculated using equations (5) and (6) and optimized ICs, the largest difference (magnitude) in accuracy was around -1.7%. In addition, the sign of the means of SSE between subjects in each group was always positive.

### 4.3 $COP_{SIP}$ Linear Measures Performance

The ability of the  $COP_{SIP(CC)}$  and  $COP_{SIP(0,0)}$  to replicate the linear measures extracted from the  $COP_{exp}$  and its respective first and second derivatives, was determined by calculating and averaging the errors per linear measure between  $COP_{exp}$  and  $COP_{SIP(CC)}$  or  $COP_{SIP(0,0)}$ , and then observing if the averages of errors between subjects were within a  $\pm 5\%$ ,  $\pm 10\%$ ,  $\pm 15\%$ , and  $\pm 20\%$ , utilizing as a filter the CrossCorr between  $COP_{exp}$  and  $COP_{SIP(CC)}$  or  $COP_{SIP(0,0)}$  and  $R_1$ ,  $R_2$ ,  $R_3$  (Section 3.3.4.1). Significance (left-tail, one-sample t-test,  $H_0 \geq 0.05$ , 0.10, 0.15, 0.20,  $\alpha = 0.05$  with multiple comparisons correction) meant that the average of errors between subjects for the extracted linear measure was within 5%,  $\pm 10\%$ ,  $\pm 15\%$ , and  $\pm 20\%$  respectively with a confidence of 95%. Examples of results that show the linear measures that fell within an error ( $\pm 15\%$ ) in a trial ( $R_2$ ) for all subject groups are in Appendix B: Figures and Tables under Section 3.1. Next, the percent of the linear measures, in each measure group, that were within the listed errors based on  $R_1$ ,  $R_2$ ,  $R_3$  and CrossCorr was calculated (Section 3.3.4.3). Results for the percent of linear measures that fell on each analyzed error per measure group ( $COP_{Pos}$ ,  $COP_{Vel}$ ,  $COP_{Acc}$ , all linear measures) are in Figure 10-Figure 13. Finally, similar to the last result, the mean between trials of the percent of linear measures that were within the listed errors was calculated without any CrossCorr restriction (Figure 21). These results were also used to further determine how sensitive  $COP_{SIP}$  was to ICs.

Regarding the extracted linear measures in the measure group  $COP_{Pos}$  (Figure 10 and Figure 21) in general: (1) Not optimizing the ICs through CrossCorr ( $IC_{CC}$ ) and using zero as ICs ( $IC_{00}$ ) reduced the percent of linear measures that fell within any of the errors for all trials ( $R_1$ ,  $R_2$ ,  $R_3$ ); (2) Filtering results by the level of CrossCorr did not increase largely the percent of linear measures that fell within certain error; and (3) No large differences were found visually between conditions EO and EC. More specifically about  $COP_{Pos}$  when  $IC_{CC}$  were used, PD-Mi had in average 88% and 96% of the linear measures within an error of  $\pm 15\%$  and  $\pm 20\%$  for EO and EC respectively; PD-Mo had in average 88% of the linear measures within an error of  $\pm 15\%$  for EO and EC. HS from the PD-Mo-Study had in average 100% of the linear measures within an error of  $\pm 20\%$  for EO, as well as 100% of them within an error of  $\pm 15\%$  for EC; while HS from the PD-Mi-Study had in average 79% of the linear measures within an error of  $\pm 20\%$  for EO and EC.

Regarding the extracted linear measures in the measure group  $COP_{Vel}$  (Figure 11 and Figure 21) in general: (1) Not finding  $IC_{CC}$  and using  $IC_{00}$ , reduced the percent of linear measures that fell within any of the errors for all trials; (2) Filtering results by the level of CrossCorr did not increase largely the number of linear measures that fell within certain error; and (3) Differences in percent of linear measures within certain errors were found visually between conditions EO and EC. More specifically about  $COP_{Vel}$  when  $IC_{CC}$  were used, PD-Mi had in average 67% of the linear measures within a  $\pm 20\%$  error for EO, and in average 75% of them within a  $\pm 20\%$  error for EC; while PD-Mo had in average 13% of the linear measures within a  $\pm 20\%$  error for EO, and a range of 25% to 75% of them between trials within a  $\pm 20\%$  error for EC. HS from the PD-Mo-Study had in average 83% of the linear measures within an error of  $\pm 20\%$  for EO and EC; while HS from the PD-Mi-Study had in average 75% of the linear measures within an error of  $\pm 20\%$  for EO, and in average 83% of them within an error of  $\pm 20\%$  for EC.

Regarding the extracted linear measures in the measure group  $COP_{Acc}$  (Figure 12 and Figure 21) in general: (1) Not finding  $IC_{CC}$  and using  $IC_{00}$  did not reduce largely the percent of linear measures that fell within any of the errors for all trials, with the only subject group that showed a large difference in performance between  $IC_{CC}$  and  $IC_{00}$  was HS from the PD-Mo-Study; (2) Filtering the results by the level of CrossCorr did not increase largely the number of linear measures that fell within certain error; and (3) Differences in percent of linear measures within certain errors were found visually only in PD-Mi between EO and EC. More specifically about  $COP_{Acc}$  when  $IC_{CC}$  were used, PD-Mi had a maximum of 50% of the linear measures within any of the errors for EO, and in average 58% of them within an error of  $\pm 20\%$  for EC; while PD-Mo had at best 25% of the linear measures within any of the errors for EO and EC.

HS from the PD-Mi-Study had in average 88% of the linear measures within an error of  $\pm 20\%$  for EO and EC; while HS from PD-Mo-Study had in average 83% and 88% of the linear measures within an error of  $\pm 20\%$  for EO and EC respectively.

Finally, looking over all the linear measures extracted (Figure 13 and Figure 21) in general: (1) Not finding  $IC_{CC}$  and using  $IC_{00}$  reduced largely the number of linear measures that fell within any of the errors for all trials; (2) Filtering the results by the level of CrossCorr did not increase largely the number of linear measures that fell within certain error; and (3) Differences in percent of linear measures between EO and EC were visually found in PD-Mi and PD-Mo at the error of  $\pm 20\%$ . More specifically about all the linear measures extracted when  $IC_{CC}$  were used, PD-Mi had in average 61% and 76% of the linear measures within an error of  $\pm 20\%$  for EO and EC respectively. PD-Mo had in average 42% of the linear measures within an error of  $\pm 15\%$  for EO, and in average 56% of them within an error of  $\pm 20\%$  for EC. HS from the PD-Mi-Study had in average 81% and 83% of the linear measures within an error of  $\pm 20\%$  for EO and EC respectively; while HS from the PD-Mo-Study had in average 90% of the linear measures within an error of  $\pm 20\%$  for EO and EC.

#### 4.4 $COP_{SIP}$ Nonlinear Measures Performance

The ability of the  $COP_{SIP(CC)}$  and  $COP_{SIP(0,0)}$  to replicate the nonlinear measures extracted from the unfiltered  $COP_{exp}$ , was determined by performing a parallel study to the linear measures analysis. Significance had the same interpretation as in Section 4.3. Examples of results that show the nonlinear measures that fell within an error ( $\pm 15\%$ ) in a trial ( $R_2$ ) for all subject groups are in Appendix B: Figures and Tables under Section 3.2. Also, results of the percent of nonlinear measures in each measure group that fell within the errors used in this study and based on CrossCorr are in Figure 14-Figure 20; while the percent of nonlinear measures that fell within the errors used in this study without CrossCorr restriction are in Figure 21. Finally, as it was mentioned in the  $COP_{SIP}$  Linear Measures Performance, these results were also to further determine how sensitive  $COP_{SIP}$  was to ICs.

Regarding the nonlinear measures  $\tau$ , EmbDim, and LLE extracted on the COP time series (Figure 14-Figure 15), it was possible to observed that neither the  $COP_{SIP(CC)}$  or  $COP_{SIP(0,0)}$  could replicate these nonlinear measures. For  $\tau$  and EmbDim (State-Space Reconstruction), both time series of  $COP_{SIP}$  could replicate an average of 25% of these nonlinear measures within an error of  $\pm 20\%$  for all subjects and conditions. However, for the LLE, both time series could not replicate any of these measures within any error for all subjects and conditions.

Regarding the nonlinear measures of the DFA on the COP time series (Figure 16 and Figure 21) in general: (1) Not finding  $IC_{CC}$  and using  $IC_{00}$  reduced the percent of DFA measures that fell within any of the errors for all trials, except for PD-Mi at an error of  $\pm 15\%$  and  $\pm 20\%$ ; (2) Filtering the results by the level of CrossCorr did not increase largely the number of DFA measures that fell within certain error; and (3) No differences were found visually between EO and EC, except on PD-Mo at an error of  $\pm 10\%$ . More specifically about the DFA measures when  $IC_{CC}$  were used, PD-Mi had in average 100% of the DFA measures within an error of  $\pm 10\%$  for EO, and 100% of them within an error of  $\pm 15\%$  for EC. PD-Mo had in average 100% of the DFA measures within an error of  $\pm 20\%$  for EO, and 100% of them within an error of  $\pm 15\%$  for EC. HS from both studies had in average 100% of the DFA measures within an error of  $\pm 10\%$  for EO and EC; except HS from the PD-Mo-Study who had 100% of the DFA measures within an error of  $\pm 15\%$  for EC.

Regarding the nonlinear measure of the SE on the COP time series (Figure 17 and Figure 21) in general: (1) Not finding  $IC_{CC}$  and using  $IC_{00}$  reduced the percent of SE measures that fell within any of the errors for all trials; (2) Filtering the results by the level of CrossCorr did not increase largely the number of SE measures that fell within certain error; and (3) Differences were found visually between EO and EC. More specifically about the SE measures when  $IC_{CC}$  were used, PD-Mi had in average 58% (high variability) of the measures within an error of  $\pm 20\%$  for EO, and 92% of them within an error of  $\pm 20\%$  for EC. PD-Mo had basically none of the SE measures within any of the errors for EO and EC. HS from the PD-Mi-Study had in average 68% of the measures within an error of  $\pm 20\%$  for EO, and 89% of them within an error of  $\pm 20\%$  for EC; while HS from the PD-Mo-Study had 100% of the measures within an error of  $\pm 20\%$  for EO and EC.

Regarding the nonlinear measure of the AE on the COP time series (Figure 18 and Figure 21) in general: (1) Not finding  $IC_{CC}$  and using  $IC_{00}$  reduced the percent of AE measures that fell within any of the errors for all trials; (2) Filtering the results by the level of CrossCorr did not increase largely the number of SE measures that fell within certain error; and (3) Differences were found visually between EO and EC. More specifically about the AE measures when  $IC_{CC}$  were used, PD-Mi had in average 53% of the measures within an error of  $\pm 20\%$  for EO, and 79% of them (high variability) within an error of  $\pm 20\%$  for EC. PD-Mo had basically none of the AE measures within any of the errors for EO and EC. HS from the PD-Mi-Study had in average 54% of the measures within an error of  $\pm 20\%$  for EO, and 92% of them within an error of  $\pm 20\%$  for EC; while HS from the PD-Mo-Study had 100% of the measures within an error of  $\pm 20\%$  for EO and EC.

Regarding all the nonlinear measures extracted on this study (Figure 19), it was possible to conclude that the  $COP_{SIP(CC)}$  was not an adequate model to replicate nonlinear measures extracted from  $COP_{exp}$ . This was a consequence of the poor results from the State-Space Reconstruction and Lyapunov Exponent nonlinear measures. However, if the overall  $COP_{SIP}$  nonlinear accuracy was based on fractality and entropy characteristics (Figure 20 and Figure 21), it was observed that better results were obtained. In general, from Figure 20: (1) Not finding  $IC_{CC}$  and using  $IC_{00}$  reduced the percent of nonlinear measures that fell within any of the errors for all trials, in fact, the difference was not large between  $COP_{SIP(CC)}$  and  $COP_{SIP(0,0)}$  when both had a poor performance; (2) Filtering the results by the level of CrossCorr did not increase the number of nonlinear measures that fell within certain error; and (3) No differences were found visually between EO and EC for the PD-Mo-Study; however, differences between EO and EC were present for the PD-Mi-Study. More specifically about all nonlinear measures (except State-Space Reconstruction and LLE) extracted when  $IC_{CC}$  were used, HS from the PD-Mi-Study had in average 74% of the nonlinear measures within a  $\pm 20\%$  for EO, and 89% of them within a  $\pm 20\%$  for EC; while HS from the PD-Mo-Study had in average 100% of the nonlinear measures within a  $\pm 20\%$  for EO and EC. PD-Mi had in average 71% of the nonlinear measures within an error of  $\pm 20\%$  for EO, and 94% of them within an error of  $\pm 20\%$  for EC. PD-Mo had in average 37% of the nonlinear measures within a  $\pm 20\%$  for EO, and 56% (high variability) of the measures within a  $\pm 20\%$  for EC.

All numerical observations explained in Sections 4.3 and 4.4, are summarized in Table 8. Red and bolded numbering means that the variability between trials was less than  $\pm 5\%$  with a 95% confidence. However, to combine the error with the percent of measures between subjects fell, the equation  $(100\% - |\%Error|) \times \%Measures$  was used. Table 9 shows the result of this multiplication where red and bolded numbering means that the variability between trials was less than  $\pm 5\%$  with a 95% confidence.

## 5 Discussion

The aim of this study was to investigate the accuracy of the  $COP_{SIP}$  in HS and PD subjects when it was compared to the  $COP_{exp}$  for bi-pedal quiet standing with EO and EC, and its sensitivity to ICs (optimized vs. zero) and the linearization of the DEQ (L-DEQ vs. N-DEQ). The primary results showed that the common practice in sway modeling studies of using zero as ICs reduced the accuracy of the  $COP_{SIP}$ . The results also showed that very little accuracy is gained by modeling the SIP using the N-DEQ (5), over using the L-DEQ (6). Regarding HS, PD-Mi and PD-Mo, results showed that the  $COP_{SIP(CC)}$  is an accurate model for quiet bi-pedal standing when the  $COP_{exp}$  is compared to the  $COP_{SIP(CC)}$  using certain linear and

nonlinear measures. Finally, it was determined that as PD progresses, the human body behaves less like a SIP, and more like a DIP.

**Hypothesis 1 claimed that the performance of the  $COP_{SIP}$  was sensitive to ICs, and based on the results of this study, hypothesis 1 is valid.** Initially, this hypothesis was tested by comparing time series similarity measures between  $COP_{exp}$  and  $COP_{SIP}$  when it was calculated using optimized and zero ICs, using both the L-DEQ (6) or N-DEQ (5) (Figure 5 and Figure 6). During this first analysis, the optimized ICs were calculated using all the optimization methods. GOF, which is a measure that calculates how much (percentage) a time series represents another time series in terms of magnitude, was only significantly different when the  $COP_{SIP}$  was calculated using zero and optimized ICs for HS from the PD-Mo-Study. Therefore, no conclusions were made based on this similarity measure. The high variability of this similarity measure was believed to come from the nature of the GOF (8). GOF has the  $COP_{exp}$  in the denominator of the equation, creating a possibility for discontinuity if the value of the  $COP_{exp}$  was equal to zero at any instance. Since the subjects were asked to align their medial-malleolus with the force plates coordinate system, it is highly likely that the  $COP_{exp}$  will have a value equal to zero since it represents a subject going from leaning forward to leaning backwards, or vice versa. On the other hand, SSE, which is similar to GOF but with the difference that it is not a percentage value (i.e. the  $COP_{exp}$  is not in the denominator), proved to be significantly different when the  $COP_{SIP}$  was calculated using zero and optimized ICs for all subjects and conditions; except PD-Mi with EO when the  $COP_{SIP}$  was calculated using the N-DEQ (5). In addition, SSE was always negative, meaning that when the  $COP_{SIP}$  was calculated using optimized ICs, it always had less error than the  $COP_{SIP}$  when it was calculated using zero as ICs. Finally, MI and CrossCorr, which measure how similar the shape of curves of two time series are, were significantly different when the  $COP_{SIP}$  was calculated using zero and optimized ICs for all subjects and conditions (32); except three cases (CrossCorr for HS from PD-Mi-Study with EC using L-DEQ and N-DEQ, and CrossCorr for PD-Mo with EC using L-DEQ). The results showed that the  $COP_{SIP}$  and  $COP_{exp}$  could have from a 10% to a 35% difference in shape of a curve when optimized ICs were not used based on all subjects. With that said, it was concluded that the ability of the  $COP_{SIP}$  to represent the  $COP_{exp}$  was sensitive to ICs, making this hypothesis valid. Therefore, it was concluded that to achieve the highest similarity between  $COP_{SIP}$  and  $COP_{exp}$ , the ICs of the model should be optimized, instead of being assumed to be zero, as it is done in the majority of previous studies (Asai et al., 2009; Bottaro et al., 2008; Chagdes et al., 2016b, 2016a; Kooij et al., 1999; Loram and Lakie, 2002; Maurer et al., 2004, p. 2; Peterka, 2002; Vette et al., 2010). This hypothesis was further tested by observing that the accuracy of the  $COP_{SIP(CC)}$  was always superior than the  $COP_{SIP(0,0)}$  when it came to replicating extracted linear and

nonlinear measures from the  $COP_{exp}$  (Figure 10-Figure 21). Our model based finding is consistent to an experimental study which investigated the sensitivity of sway on the initial position of the body before testing. Tokuno et al (Tokuno et al., 2006) concluded that the balance performance of the subjects for all sway tests was dependent on the initial location of the body. Therefore, this experimental conclusion is consistent with our first hypothesis.

**Hypothesis 2 claimed that the performance of the  $COP_{SIP}$  was not sensitive to linearizing the DEQ of motion, and based on the results of this study, hypothesis 2 is valid.** This hypothesis was tested by comparing time series similarity measures between  $COP_{exp}$  and  $COP_{SIP}$  when the latter was calculated using the L-DEQ (6) and N-DEQ (5), either with optimized or zero ICs (Figure 7 and Figure 8). Since hypothesis 1 was valid, conclusions for this hypothesis were focused only on the optimized ICs case. As the results showed, the majority of the GOF, MI and CrossCorr comparisons were significantly different when  $COP_{SIP}$  was calculated using the L-DEQ (6) and N-DEQ (5); however, the largest difference was only -1.7% based on MI for PD-Mo with EO. In addition, regardless if the similarity measures were significant, the signs of GOF, MI and CrossCorr were always negative; while the sign of SSE was always positive for all subject groups. This means that when the  $COP_{SIP}$  was calculated using the N-DEQ (5) and optimized ICs, compared to using the L-DEQ (6) and optimized ICs, all similarity measures demonstrated that the  $COP_{SIP}$  that uses the N-DEQ (5) had a larger error in magnitude and shape of curve, than the  $COP_{SIP}$  that uses the L-DEQ (6). Due to such small differences in similarity measures, and less error obtained through the L-DEQ, it was concluded that using a N-DEQ to model the SIP as some authors do (Chagdes et al., 2016b, 2016a), instead of using the L-DEQ, adds little to the accuracy to the  $COP_{SIP}$ . In fact, modeling the SIP using the L-DEQ (6) is mathematical easier since there are currently more tools to analyze linear differential equations, compared to nonlinear differential equations. Finally, linearizing the DEQ of motion on unperturbed bi-pedal sway studies is the common practice in mechanical modeling studies for sway; therefore, the validity of this hypothesis supports this current practice. In addition, the validity of this hypothesis adds to the experimental observation by Gage et al regarding the small amount of motion in quiet standing (Gage et al., 2004), i.e. around 1 to 1.5 degrees in bi-pedal quiet standing for young healthy subjects. This observation supports the use of a linearized DEQ for quiet bi-pedal sway studies in young healthy subjects. We observed that linearizing the DEQ has little effect on the error of the  $COP_{SIP}$  for both HS and PD subjects, supporting the linearization of the DEQ. This result suggests that small sway angles were present for HS and PD subjects during this study. Therefore, adding to Gage et al observation, it is possible to linearize the DEQ of motion for old healthy adults and participants with mild to moderate PD.

Before analyzing hypothesis 3 and 4 without using  $\tau$ , EmbDim and LLE, it was expected that the  $COP_{SIP}$  based on these nonlinear measures would not perform well. The low  $COP_{SIP}$  performance regarding LLE is due to its dependency to  $\tau$  and EmbDim. In fact, the  $COP_{SIP}$  could replicate only 25% of the nonlinear measures of  $\tau$  and EmbDim when an error of  $\pm 20\%$  was accepted. Since the LLE nonlinear measures are a function of  $\tau$  and EmbDim, the low performance of the LLE can be justified because errors were introduced to this calculation before even being calculated. In addition, the nonlinear measures  $\tau$ , EmbDim and LLE, in terms of differential equations, depend on the number of states, as well as the inputs and disturbances modeled in the differential equation (Steven H Strogatz, 2015). The inverse dynamics model utilized in this study only included the 2 state variables of the SIP  $(\theta, \dot{\theta})$ , and the moments and forces at the ground; while in real life there are additional inputs such as visual, vestibular, and proprioceptive feedback, as well as internal disturbances. These additional inputs and/or disturbances could increase the dimensions and complexity of the time series, to the point that they account for the error observed in these three nonlinear measures. Finally, low performance in LLE for PD sway studies had been observed in other PD sway studies (Pascolo et al., 2006, 2005).

**Hypothesis 3 claimed that the  $COP_{SIP}$  could represent at least 70% of the  $COP_{exp}$  for EO and EC, and based on the results of this study, hypothesis 3 is valid with conditions.** This hypothesis was tested by comparing the error of the extracted linear and nonlinear measures from the  $COP_{exp}$ , when the  $COP_{SIP}$  was calculated using the L-DEQ and optimized ICs for the HS from the PD-Mi- and PD-Mo-Study (Figure 10-Figure 21). We conclude that hypothesis 3 is valid with conditions, because the  $COP_{SIP(CC)}$  could represent 70% of the  $COP_{exp}$  for certain measure groups ( $COP_{Pos}$ ,  $COP_{Vel}$ , and  $COP_{Acc}$ , LLE, SE, or AE) that characterized the  $COP_{exp}$ . In fact, when results from Table 9 were based on the HS from the PD-Mo-Study, the  $COP_{SIP(CC)}$  could describe 70% or more of the  $COP_{exp}$ , when the  $COP_{exp}$  was represented by the linear measures of the  $COP_{Pos}$  (EO and EC) and  $COP_{Acc}$  (EC), as well as when it was represented by the nonlinear measures of DFA, SE and AE (EO and EC). In addition, when the results of Table 9 were based on the HS from the PD-Mi-Study, the  $COP_{SIP(CC)}$  could describe 70% or more of the  $COP_{exp}$ , when the  $COP_{exp}$  was represented by the linear measures of the  $COP_{Acc}$  (EO and EC), as well as when it was represented by the nonlinear measures of DFA (EO and EC). Regarding the HS from the PD-Mi-Study, SE and AE (EC) were measures with percentages larger than 70%; however, they were not considered since they were not significant. Therefore, hypothesis 3 is 100% valid if “representing the  $COP_{exp}$ ” consists on the  $COP_{SIP(CC)}$  replicating the DFA nonlinear measures (EO and EC), and  $COP_{Acc}$  linear measures (EC) extracted from the  $COP_{exp}$ . This allows future studies to design SIP models that replicate DFA (EO and EC) nonlinear measures and  $COP_{Acc}$  (EC) linear measures extracted from the  $COP_{exp}$ , draw conclusions from

how the SIP model recreated these measures based on its parameters and other successful studies on HS (Delignières et al., 2011; Teresa Blázquez et al., 2009), and be confident that the conclusions driven are at least 70% true. This conclusion could not be made based on the extracted linear measures on the  $COP_{Pos}$  (EO and EC), SE (EO and EC), AE (EO and EC), and  $COP_{Acc}$  (EO) since there was not an agreement between HS from both studies. Finally, hypothesis 3 is 100% invalid if “representing the  $COP_{exp}$ ” consists on the  $COP_{SIP(CC)}$  replicating the  $COP_{Vel}$  linear measures extracted from the  $COP_{exp}$ . This meant that results and conclusions from posturographic studies on  $COP_{Vel}$  such as (Gervasoni et al., 2015), could not be combined with results from SIP modeling studies.

**Hypothesis 4 claimed that as PD progresses the human body behaves more like a SIP in the AP direction due to increased rigidity at the ankles, and based on the results of this study, hypothesis 4 is invalid.** This hypothesis was tested in parallel with hypothesis 3; but instead of observing the results for the HS subjects, the results for PD-Mi and PD-Mo were observed (Figure 10-Figure 21). Using Table 9, it was possible to observe that the  $COP_{SIP(CC)}$  could better represent the  $COP_{exp}$  in PD-Mi than in PD-Mo. For every measure group and condition, the PD-Mi had a higher or equal percentage of representation of the  $COP_{exp}$  than PD-Mo. Because of this observation, and the already mentioned increase in ankle stiffness as associated with PD progression (Carpenter et al., 2004; Horak et al., 1996), it was concluded that hypothesis 4 was invalid. The invalidity of this hypothesis does not have conflict with the previously observed increase in ankle stiffness as PD progresses. On the other hand, this observation simply claims that rigidity at the ankles in PD subjects does not result in sway that can be described with a single degree of freedom or SIP model. In fact, it supports Fujiwasa et al observations (Fujisawa et al., 2005), which state that as perturbations during sway increase (reduction of stance width in Fujisawa et al’s study), the ankle motion is reduced, and the hip motion is increased to maintain balance, suggesting an increase in the degrees of freedom within the system. If PD is considered as a perturbation that increases as the disease progresses, it is possible to relate both studies and agree that as PD progresses, the ankles become stiffer, creating less motion at the ankles. However, due to the low motion at the ankles, the hips must be utilized more to keep the balance of the body, resulting in the SIP model reducing accuracy as PD progresses towards a two degree of freedom system.

Finally, it was observed that the  $COP_{SIP(CC)}$  could represent 70% of the  $COP_{exp}$  in PD-Mi and PD-Mo under certain conditions. Using the analysis done for hypothesis 3, the  $COP_{SIP(CC)}$  in PD-Mi could describe at least 70% of the  $COP_{exp}$ , when the  $COP_{exp}$  was represented by the linear measures of  $COP_{Pos}$  (EO and EC), and the nonlinear measures of the DFA (EO and EC), and SE (EC). In the case of PD-Mo, the  $COP_{SIP(CC)}$

could describe at least 70% of the  $COP_{exp}$ , when the  $COP_{exp}$  was represented by the linear measures of  $COP_{Pos}$  (EO and EC), and the nonlinear measures of the DFA (EO and EC). This allows future studies to design SIP models that replicate  $COP_{Pos}$  (EO and EC) linear measure, and nonlinear measures on DFA (EO and EC) and SE (EC) extracted from the  $COP_{exp}$ , draw conclusions from how the SIP model recreated these measures based on its parameters and other successful studies on PD (Błaszczuk et al., 2007; Mitchell et al., 1995; Pelykh et al., 2015; Schlenstedt et al., 2016; Stylianou et al., 2011), and be confident that the conclusions driven are at least 70% true.

## 6 Conclusions

In conclusion, it was identified that determining the ICs of the SIP when using it for mechanical modeling studies is a very important step. The current study, along with the study by Tokuno et al (Tokuno et al., 2006) are mathematical and experimental proof of this concept. If the ICs are assumed to be zero, it is possible to lose around 20% on accuracy regarding the shape of curve, and this assumption increases the error in magnitude on either EO and EC quiet bi-pedal stance. In addition, if the ICs of the SIP are not appropriately determined in a mechanical modeling study and assumed to be zero, the unbalance of the SIP in the model would be originated by external/internal disturbances since zero ICs do not make the SIP sway. Using zero as ICs is not realistic since the body is in a constant sway, and naturally it is very unlikely to be located at a perfect balance with zero ICs. Mechanical modeling studies need to destabilize the SIP originally using ICs and/or disturbances.

Regarding the linearization of the DEQ, it was concluded that the DEQ of motion that relates the angular position, velocity and acceleration of the SIP with the torque at the ankles can be linearized. Linearizing the DEQ of motion improved the accuracy of the model up to 2% in terms of similarity measures; however, this conclusion needs further study since the N-DEQ is meant to be a more accurate than the L-DEQ.

It was also concluded that the  $COP_{SIP}$ , when it is calculated using the L-DEQ and optimized ICs, can describe 70% or more of the  $COP_{exp}$  for HS when the  $COP_{exp}$  is represented with linear measures of the  $COP_{Acc}$  (EC) and nonlinear measures of DFA (EO and EC). In addition, the  $COP_{SIP(CC)}$  can describe 70% or more of the  $COP_{exp}$  for PD-Mi, when the  $COP_{exp}$  is represented with linear measures of the  $COP_{Pos}$  (EO and EC), and nonlinear measures of the DFA (EO and EC) and SE (EC). While for PD-Mo, the  $COP_{SIP(CC)}$  can describe 70% or more of the  $COP_{exp}$ , when the  $COP_{exp}$  is represented with linear measures of  $COP_{Pos}$  (EO and EC), and the nonlinear measures of the DFA (EO and EC).

Finally, it was possible to conclude that as the stiffness at the ankles increases due to PD progression (Carpenter et al., 2004; Horak et al., 1996), the human body behaves less as a SIP, and more as a DIP. In fact, it was observed in the current study that as PD progresses the SIP model becomes a less valid model, creating the possible need of using a DIP for PD subjects.

## 7 Tables and Figures

Table 3 - HS from PD-Mi-Study

Subject	Gender	Height [cm]	Weight [kg]	Age	UPDRS	H&Y	Years w/ PD
1001	F	160.0	60.9	76	N/A	N/A	N/A
1003	F	164.0	55.3	67	N/A	N/A	N/A
1004	M	165.5	69.4	75	N/A	N/A	N/A
1005	F	149.8	55.1	77	N/A	N/A	N/A
1006	M	172.0	74.9	67	N/A	N/A	N/A
1007	F	162.0	68.0	62	N/A	N/A	N/A
1008	F	150.5	69.9	71	N/A	N/A	N/A
1010	M	170.0	72.6	71	N/A	N/A	N/A
1011	M	170.0	77.4	72	N/A	N/A	N/A
1012	M	187.5	91.2	61	N/A	N/A	N/A
1013	F	169.5	66.7	50	N/A	N/A	N/A
1014	F	168.5	65.8	48	N/A	N/A	N/A
<b>Mean (SD)</b>		165.8 (9.6)	68.9 (9.5)	66.4 (9.2)	N/A	N/A	N/A

Table 4 - PD-Mi from PD-Mi-Study

Subject	Gender	Height [cm]	Weight [kg]	Age	UPDRS	H&Y	Years w/ PD
3001	F	168.5	70.3	55	48	2	3.5
3002	M	181.5	83.9	64	51	2	16.0
3003	M	173.2	79.6	77	37	2	1.0
3004	M	170.0	94.5	62	34	2	5.0
3005	F	162.0	78.2	65	10	2	4.0
3006	M	162.0	71.5	56	25	2	8.0
3008	M	176.5	82.3	64	33	2	13.0
3009	F	157.5	81.6	73	22	2	3.0
3010	M	169.5	78.1	51	30	2	2.0
3011	F	167.0	55.3	48	11	2	2.0
3013	F	161.0	58.2	63	18	2	12.0
3014	F	159.5	59.6	60	12	2	1.0
<b>Mean (SD)</b>		167.4 (7.0)	74.4 (11.3)	61.5 (8.0)	27.6 (13.2)	2 (0)	5.9 (4.9)

Table 5 - HS from PD-Mo-Study

Subject	Gender	Height [cm]	Weight [kg]	Age	UPDRS	H&Y	Years w/ PD
1001	F	171.0	55.1	63	N/A	N/A	N/A
1002	M	171.5	86.2	67	N/A	N/A	N/A
1003	M	169.5	66.2	63	N/A	N/A	N/A
1005	M	170.5	69.9	68	N/A	N/A	N/A
1006	M	185.7	88.0	65	N/A	N/A	N/A
1007	M	175.4	91.6	70	N/A	N/A	N/A
1008	M	181.0	71.1	62	N/A	N/A	N/A
1009	F	169.5	61.6	73	N/A	N/A	N/A
1010	M	176.0	73.5	78	N/A	N/A	N/A
<b>Mean (SD)</b>		174.5 (5.4)	73.7 (11.8)	67.7 (5.0)	N/A	N/A	N/A

Table 6 - PD-Mo from PD-Mo-Study

Subject	Gender	Height [cm]	Weight [kg]	Age	UPDRS	H&Y	Years w/ PD
4001	M	172.0	86.7	72	66	3	5.0
4002	F	157.0	64.4	71	47	3	13.0
4004	M	170.0	115.8	61	36	3	10.0
4005	M	166.5	90.0	69	57	3	3.0
4006	M	186.0	103.0	71	47	3	7.0
4007	M	179.0	85.8	66	35	3	2.0
4008	M	182.0	89.4	63	65	3	9.0
4009	M	181.0	97.5	68	31	3	2.5
4010	M	184.5	90.3	65	44	3	9.0
4011	M	171.5	97.1	68	53	3	10.0
<b>Mean (SD)</b>		175.0 (8.7)	92.0 (12.6)	67.4 (3.4)	48.1 (11.6)	3 (0)	7.1 (3.6)

Table 7 - Anthropometric Equations for the SIP Model Constants

Parameter	HAT	Thighs	Calfs	Feet
<b><i>m</i></b>	0.678 <i>M</i>	2×0.1 <i>M</i>	2×0.0465 <i>M</i>	0.029 <i>M</i>
<b><i>l</i></b>	(0.818 – 0.530) <i>H</i>	Measured	Measured	Measured
<b><i>COM</i></b>	0.374 <i>l</i> <sub>HAT</sub>	0.567 <i>l</i> <sub>thigh</sub>	0.567 <i>l</i> <sub>calf</sub>	0.5 <i>l</i> <sub>feet</sub>
<b><i>J</i></b>	$m_{HAT}(0.496l_{HAT})^2 + m_{HAT}(l_{calf} + l_{thigh} + COM_{HAT})^2$	$2 \times [m_{thigh}(0.323l_{thigh})^2 + m_{thigh}(l_{calf} + COM_{thigh})^2]$	$2 \times m_{calf}(0.643l_{calf})^2$	N/A

Table 8 - Average Percent between Trials of Linear and Nonlinear Measures within Defined Error for COP<sub>SIP</sub> with Optimized ICs

		COP <sub>Pos</sub>		COP <sub>Vel</sub>		COP <sub>Acc</sub>		All Linear Measures		DFA		SE		AE		All Nonlinear Measures	
		EO	EC	EO	EC	EO	EC	EO	EC	EO	EC	EO	EC	EO	EC	EO	EC
		PD-Mi-Study	HS	79%	79%	<b>75%</b>	83%	<b>88%</b>	<b>88%</b>	<b>81%</b>	<b>83%</b>	<b>100%</b>	<b>100%</b>	68%	89%	<b>54%</b>	92%
PD-Mi-Study	PD-Mi	<b>88%</b>	96%	67%	75%	29%	58%	61%	76%	<b>100%</b>	<b>100%</b>	58%	92%	53%	79%	71%	94%
PD-Mo-Study	HS	<b>100%</b>	<b>100%</b>	83%	83%	83%	<b>88%</b>	<b>89%</b>	<b>90%</b>	<b>100%</b>	<b>100%</b>						
PD-Mo-Study	PD-Mo	<b>88%</b>	<b>88%</b>	<b>13%</b>	54%	<b>25%</b>	<b>25%</b>	<b>42%</b>	56%	<b>100%</b>	<b>100%</b>	<b>8%</b>	42%	3%	26%	<b>37%</b>	56%

±10% Error     
  ±15% Error     
  ±20% Error

Red and bolded numbering means that the variability between trials was less than ±5% ( $\alpha = 0.05$ )

Table 9 - Average Percent between Trials of Linear and Nonlinear Measures with Error Applied for COP<sub>SIP</sub> with Optimized ICs

		COP <sub>Pos</sub>		COP <sub>Vel</sub>		COP <sub>Acc</sub>		All Linear Measures		DFA		SE		AE		All Nonlinear Measures	
		EO	EC	EO	EC	EO	EC	EO	EC	EO	EC	EO	EC	EO	EC	EO	EC
		PD-Mi-Study	HS	63%	63%	<b>60%</b>	66%	<b>70%</b>	<b>70%</b>	<b>65%</b>	<b>66%</b>	<b>90%</b>	<b>85%</b>	54%	71%	<b>43%</b>	74%
PD-Mi-Study	PD-Mi	<b>75%</b>	77%	54%	60%	23%	46%	49%	61%	<b>90%</b>	<b>85%</b>	46%	74%	42%	63%	57%	75%
PD-Mo-Study	HS	<b>80%</b>	<b>85%</b>	66%	66%	66%	<b>70%</b>	<b>72%</b>	<b>72%</b>	<b>90%</b>	<b>90%</b>	<b>80%</b>	<b>80%</b>	<b>80%</b>	<b>80%</b>	<b>80%</b>	<b>80%</b>
PD-Mo-Study	PD-Mo	<b>75%</b>	<b>75%</b>	<b>10%</b>	43%	<b>20%</b>	<b>20%</b>	<b>36%</b>	45%	<b>80%</b>	<b>85%</b>	<b>6%</b>	34%	2%	21%	<b>30%</b>	45%

Average percent between trials and error are combined using  $\%Measures \times (100\% - |\%Error|)$ . Red and bolded numbering means that the variability between trials was less than ±5% ( $\alpha = 0.05$ )

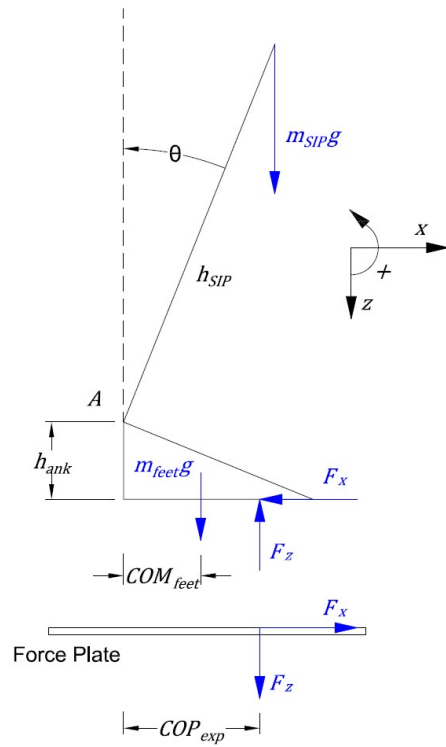


Figure 2 - SIP Free Body Diagram: Kinetic Study of SIP

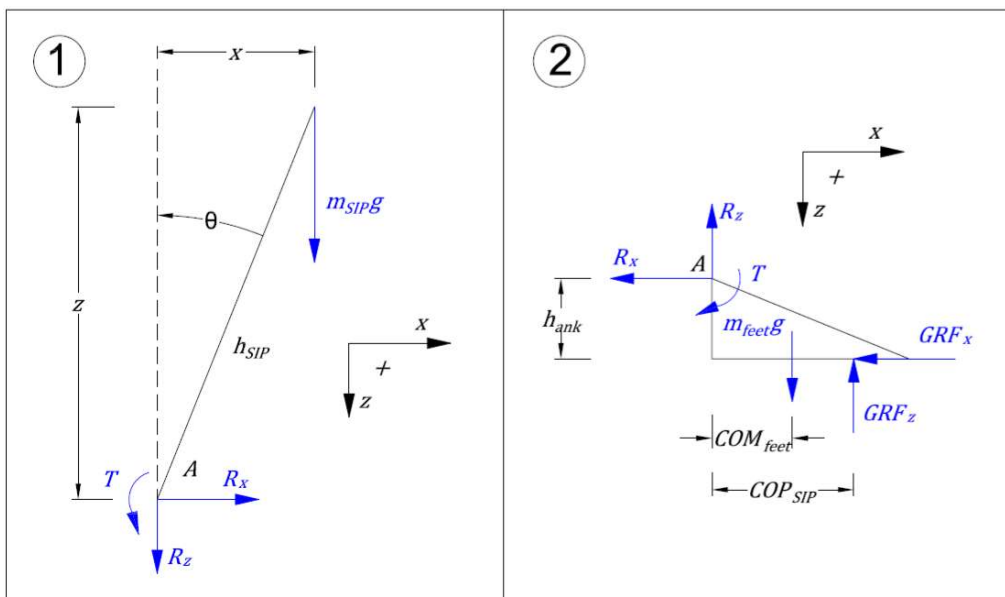


Figure 3 - SIP Free Body Diagram: Kinetic Study of Stationary Foot

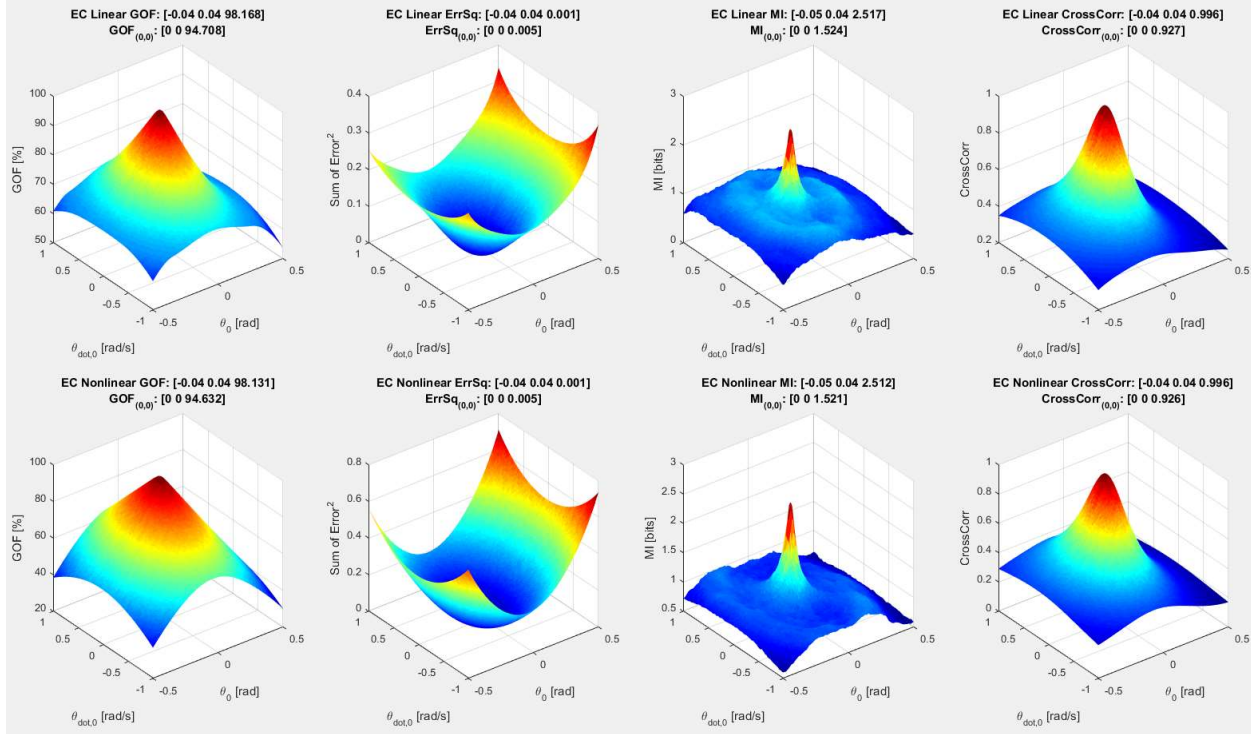


Figure 4 - PD-Mi-Study (Sub 1013): ICs Optimization for Nonlinear/Linear Differential Equation

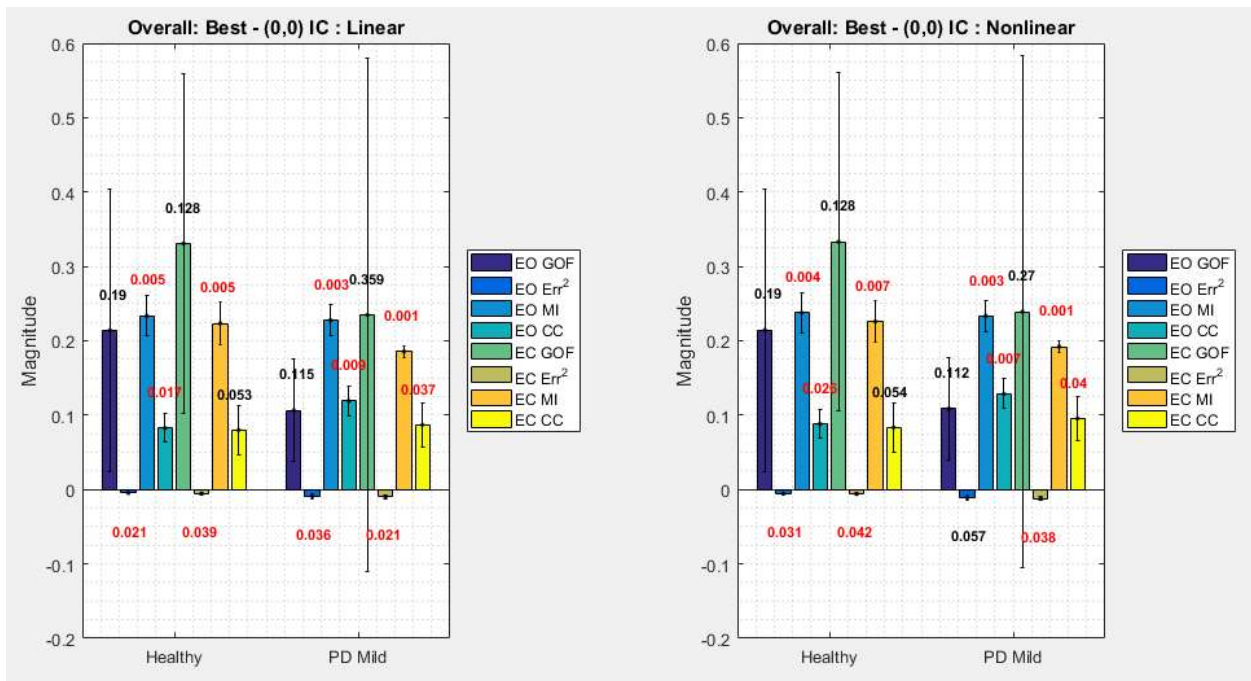


Figure 5 - PD-Mi-Study: Overall Comparison of Optimized and Zero ICs in EO and EC

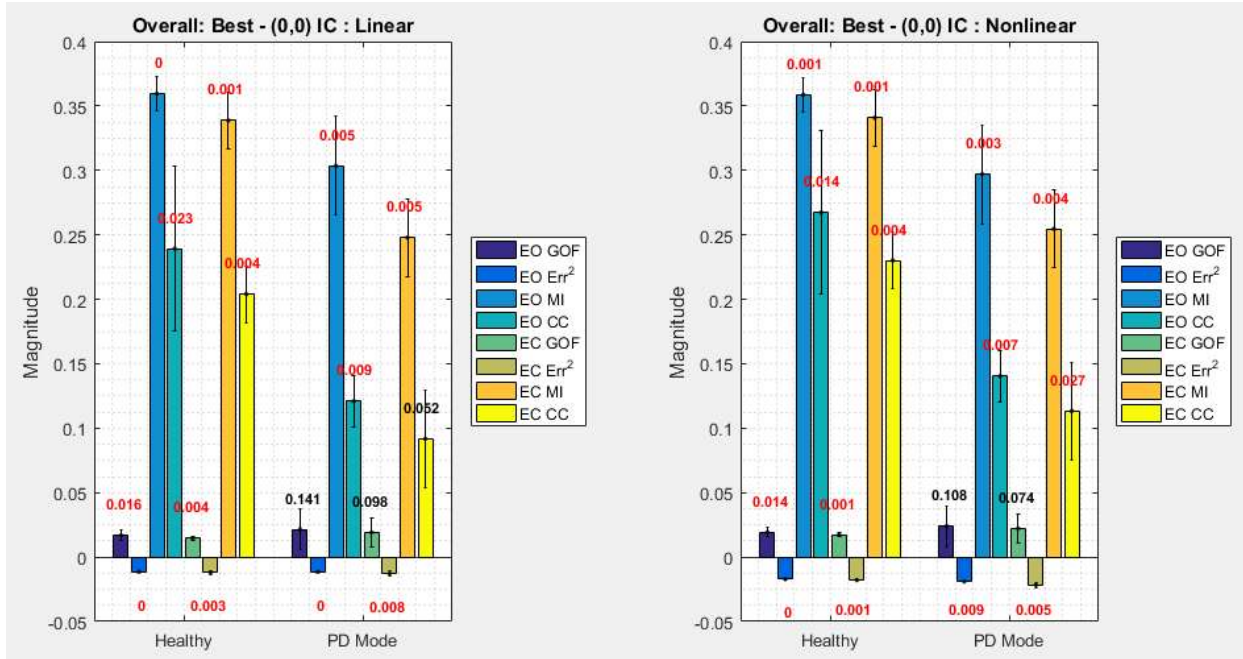


Figure 6 - PD-Mo-Study: Overall Comparison of Optimized and Zero ICs in EO and EC

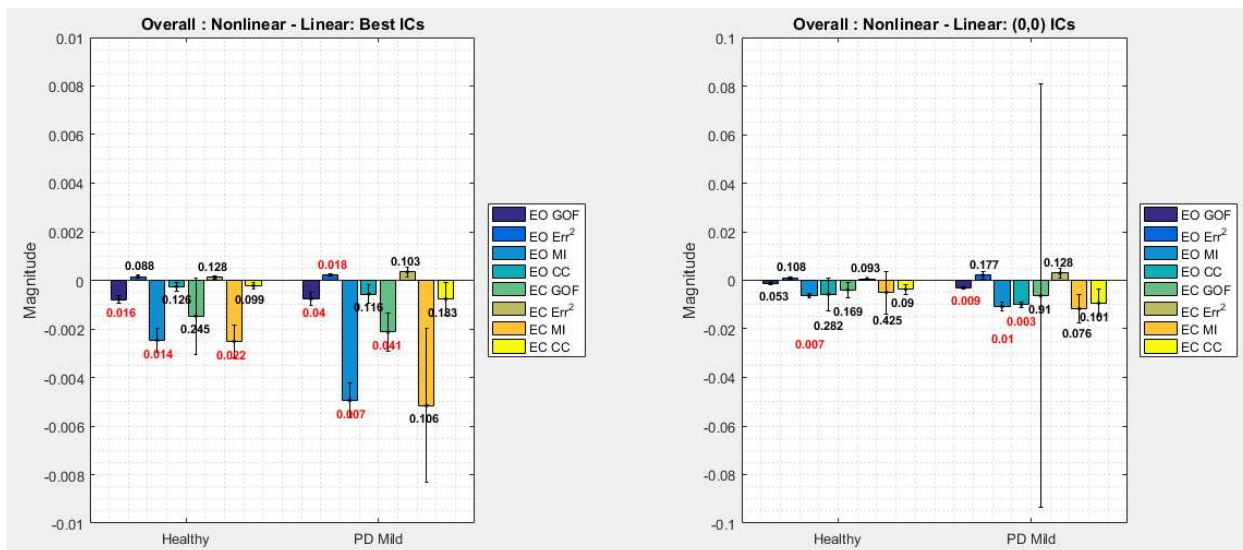


Figure 7 - PD-Mi-Study: Overall Comparison of Nonlinear/Linear Differential Equation

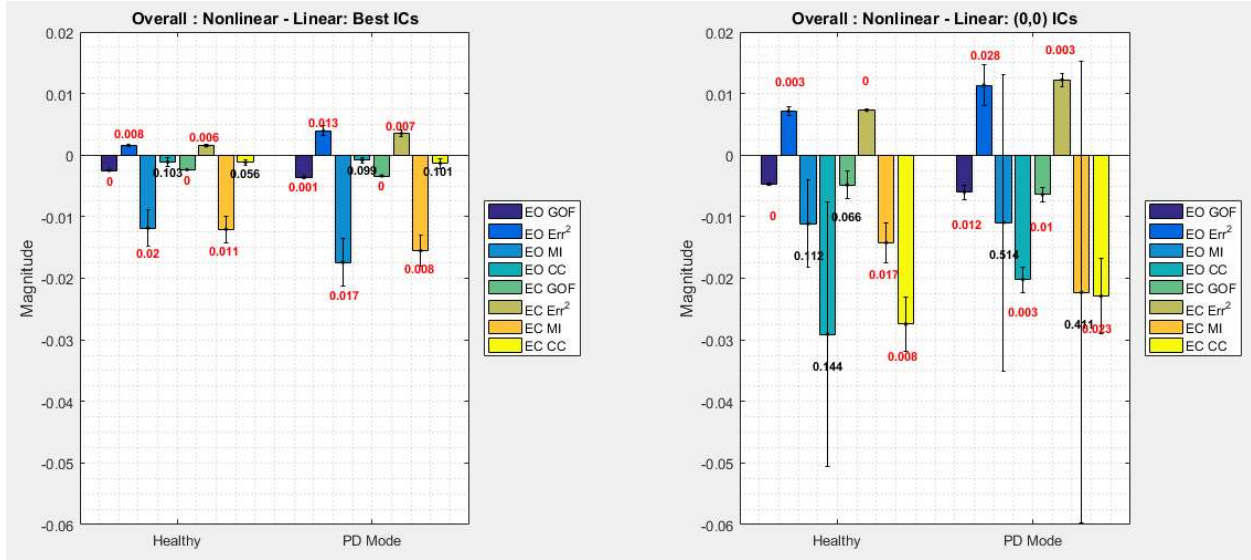


Figure 8 - PD-Mo-Study: Overall Comparison of Nonlinear/Linear Differential Equation

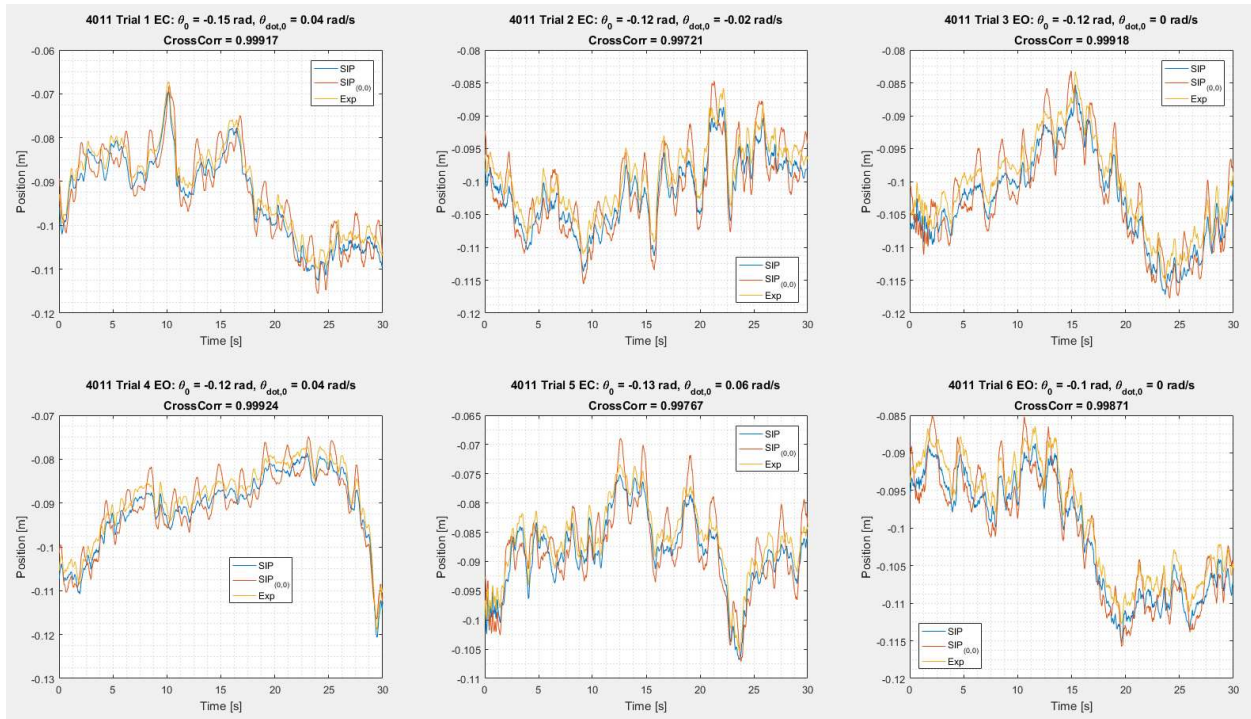


Figure 9 - PD-Mo-Study (Sub 4011): Comparison of  $COP_{exp}$  and  $COP_{SIP}$  with Optimized/Zero ICs

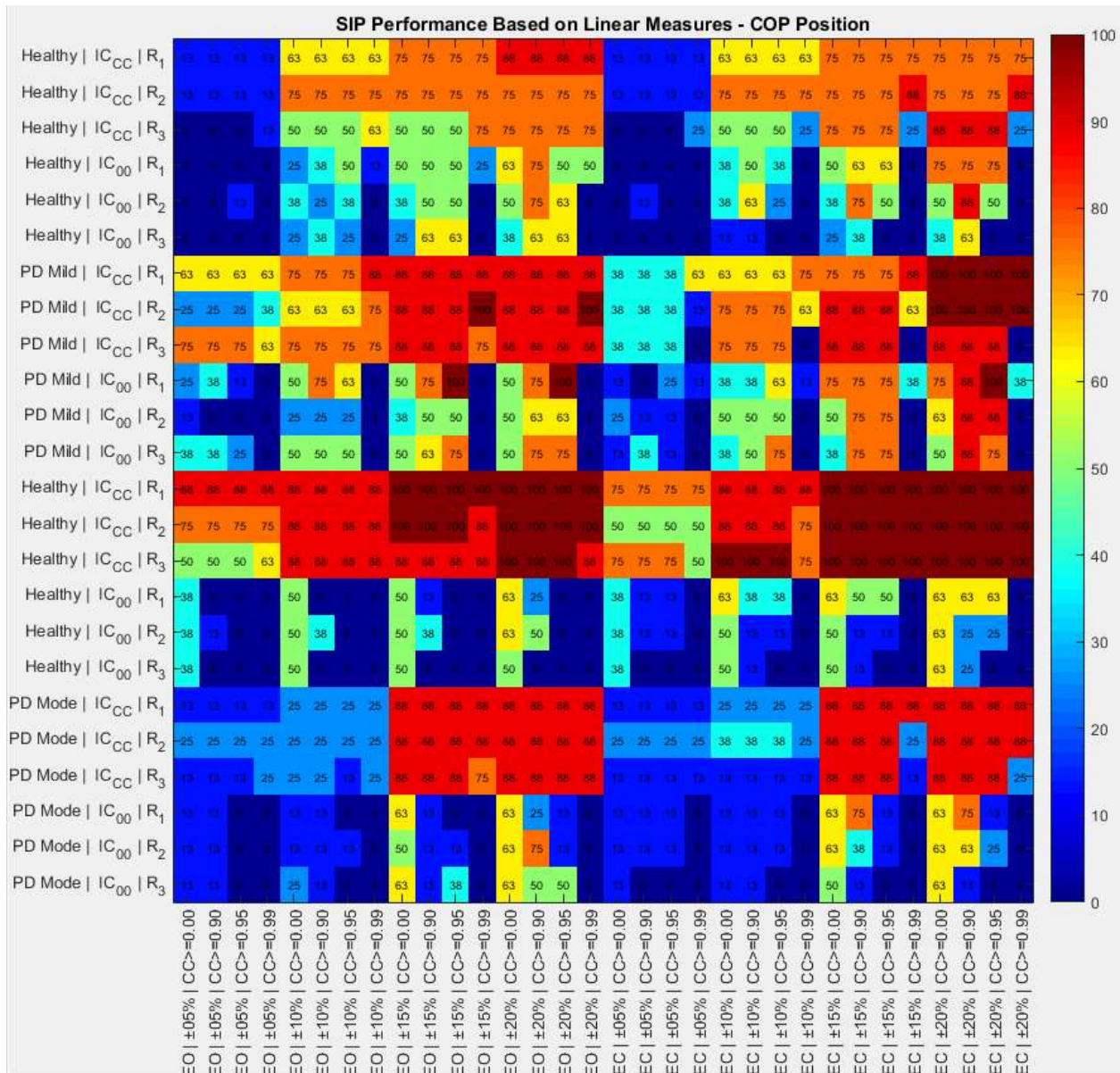


Figure 10 - SIP Linear Performance Based on Linear Measures on COP<sub>Pos</sub>

Percent of linear measures extracted from the  $COP_{SIP(CC)}$  and  $COP_{SIP(0,0)}$  that had an average error when compared to  $COP_{exp}$  within a  $\pm 5\%$ ,  $\pm 10\%$ ,  $\pm 15\%$ , and  $\pm 20\%$  ( $\alpha = 0.05$ ) based on subject groups, EO and EC, trials ( $R_1, R_2, R_3$ ), and similarity between  $COP_{exp}$  and  $COP_{SIP(CC)}$  or  $COP_{SIP(0,0)}$  (CrossCorr > 0, 0.9, 0.95, 0.99)

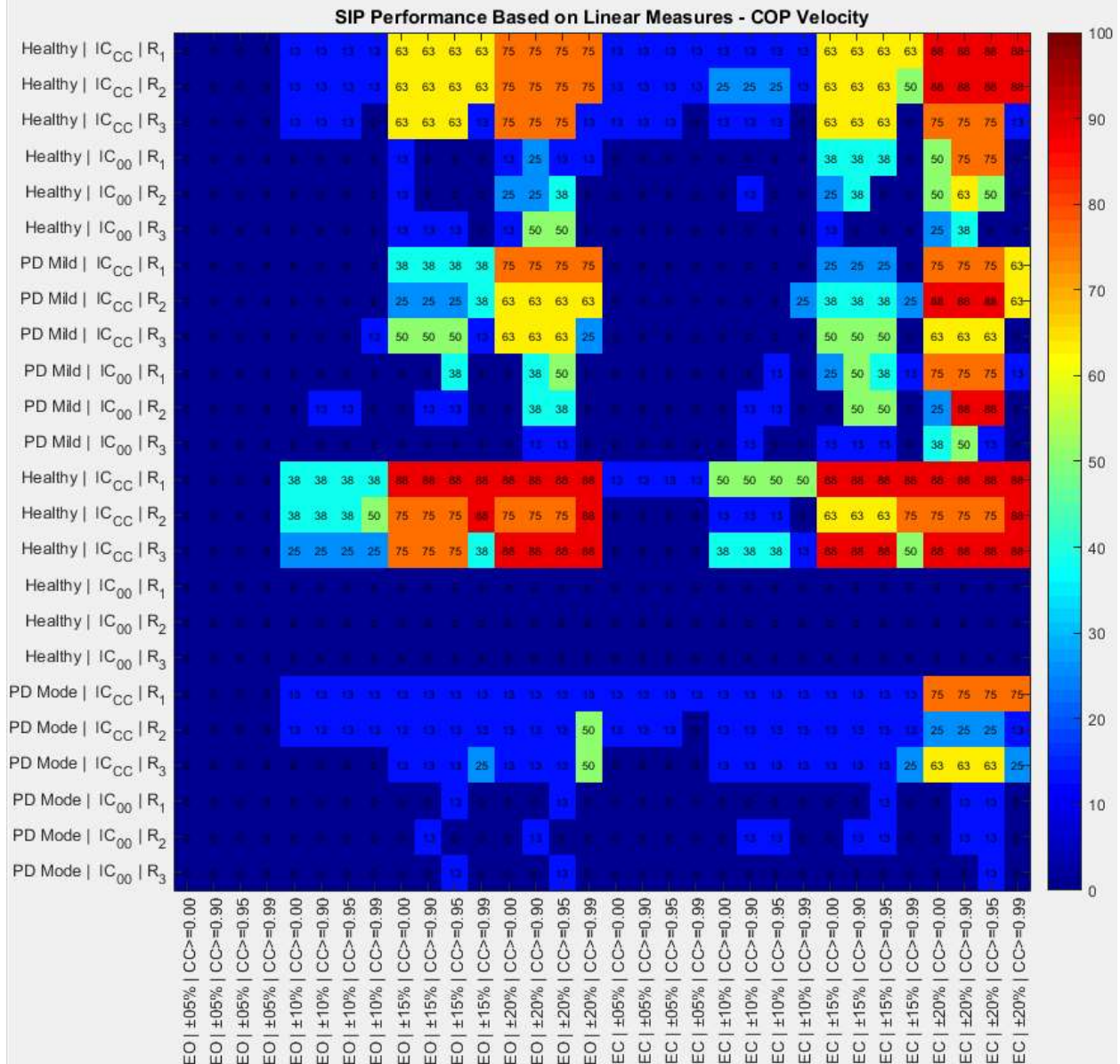


Figure 11 - SIP Linear Performance Based on Linear Measures on COP<sub>vel</sub>

Percent of linear measures extracted from the first derivative of  $COP_{SIP(CC)}$  and  $COP_{SIP(0,0)}$  with respect to time that had an average error when compared to  $COP_{exp}$  within a  $\pm 5\%$ ,  $\pm 10\%$ ,  $\pm 15\%$ , and  $\pm 20\%$  ( $\alpha = 0.05$ ) based on subject groups, EO and EC, trials ( $R_1, R_2, R_3$ ), and similarity between  $COP_{exp}$  and  $COP_{SIP(CC)}$  or  $COP_{SIP(0,0)}$  ( $CrossCorr > 0, 0.9, 0.95, 0.99$ )

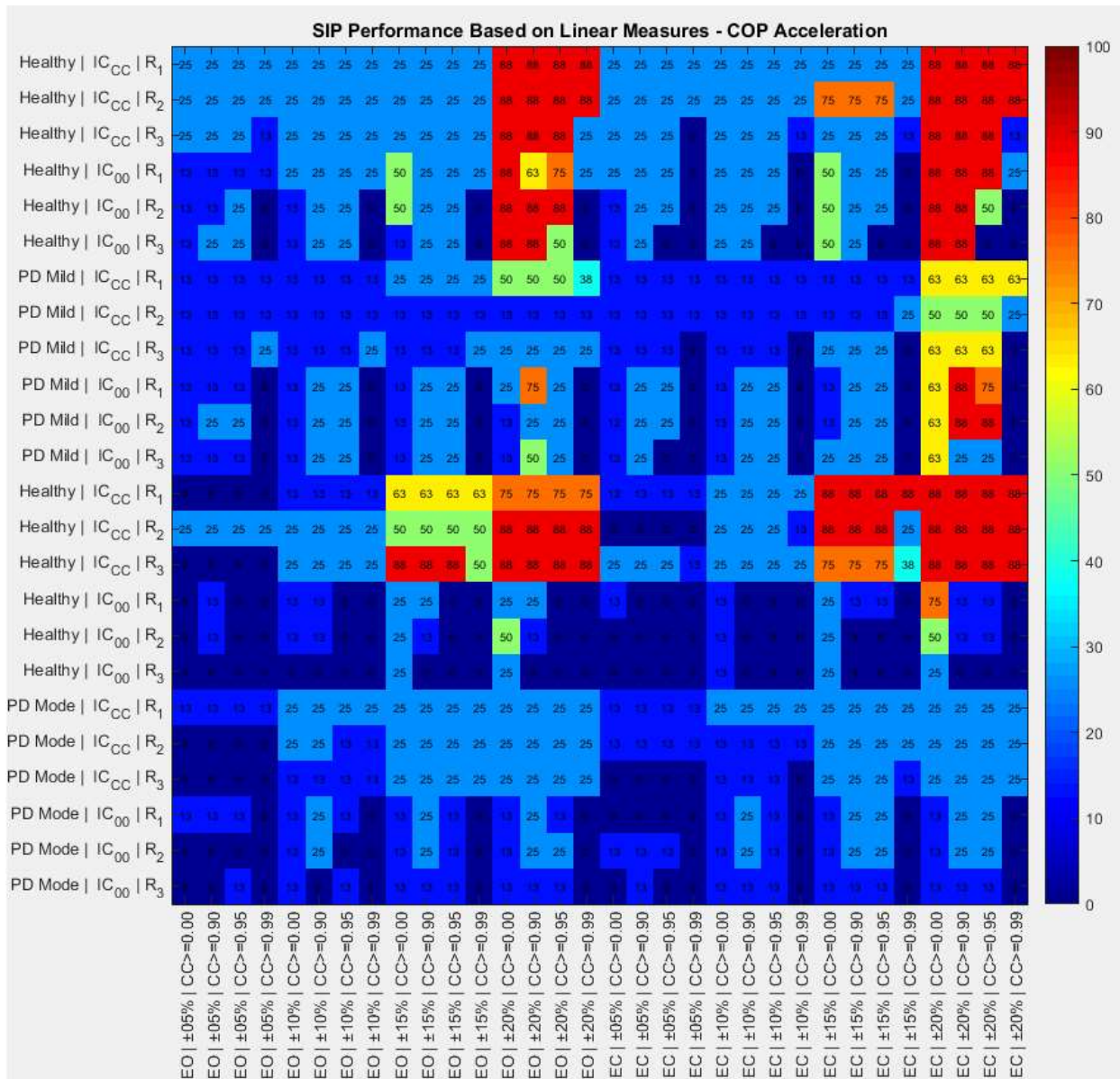


Figure 12 - SIP Linear Performance Based on Linear Measures on COP<sub>Acc</sub>

Percent of linear measures extracted from the second derivative of  $COP_{SIP(CC)}$  and  $COP_{SIP(0,0)}$  with respect to time that had an average error when compared to  $COP_{exp}$  within a  $\pm 5\%$ ,  $\pm 10\%$ ,  $\pm 15\%$ , and  $\pm 20\%$  ( $\alpha = 0.05$ ) based on subject groups, EO and EC, trials ( $R_1, R_2, R_3$ ), and similarity between  $COP_{exp}$  and  $COP_{SIP(CC)}$  or  $COP_{SIP(0,0)}$  (CrossCorr > 0, 0.9, 0.95, 0.99)

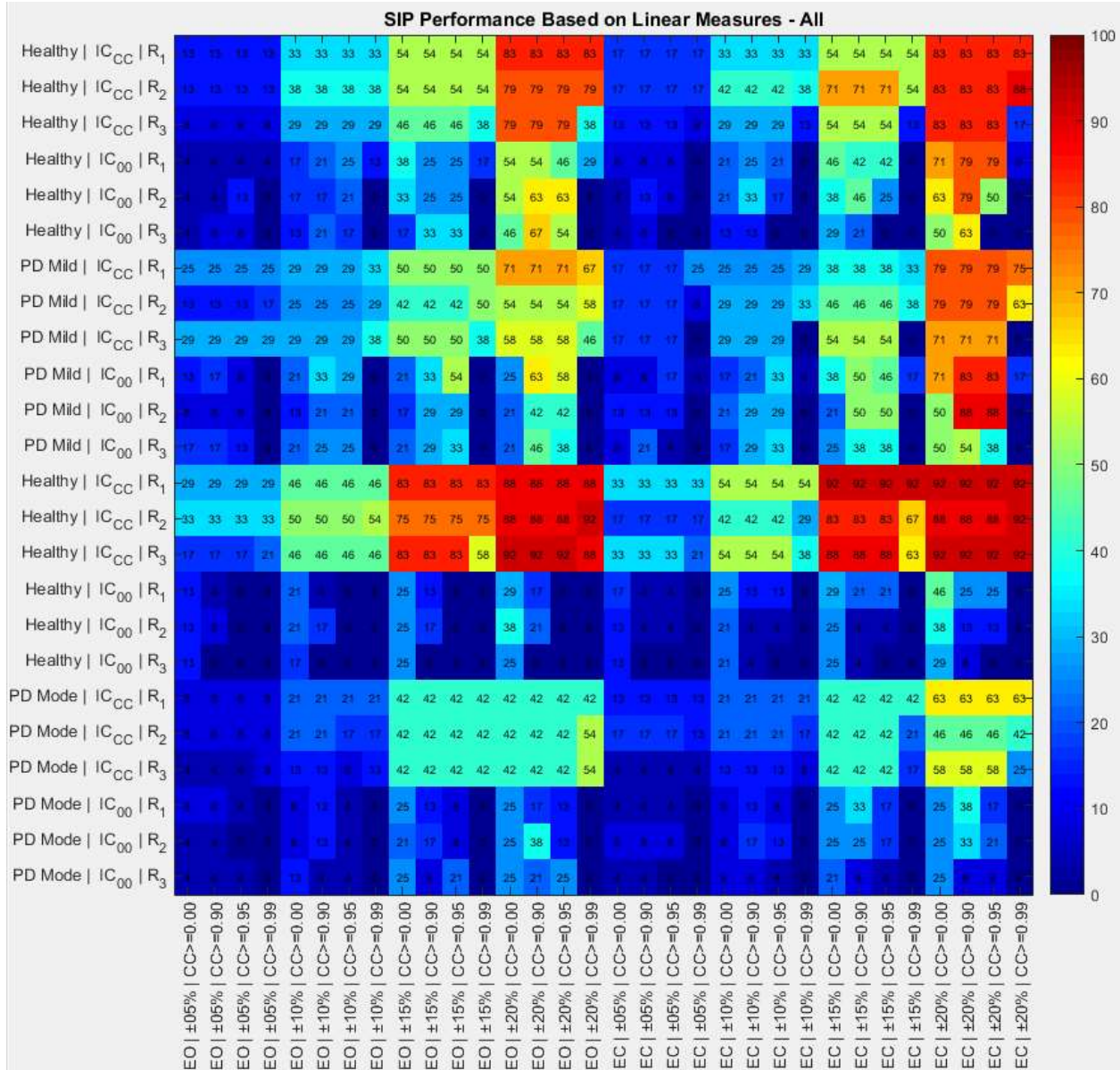


Figure 13 - SIP Linear Performance Based on Linear Measures on  $COP_{Pos}$ ,  $COP_{Vel}$  and  $COP_{Acc}$

Percent of linear measures extracted from the  $COP_{SIP(CC)}$  and  $COP_{SIP(0,0)}$ , and their first and second derivatives, that had an average error when compared to  $COP_{exp}$  within a  $\pm 5\%$ ,  $\pm 10\%$ ,  $\pm 15\%$ , and  $\pm 20\%$  ( $\alpha = 0.05$ ) based on subject groups, EO and EC, trials ( $R_1$ ,  $R_2$ ,  $R_3$ ), and similarity between  $COP_{exp}$  and  $COP_{SIP(CC)}$  or  $COP_{SIP(0,0)}$  ( $CrossCorr > 0, 0.9, 0.95, 0.99$ )

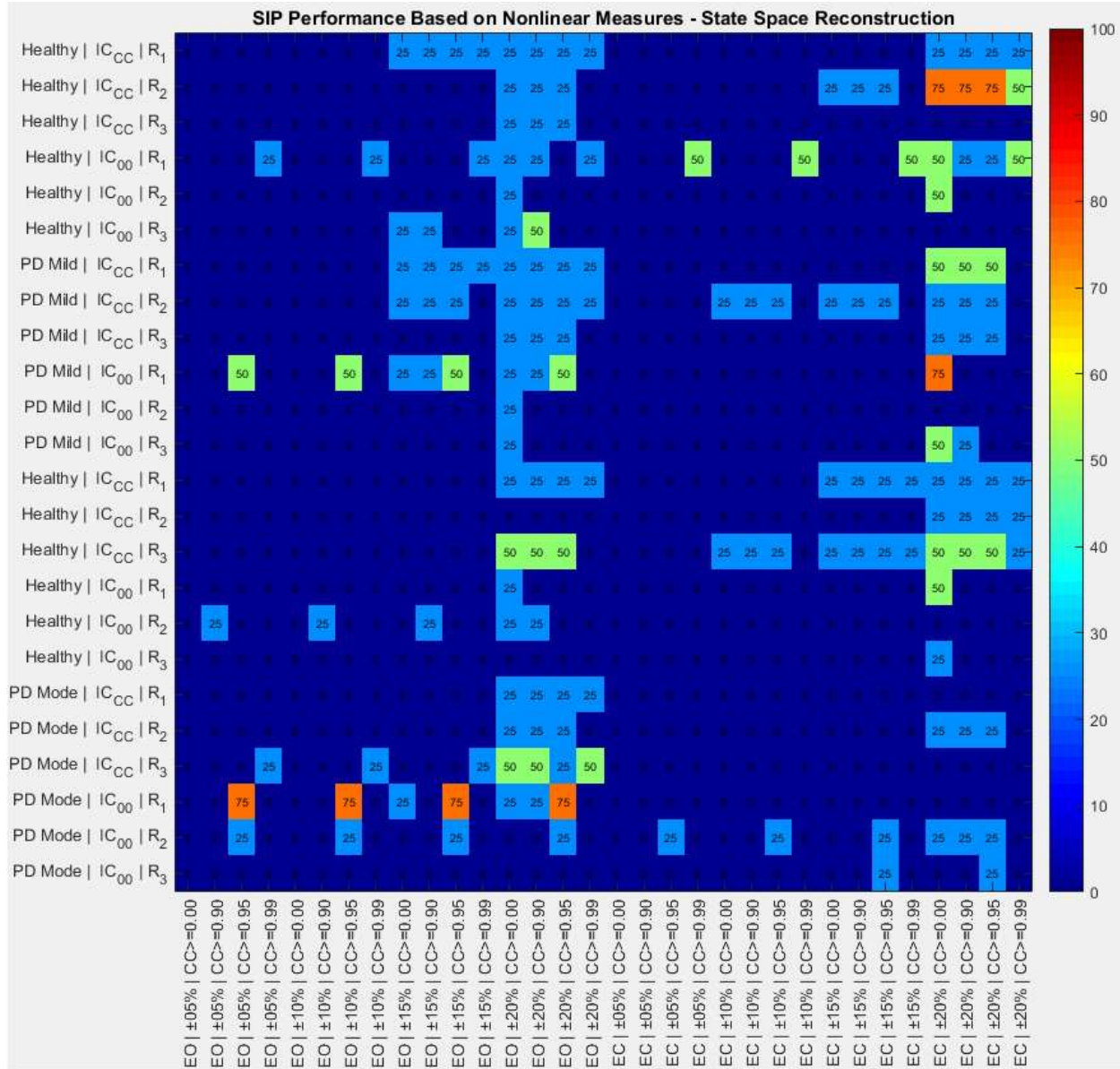


Figure 14 - SIP Nonlinear Performance Based on  $\tau$  and EmbDim

Percent of State-Space Reconstruction nonlinear measures extracted from the  $COP_{SIP(CC)}$  and  $COP_{SIP(0,0)}$  that had an average error when compared to  $COP_{exp}$  within a  $\pm 5\%$ ,  $\pm 10\%$ ,  $\pm 15\%$ , and  $\pm 20\%$  ( $\alpha = 0.05$ ) based on subject groups, EO and EC, trials ( $R_1$ ,  $R_2$ ,  $R_3$ ), and similarity between  $COP_{exp}$  and  $COP_{SIP(CC)}$  or  $COP_{SIP(0,0)}$  (CrossCorr > 0.9, 0.95, 0.99)

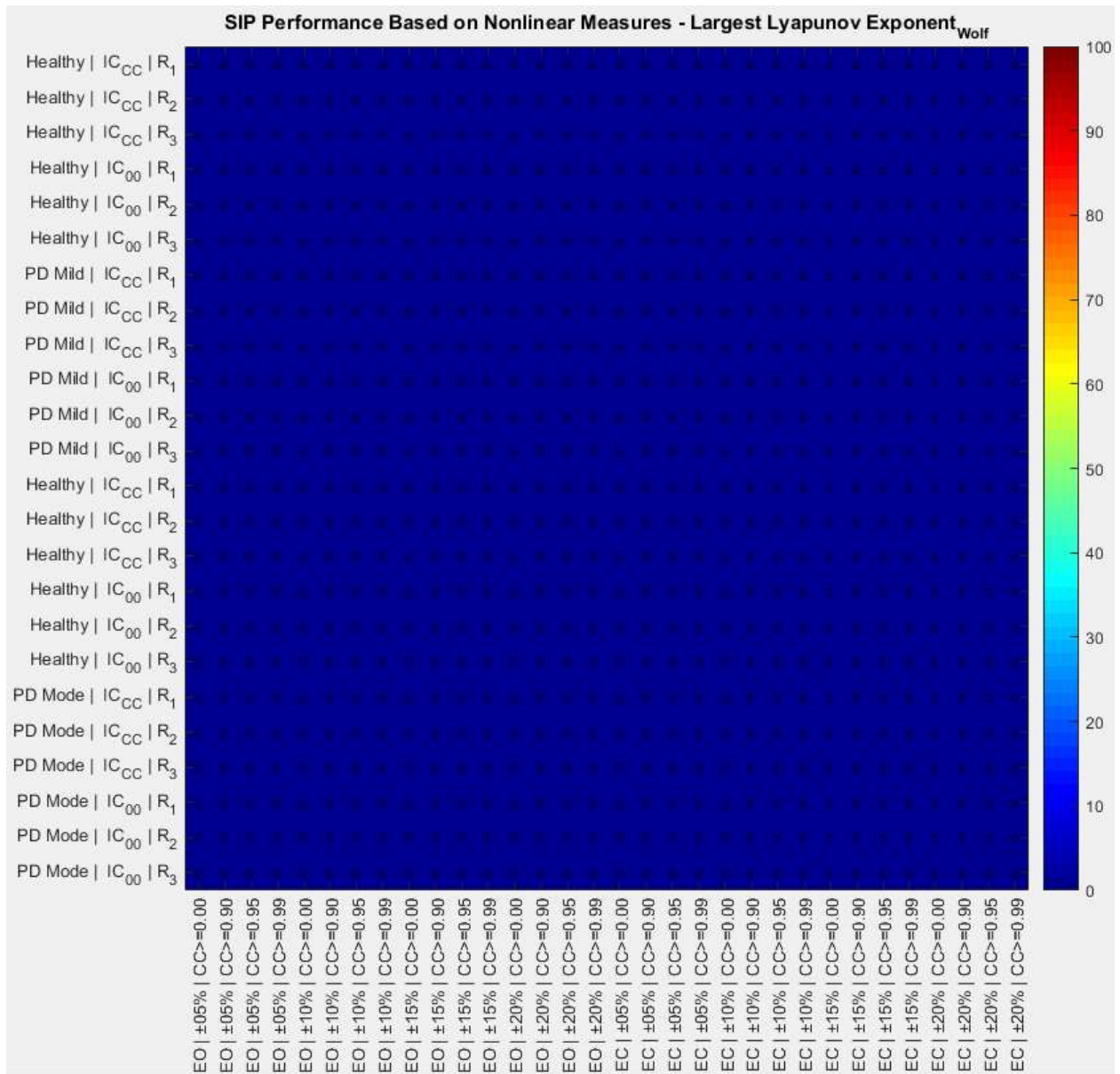


Figure 15 - SIP Nonlinear Performance Based on LLE

Percent of Largest Lyapunov Exponent nonlinear measures extracted from the  $COP_{SIP(CC)}$  and  $COP_{SIP(0,0)}$  that had an average error when compared to  $COP_{exp}$  within a  $\pm 5\%$ ,  $\pm 10\%$ ,  $\pm 15\%$ , and  $\pm 20\%$  ( $\alpha = 0.05$ ) based on subject groups, EO and EC, trials ( $R_1$ ,  $R_2$ ,  $R_3$ ), and similarity between  $COP_{exp}$  and  $COP_{SIP(CC)}$  or  $COP_{SIP(0,0)}$  (CrossCorr > 0, 0.9, 0.95, 0.99)

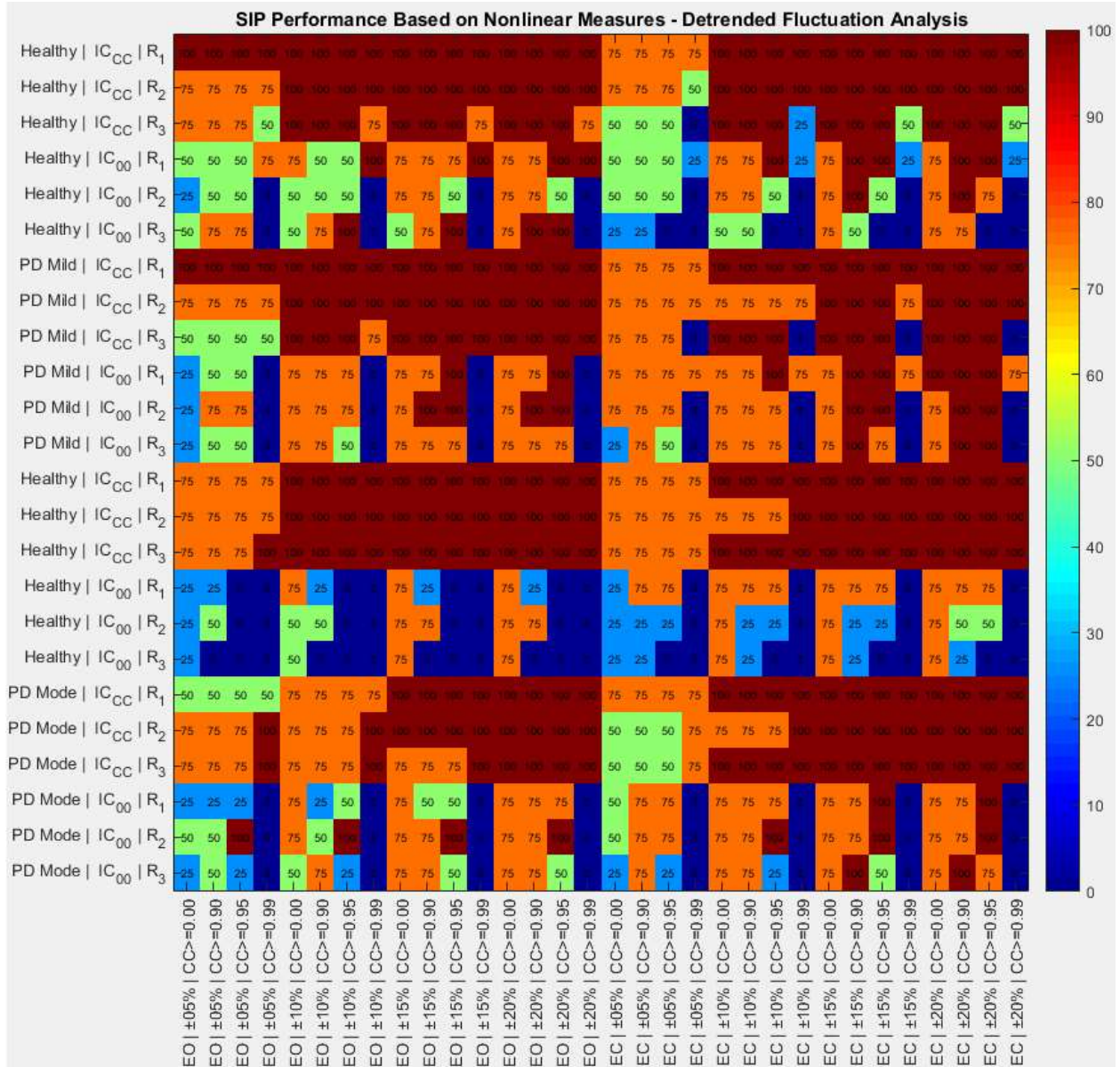


Figure 16 - SIP Nonlinear Performance Based on DFA

Percent of Detrended Fluctuation Analysis nonlinear measures extracted from the COPSIP (CC) and COPSIP (0,0) that had an average error when compared to COPexp within a  $\pm 5\%$ ,  $\pm 10\%$ ,  $\pm 15\%$ , and  $\pm 20\%$  ( $\alpha = 0.05$ ) based on subject groups, EO and EC, trials ( $R_1$ ,  $R_2$ ,  $R_3$ ), and similarity between COPexp and COPSIP (CC) or COPSIP (0,0) (CrossCorr > 0, 0.9, 0.95, 0.99)

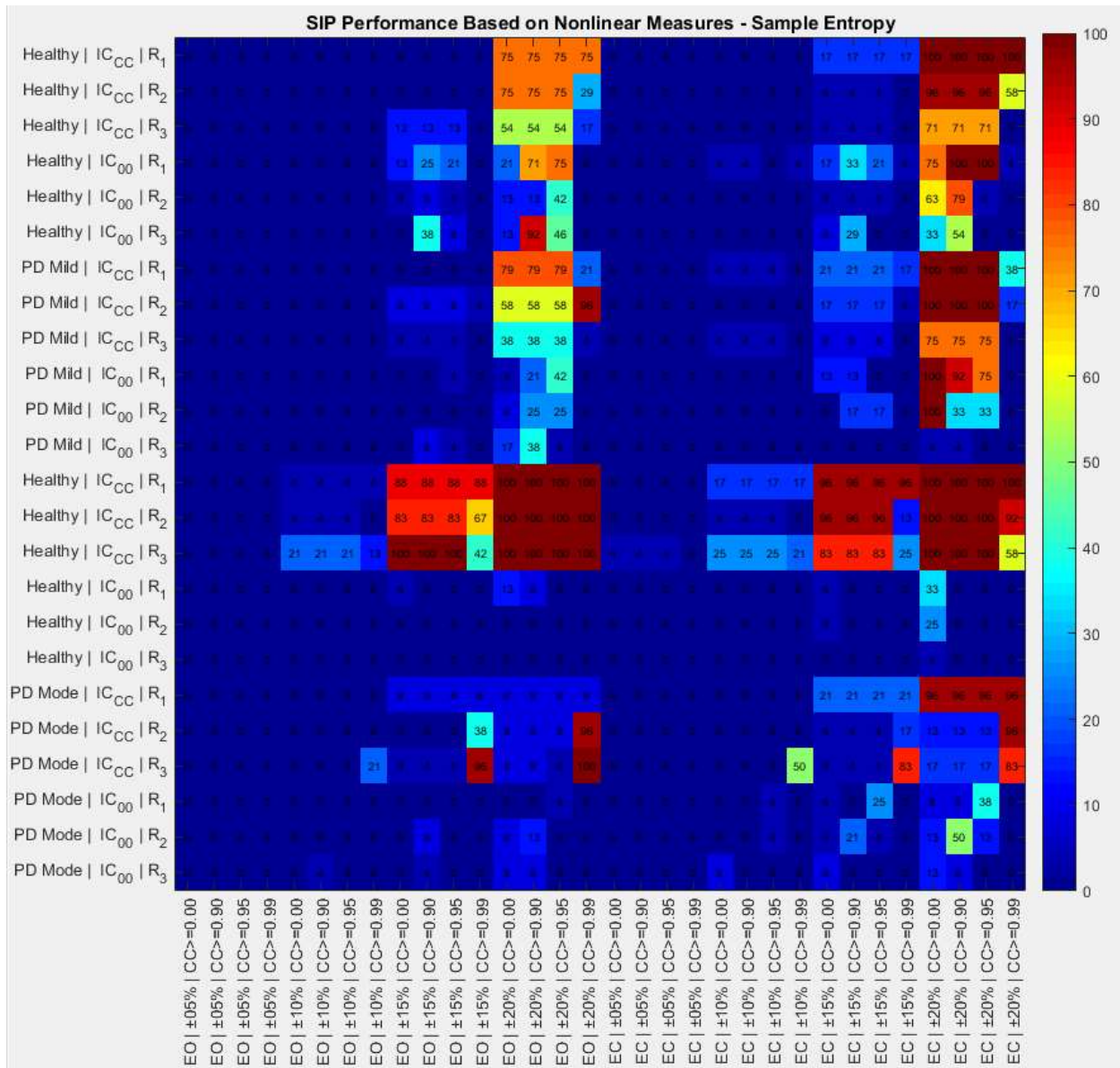


Figure 17 - SIP Nonlinear Performance Based on SE

Percent of Sample Entropy nonlinear measures extracted from the  $COP_{SIP(CC)}$  and  $COP_{SIP(0,0)}$  that had an average error when compared to  $COP_{exp}$  within a  $\pm 5\%$ ,  $\pm 10\%$ ,  $\pm 15\%$ , and  $\pm 20\%$  ( $\alpha = 0.05$ ) based on subject groups, EO and EC, trials ( $R_1, R_2, R_3$ ), and similarity between  $COP_{exp}$  and  $COP_{SIP(CC)}$  or  $COP_{SIP(0,0)}$  (CrossCorr > 0, 0.9, 0.95, 0.99)

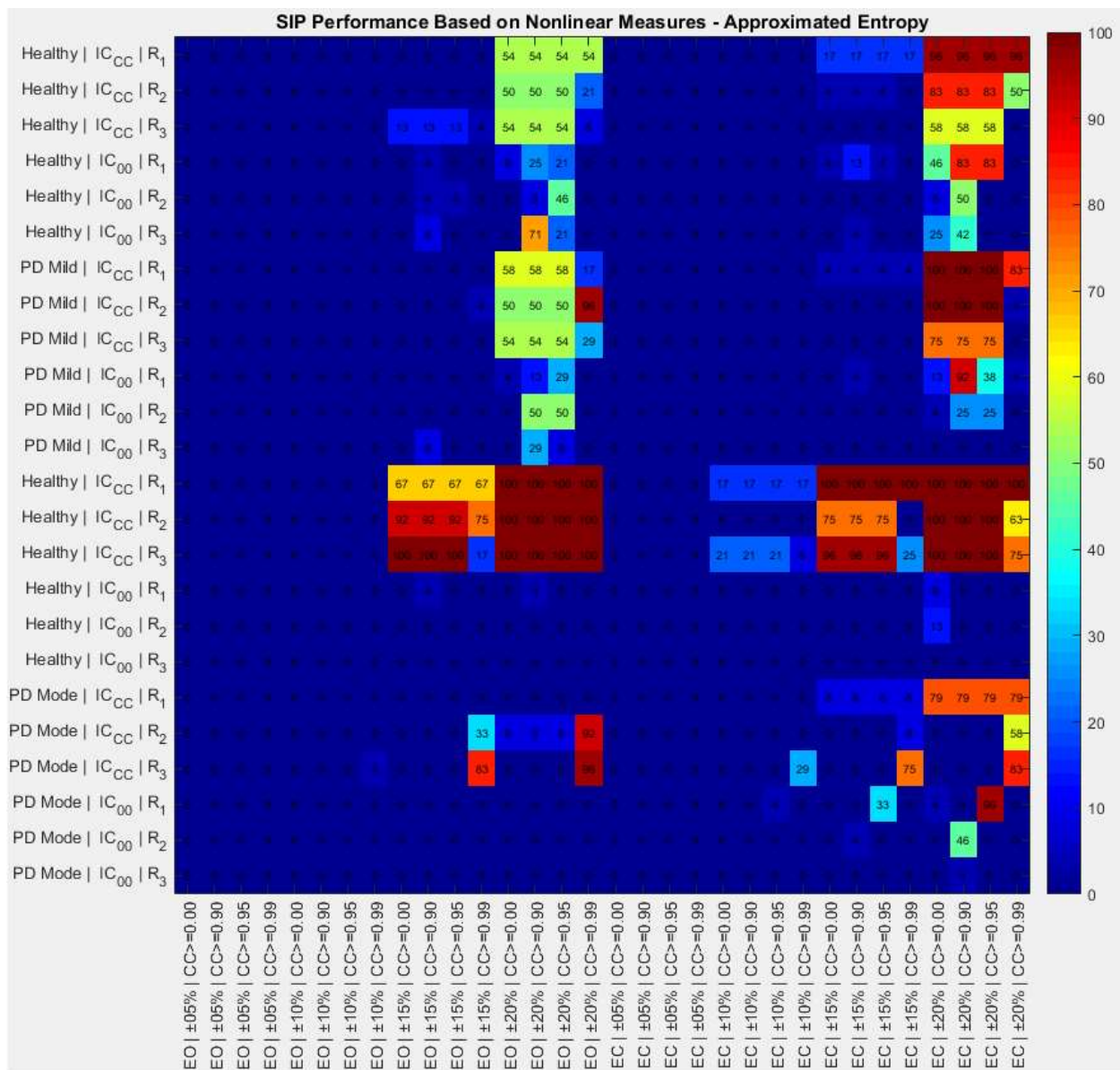


Figure 18 - SIP Nonlinear Performance Based on AE

Percent of Approximated Entropy nonlinear measures extracted from the  $COP_{SIP(CC)}$  and  $COP_{SIP(0,0)}$  that had an average error when compared to  $COP_{exp}$  within a  $\pm 5\%$ ,  $\pm 10\%$ ,  $\pm 15\%$ , and  $\pm 20\%$  ( $\alpha = 0.05$ ) based on subject groups, EO and EC, trials ( $R_1, R_2, R_3$ ), and similarity between  $COP_{exp}$  and  $COP_{SIP(CC)}$  or  $COP_{SIP(0,0)}$  (CrossCorr > 0, 0.9, 0.95, 0.99)

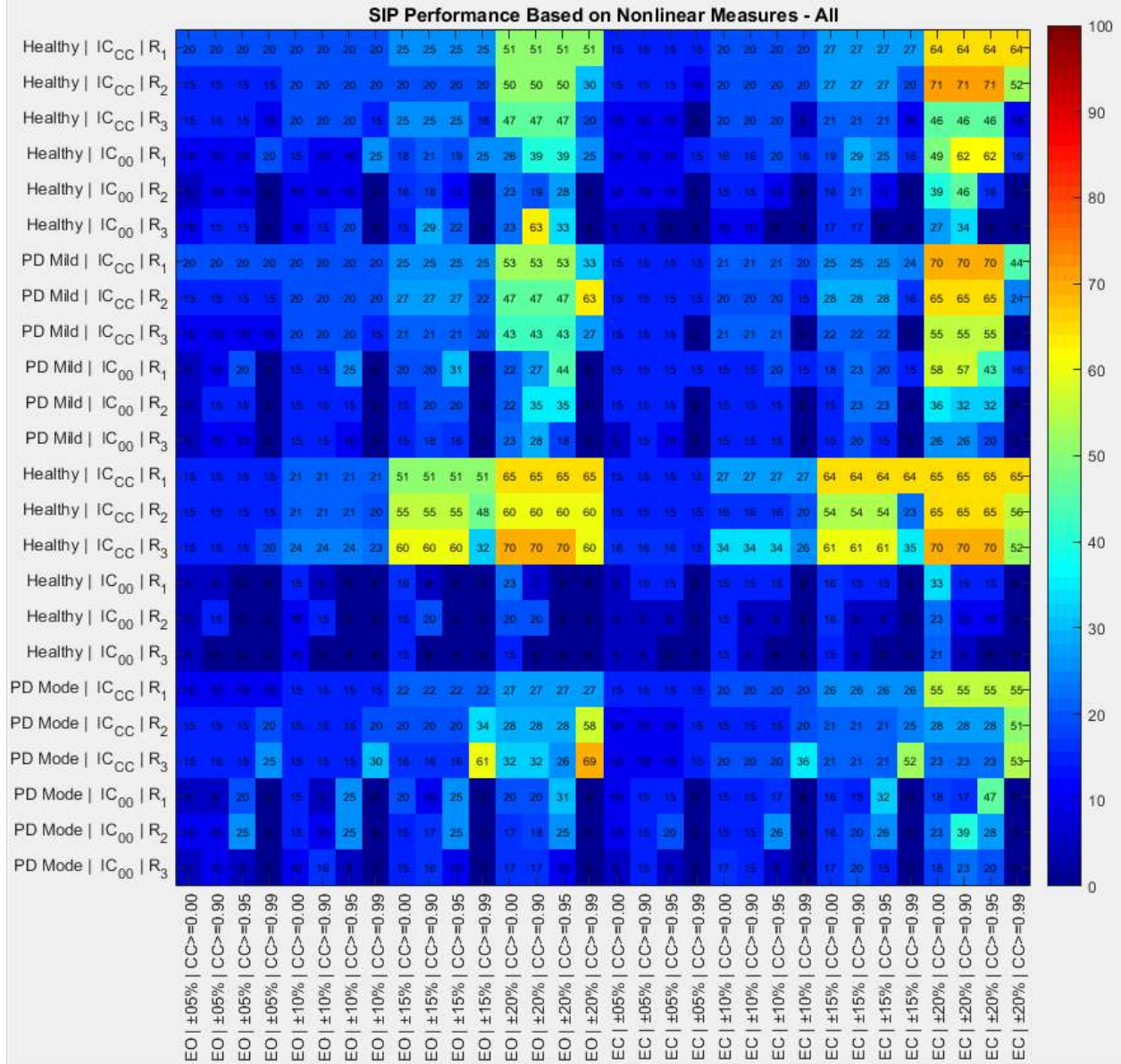


Figure 19 - SIP Nonlinear Performance Based on All Nonlinear Measures

Percent of all nonlinear measures extracted from the  $COP_{SIP(CC)}$  and  $COP_{SIP(0,0)}$  that had an average error when compared to  $COP_{exp}$  within a  $\pm 5\%$ ,  $\pm 10\%$ ,  $\pm 15\%$ , and  $\pm 20\%$  ( $\alpha = 0.05$ ) based on subject groups, EO and EC, trials ( $R_1$ ,  $R_2$ ,  $R_3$ ), and similarity between  $COP_{exp}$  and  $COP_{SIP(CC)}$  or  $COP_{SIP(0,0)}$  (CrossCorr > 0, 0.9, 0.95, 0.99)

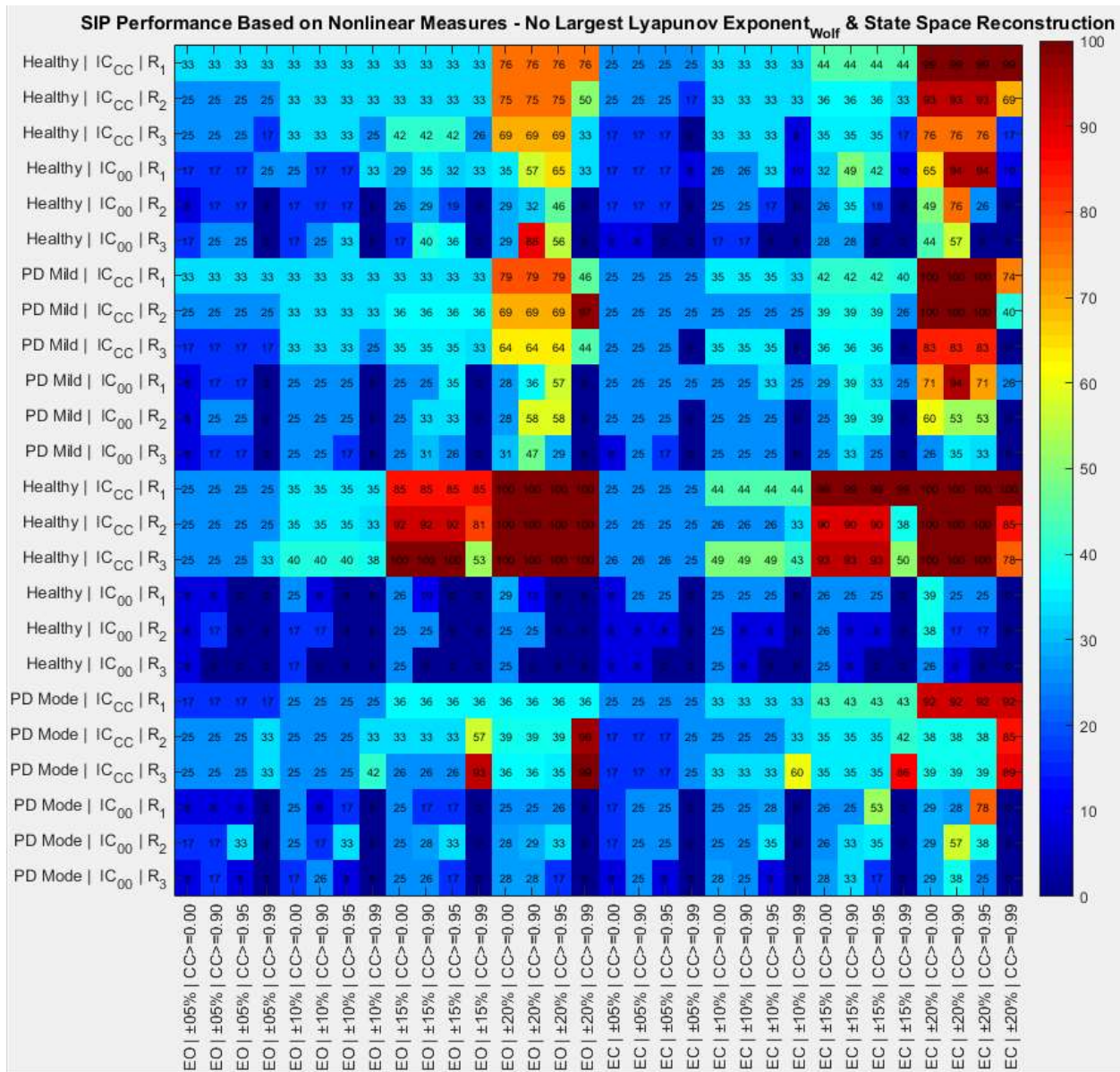


Figure 20 - SIP Nonlinear Performance Based on All Nonlinear Measures (Except  $\tau$ , EmbDim, and LLE)

Percent of all nonlinear measures (Except  $\tau$ , EmbDim, and LLE) extracted from the  $COP_{SIP(CC)}$  and  $COP_{SIP(0,0)}$  that had an average error when compared to  $COP_{exp}$  within a  $\pm 5\%$ ,  $\pm 10\%$ ,  $\pm 15\%$ , and  $\pm 20\%$  ( $\alpha = 0.05$ ) based on subject groups, EO and EC, trials ( $R_1$ ,  $R_2$ ,  $R_3$ ), and similarity between  $COP_{exp}$  and  $COP_{SIP(CC)}$  or  $COP_{SIP(0,0)}$  (CrossCorr > 0, 0.9, 0.95, 0.99)

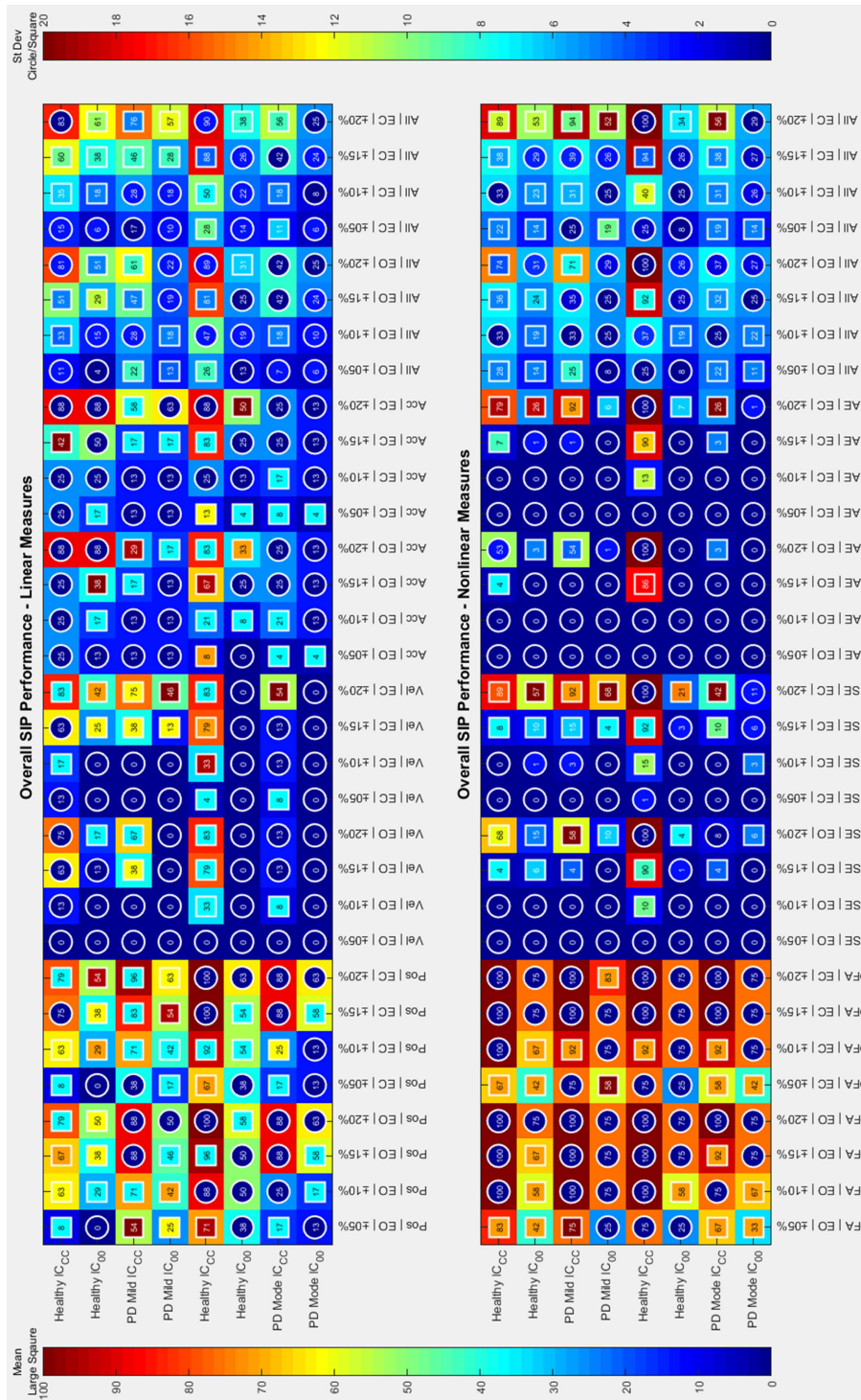


Figure 21 - SIP Linear and Nonlinear Overall Performance

Average between trials without CrossCorr restrictions (CrossCorr > 0) of percent of linear ( $COP_{Pos}$ ,  $COP_{Vel}$ ,  $COP_{Acc}$ , and All linear measures) and nonlinear (DFA, SE, AE, and All nonlinear measures except  $\tau$ , EmbDim, LLE) measures extracted from the  $COP_{SIP(CC)}$  and  $COP_{SIP(0,0)}$  that had an average error when compared to  $COP_{exp}$  within a  $\pm 5\%$ ,  $\pm 10\%$ ,  $\pm 15\%$ , and  $\pm 20\%$  ( $\alpha = 0.05$ ) based on subject groups, and EO and EC. Outside color (left color bar) represents the average between trials, while inside color (right color bar) represents the standard deviation. Average values enclosed by a circle indicate that the variability of percentages between trials was less than  $\pm 5\%$  ( $\alpha = 0.05$ ); otherwise the average value is enclosed by a square.

## 8 References

- Asai, Y., Tasaka, Y., Nomura, K., Nomura, T., Casadio, M., Morasso, P., 2009. A model of postural control in quiet standing: robust compensation of delay-induced instability using intermittent activation of feedback control. *PLoS One* 4, e6169. doi:10.1371/journal.pone.0006169
- Barnds, A.N., 2015. Biomechanical markers as indicators of postural instability progression in Parkinson's disease (D.Eng.). University of Kansas, United States -- Kansas.
- Benjamini, Y., Hochberg, Y., 1995. Controlling the False Discovery Rate: A Practical and Powerful Approach to Multiple Testing. *J. R. Stat. Soc. Ser. B Methodol.* 57, 289–300.
- Błaszczyk, J.W., Orawiec, R., Duda-Kłodowska, D., Opala, G., 2007. Assessment of postural instability in patients with Parkinson's disease. *Exp. Brain Res.* 183, 107–114. doi:10.1007/s00221-007-1024-y
- Bloem, B.R., Hausdorff, J.M., Visser, J.E., Giladi, N., 2004. Falls and freezing of gait in Parkinson's disease: a review of two interconnected, episodic phenomena. *Mov. Disord. Off. J. Mov. Disord. Soc.* 19, 871–884. doi:10.1002/mds.20115
- Boonstra, T.A., Schouten, A.C., Van der Kooij, H., 2013. Identification of the contribution of the ankle and hip joints to multi-segmental balance control. *J. NeuroEngineering Rehabil. JNER* 10, 1–18. doi:10.1186/1743-0003-10-23
- Bottaro, A., Yasutake, Y., Nomura, T., Casadio, M., Morasso, P., 2008. Bounded stability of the quiet standing posture: An intermittent control model. *Hum. Mov. Sci.* 27, 473–495. doi:10.1016/j.humov.2007.11.005
- Boyas, S., Hajj, M., Bilodeau, M., 2013. Influence of ankle plantarflexor fatigue on postural sway, lower limb articular angles, and postural strategies during unipedal quiet standing. *Gait Posture* 37, 547–551. doi:10.1016/j.gaitpost.2012.09.014
- Carpenter, M.G., Allum, J.H.J., Honegger, F., Adkin, A.L., Bloem, B.R., 2004. Postural abnormalities to multidirectional stance perturbations in Parkinson's disease. *J. Neurol. Neurosurg. Psychiatry* 75, 1245–1254. doi:10.1136/jnnp.2003.021147
- Chagdes, J.R., Huber, J.E., Saletta, M., Darling-White, M., Raman, A., Rietdyk, S., Zelaznik, H.N., Haddad, J.M., 2016a. The relationship between intermittent limit cycles and postural instability associated with Parkinson's disease. *J. Sport Health Sci.* 5, 14–24. doi:10.1016/j.jshs.2016.01.005
- Chagdes, J.R., Rietdyk, S., Haddad, J.M., Zelaznik, H.N., Cinelli, M.E., Denomme, L.T., Powers, K.C., Raman, A., 2016b. Limit cycle oscillations in standing human posture. *J. Biomech.* 49, 1170–1179. doi:10.1016/j.jbiomech.2016.03.005
- Collins, J.J., De Luca, C.J., 1994. Random Walking during Quiet Standing. *Phys. Rev. Lett.* 73, 764–767. doi:10.1103/PhysRevLett.73.764
- Costello, K.E., Matrangola, S.L., Madigan, M.L., 2012. Independent effects of adding weight and inertia on balance during quiet standing. *Biomed. Eng. Online* 11, 20. doi:10.1186/1475-925X-11-20
- Crétual, A., 2015. Which biomechanical models are currently used in standing posture analysis? *Neurophysiol. Clin. Clin. Neurophysiol.* 45, 285–295. doi:10.1016/j.neucli.2015.07.004
- de Lau, L.M.L., Breteler, M.M.B., 2006. Epidemiology of Parkinson's disease. *Lancet Neurol.* 5, 525–535. doi:10.1016/S1474-4422(06)70471-9
- Delignières, D., Torre, K., Bernard, P.-L., 2011. Transition from Persistent to Anti-Persistent Correlations in Postural Sway Indicates Velocity-Based Control. *PLoS Comput. Biol.* 7, 1–10. doi:10.1371/journal.pcbi.1001089
- Doná, F., Aquino, C.C., Gazzola, J.M., Borges, V., Silva, S.M.C.A., Ganança, F.F., Caovilla, H.H., Ferraz, H.B., 2016. Changes in postural control in patients with Parkinson's disease: a posturographic study. *Physiotherapy* 102, 272–279. doi:10.1016/j.physio.2015.08.009
- Federolf, P., Roos, L., Nigg, B.M., 2013. Analysis of the multi-segmental postural movement strategies utilized in bipedal, tandem and one-leg stance as quantified by a principal component

- decomposition of marker coordinates. *J. Biomech.* 46, 2626–2633.  
doi:10.1016/j.jbiomech.2013.08.008
- Fraser, null, Swinney, null, 1986. Independent coordinates for strange attractors from mutual information. *Phys. Rev. Gen. Phys.* 33, 1134–1140.
- Fujisawa, N., Masuda, T., Inaoka, H., Fukuoka, Y., Ishida, A., Minamitani, H., 2005. Human standing posture control system depending on adopted strategies. *Med. Biol. Eng. Comput.* 43, 107–114.  
doi:10.1007/BF02345130
- Gage, W.H., Winter, D.A., Frank, J.S., Adkin, A.L., 2004. Kinematic and kinetic validity of the inverted pendulum model in quiet standing. *Gait Posture* 19, 124–132. doi:10.1016/S0966-6362(03)00037-7
- Gervasoni, E., Cattaneo, D., Messina, P., Casati, E., Montesano, A., Bianchi, E., Beghi, E., 2015. Clinical and stabilometric measures predicting falls in Parkinson disease/parkinsonisms. *Acta Neurol. Scand.* 132, 235–241. doi:10.1111/ane.12388
- Günther, M., Grimmer, S., Siebert, T., Blickhan, R., 2009. All leg joints contribute to quiet human stance: A mechanical analysis. *J. Biomech.* 42, 2739–2746. doi:10.1016/j.jbiomech.2009.08.014
- Horak, F.B., Frank, J., Nutt, J., 1996. Effects of dopamine on postural control in parkinsonian subjects: scaling, set, and tone. *J. Neurophysiol.* 75, 2380–2396.
- Horak, F.B., Nashner, L.M., 1986. Central programming of postural movements: adaptation to altered support-surface configurations. *J. Neurophysiol.* 55, 1369–1381.
- Hu, K., Ivanov, P.C., Chen, Z., Carpena, P., Stanley, H.E., 2001. Effect of Trends on Detrended Fluctuation Analysis. *Phys. Rev. E* 64. doi:10.1103/PhysRevE.64.011114
- Karimi, M., Sadeghisani, M., Omar, A., Kouchaki, E., Mirahmadi, M., Fatoye, F., 2015. STABILITY ANALYSIS IN PATIENTS WITH NEUROLOGICAL AND MUSCULOSKELETAL DISORDERS USING LINEAR AND NON-LINEAR APPROACHES. *J. Mech. Med. Biol.* 15. doi:10.1142/S0219519415300045
- Kennel, M.B., Brown, R., Abarbanel, H.D.I., 1992. Determining embedding dimension for phase-space reconstruction using a geometrical construction. *Phys. Rev. A* 45, 3403–3411.  
doi:10.1103/PhysRevA.45.3403
- Kooij, H. van der, Jacobs, R., Koopman, B., Grootenboer, H., 1999. A multisensory integration model of human stance control. *Biol. Cybern.* 80, 299–308. doi:10.1007/s004220050527
- Loram, I.D., Lakie, M., 2002. Human balancing of an inverted pendulum: position control by small, ballistic-like, throw and catch movements. *J. Physiol.* 540, 1111–1124.  
doi:10.1113/jphysiol.2001.013077
- Mancini, M., Salarian, A., Carlson-Kuhta, P., Zampieri, C., King, L., Chiari, L., Horak, F.B., 2012. ISway: a sensitive, valid and reliable measure of postural control. *J. NeuroEngineering Rehabil.* JNER 9, 59–66. doi:10.1186/1743-0003-9-59
- Masani, K., Vette, A.H., Kouzaki, M., Kanehisa, H., Fukunaga, T., Popovic, M.R., 2007. Larger center of pressure minus center of gravity in the elderly induces larger body acceleration during quiet standing. *Neurosci. Lett.* 422, 202–206. doi:10.1016/j.neulet.2007.06.019
- Maurer, C., Mergner, T., Peterka, R.J., 2004. Abnormal resonance behavior of the postural control loop in Parkinson's disease. *Exp. Brain Res.* 157, 369–376. doi:10.1007/s00221-004-1852-y
- McCollum, G., Leen, T.K., 1989. Form and exploration of mechanical stability limits in erect stance. *J. Mot. Behav.* 21, 225–244.
- Mitchell, S.L., Collins, J.J., De Luca, C.J., Burrows, A., Lipsitz, L.A., 1995. Open-loop and closed-loop postural control mechanisms in Parkinson's disease: increased mediolateral activity during quiet standing. *Neurosci. Lett.* 197, 133–136.
- Ni, M., Signorile, J.F., Mooney, K., Balachandran, A., Potiaumpai, M., Luca, C., Moore, J.G., Kuenze, C.M., Eltoukhy, M., Perry, A.C., 2016. Comparative Effect of Power Training and High-Speed Yoga on

- Motor Function in Older Patients With Parkinson Disease. *Arch. Phys. Med. Rehabil.* 97, 345–354.e15. doi:10.1016/j.apmr.2015.10.095
- Pahwa, R., Lyons, K.E., William C. Koller, 2003. *Handbook of Parkinson's disease*, 3rd ed.. ed, Neurological disease and therapy ; v. 59. Dekker, New York.
- Park, J.-H., Youm, S., Jeon, Y., Park, S.-H., 2015. Development of a balance analysis system for early diagnosis of Parkinson's disease. *Int. J. Ind. Ergon.* 48, 139–148. doi:10.1016/j.ergon.2015.05.005
- Park, S., Horak, F.B., Kuo, A.D., 2004. Postural feedback responses scale with biomechanical constraints in human standing. *Exp. Brain Res.* 154, 417–427. doi:10.1007/s00221-003-1674-3
- Pascolo, P., Barazza, F., Carniel, R., 2006. Considerations on the application of the chaos paradigm to describe the postural sway. *Chaos Solitons Fractals* 27, 1339–1346. doi:10.1016/j.chaos.2005.04.111
- Pascolo, P.B., Marini, A., Carniel, R., Barazza, F., 2005. Posture as a chaotic system and an application to the Parkinson's disease. *Chaos Solitons Fractals* 24, 1343–1346. doi:10.1016/j.chaos.2004.09.062
- Pelykh, O., Klein, A.-M., Bötzel, K., Kosutzka, Z., Ilmberger, J., 2015. Dynamics of postural control in Parkinson patients with and without symptoms of freezing of gait. *Gait Posture* 42, 246–250. doi:10.1016/j.gaitpost.2014.09.021
- Peng, C.-K., Buldyrev, S.V., Havlin, S., Simons, M., Stanley, H.E., Goldberger, A.L., 1994. Mosaic organization of DNA nucleotides. *Phys. Rev. E* 49, 1685–1689. doi:10.1103/PhysRevE.49.1685
- Peterka, R.J., 2002. Sensorimotor Integration in Human Postural Control. *J. Neurophysiol.* 88, 1097–1118.
- Pincus, S.M., 1991. Approximate entropy as a measure of system complexity. *Proc. Natl. Acad. Sci. U. S. A.* 88, 2297–2301.
- Ramdani, S., Seigle, B., Lagarde, J., Bouchara, F., Bernard, P.L., 2009. On the use of sample entropy to analyze human postural sway data. *Med. Eng. Phys.* 31, 1023–1031. doi:10.1016/j.medengphy.2009.06.004
- Richman, J.S., Moorman, J.R., 2000. Physiological time-series analysis using approximate entropy and sample entropy. *Am. J. Physiol. - Heart Circ. Physiol.* 278, H2039–H2049.
- Rocchi, L., Chiari, L., Cappello, A., Horak, F.B., 2006. Identification of distinct characteristics of postural sway in Parkinson's disease: A feature selection procedure based on principal component analysis. *Neurosci. Lett.* 394, 140–145. doi:10.1016/j.neulet.2005.10.020
- Rusaw, D.F., Ramstrand, S., 2016. Validation of the Inverted Pendulum Model in standing for transtibial prosthesis users. *Clin. Biomech.* 31, 100–106. doi:10.1016/j.clinbiomech.2015.09.014
- Sasagawa, S., Ushiyama, J., Kouzaki, M., Kanehisa, H., 2009. Effect of the hip motion on the body kinematics in the sagittal plane during human quiet standing. *Neurosci. Lett.* 450, 27–31. doi:10.1016/j.neulet.2008.11.027
- Schlenstedt, C., Muthuraman, M., Witt, K., Weisser, B., Fasano, A., Deuschl, G., 2016. Postural control and freezing of gait in Parkinson's disease. *Parkinsonism Relat. Disord.* 24, 107–112. doi:10.1016/j.parkreldis.2015.12.011
- Smania, N., Corato, E., Tinazzi, M., Stanzani, C., Fiaschi, A., Girardi, P., Gandolfi, M., 2010. Effect of Balance Training on Postural Instability in Patients With Idiopathic Parkinson's Disease. *Neurorehabil. Neural Repair* 24, 826–834. doi:10.1177/1545968310376057
- Steven H Strogatz, author, 2015. *Nonlinear dynamics and chaos: with applications to physics, biology, chemistry, and engineering*, Second edition.. ed. Westview Press, a member of the Perseus Books Group, Boulder, CO.

- Stylianou, A.P., McVey, M.A., Lyons, K.E., Pahwa, R., Luchies, C.W., 2011. Postural Sway in Patients with Mild to Moderate Parkinson's Disease. *Int. J. Neurosci.* 121, 614–621. doi:10.3109/00207454.2011.602807
- Suzuki, Y., Nomura, T., Casadio, M., Morasso, P., 2012. Intermittent control with ankle, hip, and mixed strategies during quiet standing: A theoretical proposal based on a double inverted pendulum model. *J. Theor. Biol.* 310, 55–79. doi:10.1016/j.jtbi.2012.06.019
- Teresa Blázquez, M., Anguiano, M., de Saavedra, F.A., Lallena, A.M., Carpena, P., 2009. Study of the human postural control system during quiet standing using detrended fluctuation analysis. *Phys. Stat. Mech. Its Appl.* 388, 1857–1866. doi:10.1016/j.physa.2009.01.001
- Tokuno, C.D., Carpenter, M.G., Thorstensson, A., Cresswell, A.G., 2006. The influence of natural body sway on neuromuscular responses to an unpredictable surface translation. *Exp. Brain Res.* 174, 19–28. doi:10.1007/s00221-006-0414-x
- Vette, A.H., Masani, K., Nakazawa, K., Popovic, M.R., 2010. Neural-Mechanical Feedback Control Scheme Generates Physiological Ankle Torque Fluctuation During Quiet Stance. *IEEE Trans. Neural Syst. Rehabil. Eng.* 18, 86–95. doi:10.1109/TNSRE.2009.2037891
- Winter, D.A., 1990. *Biomechanics and motor control of human movement*, 2nd ed.. ed. Wiley, New York.
- Winter, D.A., Prince, F., Patla, A., 1997. Validity of the inverted pendulum model of balance in quiet standing. *Gait Posture* 5, 153–154. doi:10.1016/S0966-6362(97)83376-0
- Wolf, A., Swift, J.B., Swinney, H.L., Vastano, J.A., 1985. Determining Lyapunov exponents from a time series. *Phys. Nonlinear Phenom.* 16, 285–317. doi:10.1016/0167-2789(85)90011-9
- World Health Organization, 2008. *The world health report 2008 primary health care: now more than ever*. World Health Organization, Geneva.
- Yamamoto, A., Sasagawa, S., Oba, N., Nakazawa, K., 2015. Behavioral effect of knee joint motion on body's center of mass during human quiet standing. *Gait Posture* 41, 291–294. doi:10.1016/j.gaitpost.2014.08.016
- Yentes, J.M., Hunt, N., Schmid, K.K., Kaipust, J.P., McGrath, D., Stergiou, N., 2013. The appropriate use of approximate entropy and sample entropy with short data sets. *Ann. Biomed. Eng.* 41, 349–365. doi:10.1007/s10439-012-0668-3
- Yu, E., Abe, M., Masani, K., Kawashima, N., Eto, F., Haga, N., Nakazawa, K., 2008. Evaluation of postural control in quiet standing using center of mass acceleration: comparison among the young, the elderly, and people with stroke. *Arch. Phys. Med. Rehabil.* 89, 1133–1139. doi:10.1016/j.apmr.2007.10.047

## Chapter Four: Summary

### 1 Summary of Study

The goal of this study was to validate the SIP model for bi-pedal quiet standing on healthy old adults and people with PD by comparing the linear and nonlinear measures extracted from the COP that the SIP creates ( $COP_{SIP}$ ), and the ones extracted from the experimental COP ( $COP_{exp}$ ). In addition, this study intended to determine if the accuracy of the  $COP_{SIP}$  to replicate the  $COP_{exp}$  was sensitive to the current practice of assuming zero as initial conditions (ICs) when using the differential equation (DEQ) of the SIP. As well as if the accuracy of the  $COP_{SIP}$  was sensitive to the linearization of the DEQ of the SIP.

The results of this study showed that assuming zero as ICs increments significantly the error of the  $COP_{SIP}$  time series in magnitude, and shape of curve (10% to 35%) when compared to the  $COP_{exp}$  time series. In addition, when the ICs are assumed to be zero, the  $COP_{SIP}$  replicates less linear and nonlinear measures extracted from the  $COP_{exp}$  when errors from  $\pm 5\%$  to  $\pm 20\%$  are accepted, than when the ICs are optimized. Regarding the optimization of ICs, the study showed that the best practice to find them is by calculating the  $COP_{SIP}$  using the linear version of the SIP DEQ, and finding the ICs that maximize the cross correlation between the  $COP_{SIP}$  and  $COP_{exp}$ . This study also showed that linearizing the SIP DEQ is a safe practice since the change in accuracy of the  $COP_{SIP}$  was at the most 3% when the nonlinear DEQ was used instead of the linear version.

Regarding the ability of the  $COP_{SIP}$  to represent the  $COP_{exp}$  based on linear and nonlinear measures, it was determined that the  $COP_{SIP}$  can describe 70% of the  $COP_{exp}$  for healthy subjects if “representing the  $COP_{exp}$ ” consists of replicating the nonlinear measures of a detrended fluctuation analysis (eyes open and closed), and the linear measures of the second derivative of the COP time series with respect to time (eyes closed). In addition, the  $COP_{SIP}$  can represent 70% of the  $COP_{exp}$  for subjects with mild PD, when the  $COP_{exp}$  is described by the linear measures of the COP (eyes open and closed), and nonlinear measures of a detrended fluctuations analysis (eyes open and closed), and sample entropy (eyes closed). Finally, the  $COP_{SIP}$  can represent 70% of the  $COP_{exp}$  for subject with moderate PD, when the  $COP_{exp}$  is described by the linear measures of the COP (eyes open and closed), and the nonlinear measures of a detrended fluctuation analysis (eyes open and closed). Also, it was shown that as PD progresses, the SIP becomes a less accurate model to represent bi-pedal quiet standing.

## 2 Conclusions and Recommendations

The main conclusion of this study was that the current practice of assuming zero for the initial conditions in the SIP model significantly decreases the accuracy of the model results. This reduces the similarity between the  $COP_{SIP}$  to the  $COP_{exp}$  time series, and the ability of the  $COP_{SIP}$  to replicate linear and nonlinear measures used to characterize the  $COP_{exp}$ . Therefore, an alternative approach is recommended to determine more accurate initial conditions by finding the set that maximizes the cross correlation between the  $COP_{SIP}$  and  $COP_{exp}$ . It is also recommended to use linearized differential equations within the SIP model when calculating the  $COP_{SIP}$  time series, since using the nonlinear differential equation results in a very small increase in accuracy.

It is also concluded that the SIP can be a valid model for unperturbed sway studies on healthy old adults and people with mild and moderate PD, when validation is defined as a maximum error of 30% or less. In other words, if a study on healthy old adults and people with PD is defining their  $COP_{exp}$  using detrended fluctuation analysis, it is possible to design a SIP mechanical system that replicates those nonlinear measures, and draw conclusions from this mechanical system knowing that they are at least 70% correct. Therefore, it is recommended that SIP mechanical systems are designed with the goal of replicating the linear and nonlinear measures that assure 70% of the  $COP_{exp}$  (Table 9), and linear and nonlinear measures that have already been analyzed in posturographic studies. This would allow a connection between posturographic and mechanical modeling studies that is at least 70% correct.

Finally, it was concluded that as PD progresses, the SIP model becomes less valid. Therefore, it is recommended to explore the use of a double inverted pendulum when people with moderate PD ( $H\&Y \geq 3$ ) are included in the study.

## 3 Limitations and Future Work

This study had a few limitations. For example, the PD subjects were only tested in their ON medication state. Therefore we could not determine if the SIP could model their sway during the OFF medication state, so no insight is available regarding the use of the SIP model for diagnosis of balance deficits in the off medication state. Another limitation was that the stance width was not controlled. Therefore, we could not analyze the COP in the medial-lateral direction, since not controlling the width would introduce additional variability that would skew the results. The participants with PD, compared to the healthy controls, naturally chose a wider stance width, providing an increase lateral base of support an improved stability.

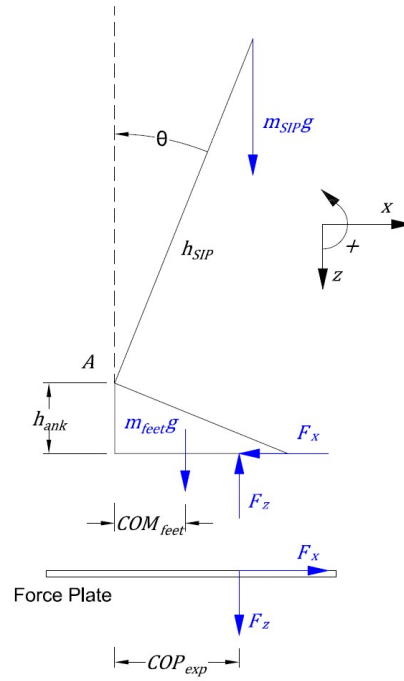
Future studies should consider improving the validation technique proposed in this study. Additional nonlinear measures such as Recurrence Quantification Analysis (RQA), or Adaptive Fractal Analysis (AFA) could be added to the list of nonlinear measures. In addition, future studies should control the stance width of the participants and analyze if the SIP could be a valid model within a defined error for the medial-lateral direction. Finally, using the same validation technique of this study, the double inverted pendulum should be analyzed and observe if the results improve. In fact, this study should be focused more on people with moderate PD since that is where the SIP cannot be considerate a very valid model.

## Appendices

### 1 Appendix A: Equations

#### 1.1 SIP Free Body Diagram: Kinetic Study of SIP

Based on Figure 2, these are the steps to obtain the differential equation that determines the angular position, velocity and acceleration (AP direction) of the SIP when the  $COP_{exp}$  (AP direction) and force plate measures ( $F_x$ ,  $F_z$ ) are known. It is assumed that the feet are a single rigid body that is stationary in all degrees of freedom.



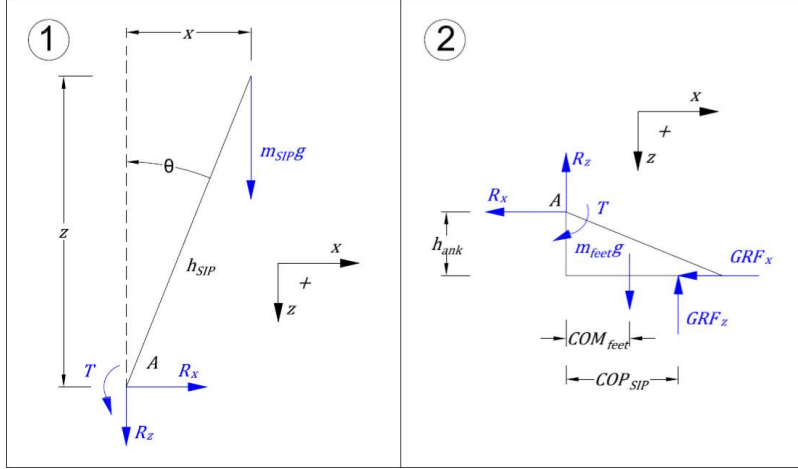
$$\sum M_A = J_{SIP} \ddot{\theta}$$

$$-m_{SIP} g h_{SIP} \sin \theta - m_{feet} g COM_{feet} - F_x h_{ank} + F_z COP_{exp} = J_{SIP} \ddot{\theta}$$

$$\ddot{\theta} = \frac{1}{J_{SIP}} (F_z COP_{exp} - m_{SIP} g h_{SIP} \sin \theta - m_{feet} g COM_{feet} - F_x h_{ank})$$

#### 1.2 SIP Free Body Diagram: Kinetic Study of Stationary Foot

Based on Figure 3, these are the steps to obtain the ground reaction forces ( $GRF_x$ ,  $GRF_z$ ) and COP in the AP direction ( $COP_{SIP}$ ) that a force plate would measure if the human body is a SIP. Same assumptions, and angular position, velocity and acceleration previously determined from Appendix A: Equations – Section 1.1.



From window 1:

$$\begin{aligned} \sum F_x &= m_{SIP}\ddot{x} & \sum F_y &= m_{SIP}\ddot{z} & \sum M_A &= J_{SIP}\ddot{\theta} \\ R_x &= m_{SIP}\ddot{x} & m_{SIP}g + R_z &= m_{SIP}\ddot{z} & -m_{SIP}gh_{SIP}\sin\theta + T &= J_{SIP}\ddot{\theta} \\ R_z &= m_{SIP}(\ddot{z} - g) & T &= J_{SIP}\ddot{\theta} + m_{SIP}gh_{SIP}\sin\theta \end{aligned}$$

From window 2:

$$\begin{aligned} \sum F_x &= 0 & \sum F_y &= 0 & \sum M_A &= 0 \\ -R_x - GRF_x &= 0 & -R_z + m_{feet}g - GRF_z &= 0 & -T - m_{feet}gCOM_{feet} - GRF_x h_{ank} + GRF_z COP_{SIP} &= 0 \\ GRF_x &= -R_x & GRF_z &= -R_z + m_{feet}g & COP_{SIP} &= \frac{1}{GRF_z}(T + m_{feet}gCOM_{feet} + GRF_x h_{ank}) \end{aligned}$$

Knowing that  $\ddot{x}$  and  $\ddot{z}$  in terms of  $h_{SIP}$  and  $\theta$  are:

$$\begin{aligned} x &= h_{SIP}\sin\theta & z &= -h_{SIP}\cos\theta \\ \dot{x} &= h_{SIP}\dot{\theta}\cos\theta & \dot{z} &= h_{SIP}\dot{\theta}\sin\theta \\ \ddot{x} &= h_{SIP}\ddot{\theta}\cos\theta - h_{SIP}\dot{\theta}^2\sin\theta & \ddot{z} &= h_{SIP}\ddot{\theta}\sin\theta + h_{SIP}\dot{\theta}^2\cos\theta \end{aligned}$$

## 2 Appendix C: Selecting the Final Optimized ICs

As mentioned in Section 3.3.4, there were 8 ways to select the ICs to calculate the  $COP_{SIP}$  that used optimized ICs. These ways were based on the similarity measure that was optimized (GOF, SSE, MI or CrossCorr), and the DEQ (N-DEQ (5) or L-DEQ (6)).

To select the DEQ, results from Section 4.2 were analyzed. It was found that the differences of GOF, MI and CrossCorr between  $COP_{exp}$  and  $COP_{SIP}$  when the N-DEQ and L-DEQ were used with optimized ICs, were in average less than 2% in the worst-case scenario. In addition, it was found that the difference in SSE was negative for all comparisons, meaning that the N-DEQ had in average more error than the L-DEQ. Due to these observations, it was decided to use the L-DEQ (6) to calculate the  $COP_{SIP}$ , instead of using the N-DEQ (5).

To select which similarity measure was going to be optimized and used to select the optimized ICs, the following analysis was performed. Using the L-DEQ (6) to calculate the  $COP_{SIP}$ , a set of optimized ICs was determined for each similarity measure using their respective optimization method (maximization for GOF, MI and CrossCorr; and minimization for SSE). Next the absolute differences of all optimized ICs were calculated for each subject and trials. These absolute differences were then separated by subject groups (HS, PD-Mi and PD-Mo) and condition (EO and EC), and averaged between all trials. In other words, the difference  $|IC_{Similarity\ Measure\ x} - IC_{Similarity\ Measure\ y}|$  was performed for all permutations of  $HS_{PD-Mi-Study}/PD-Mi/HS_{PD-Mo-Study}/PD-Mo \cap EO/EC$ , and the average of all trials per condition in each group of subjects was calculated. Finally, to determine if the absolute differences between ICs calculated from various optimization methods were significant different, a left-tail one-sample t-test with  $\alpha = 0.05$  and  $H_0 \geq 0.02$  was performed. Significance meant that the difference between ICs ( $\theta_0 = 0, \dot{\theta}_0 = 0$ ) was less than 0.02 in magnitude with a 95% confidence. Results from this analysis are in Figure 22 and Figure 23, in which the p-value of each comparison is displayed, red font meaning  $p \leq 0.05$ .

Results showed that the optimized ICs calculated using GOF differ the most (EO and EC) for both studies when compared with the other optimized ICs calculated using MI, SSE, and CrossCorr. The most number of significant differences between optimized ICs was found when SSE, MI and CrossCorr were compared. In fact, the absolute difference between optimized ICs was always smaller in comparisons that were between SSE, MI and CrossCorr, than in any other comparison that involved GOF. This meant that the agreement of optimized ICs was stronger between SSE, MI and CrossCorr, than between GOF and any other similarity measure. Due to these observations, and the nature of CrossCorr (bounded from 0 to 1), it was decided to use CrossCorr as the similarity measure to find ICs in this study.

In conclusion, the method to select the final optimized ICs (used in Section 3.3.4) consisted on calculating  $COP_{SIP}$  using the L-DEQ (6) with all the possible combinations of ICs in  $-0.5\ rad \leq \theta_0 \leq$

$0.5 \text{ rad} \cap -1 \frac{\text{rad}}{\text{s}} \leq \dot{\theta}_0 \leq 1 \frac{\text{rad}}{\text{s}}$  using  $\Delta\theta_0 = 0.01 \text{ rad} \cap \Delta\dot{\theta}_0 = 0.02 \frac{\text{rad}}{\text{s}}$ , and then selecting the ICs that maximized the CrossCorr between  $\text{COP}_{\text{exp}}$  and  $\text{COP}_{\text{SIP}}$ .

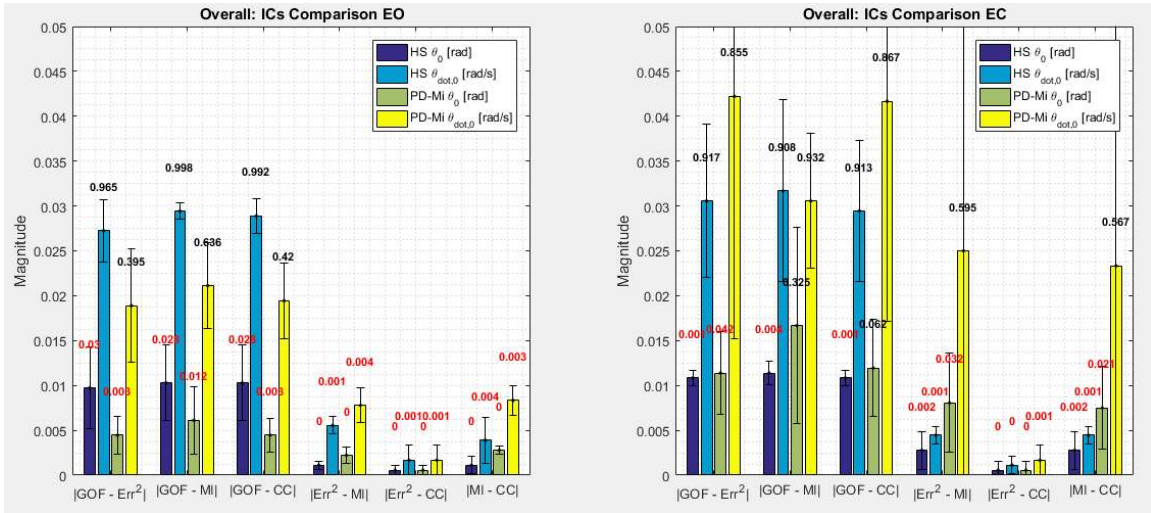


Figure 22 - PD-Mi-Study: Overall Comparison of ICs between Similarity Measures for EO and EC

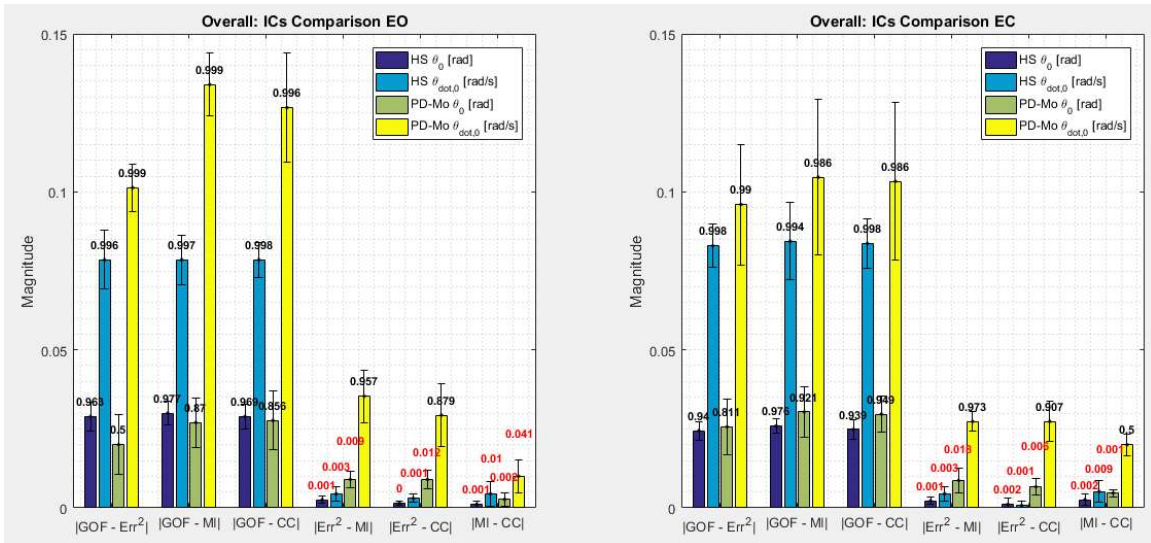


Figure 23 - PD-Mo-Study: Overall Comparison of ICs between Similarity Measures for EO and EC

### 3 Appendix B: Figures and Tables

#### 3.1 SIP Linear Measure Accuracy between Subjects

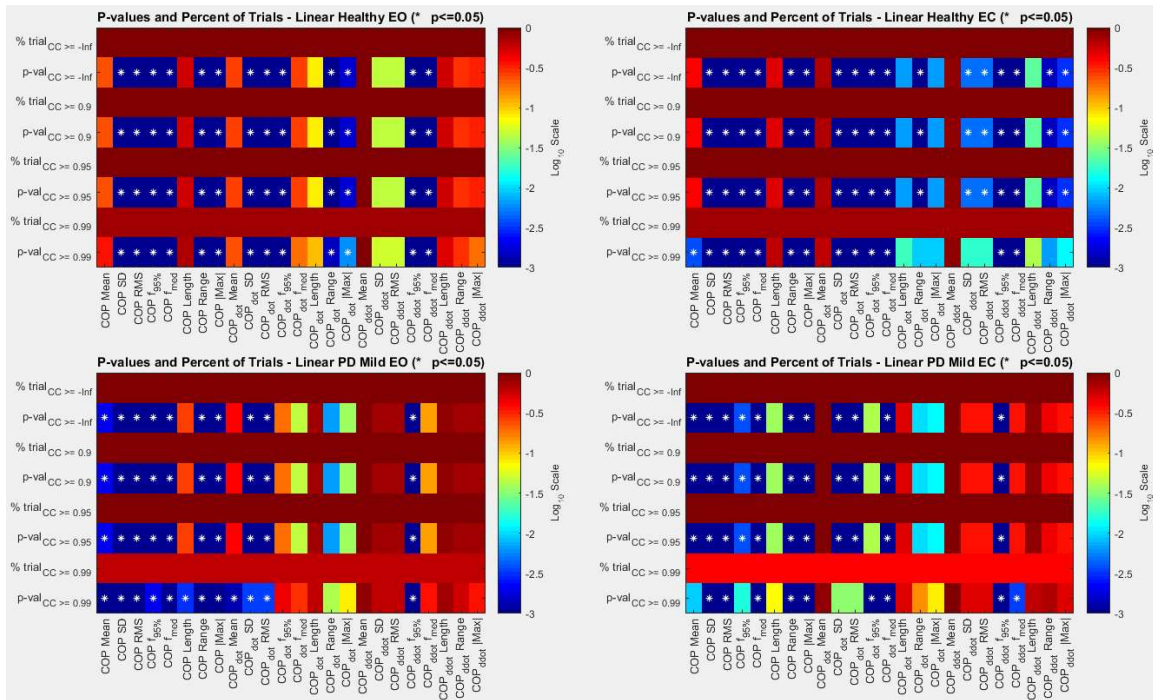


Figure 24 - PD-Mi-Study: Linear Accuracy ( $\pm 15\%$ ) for SIP ( $R_2$ ) with Optimized ICs

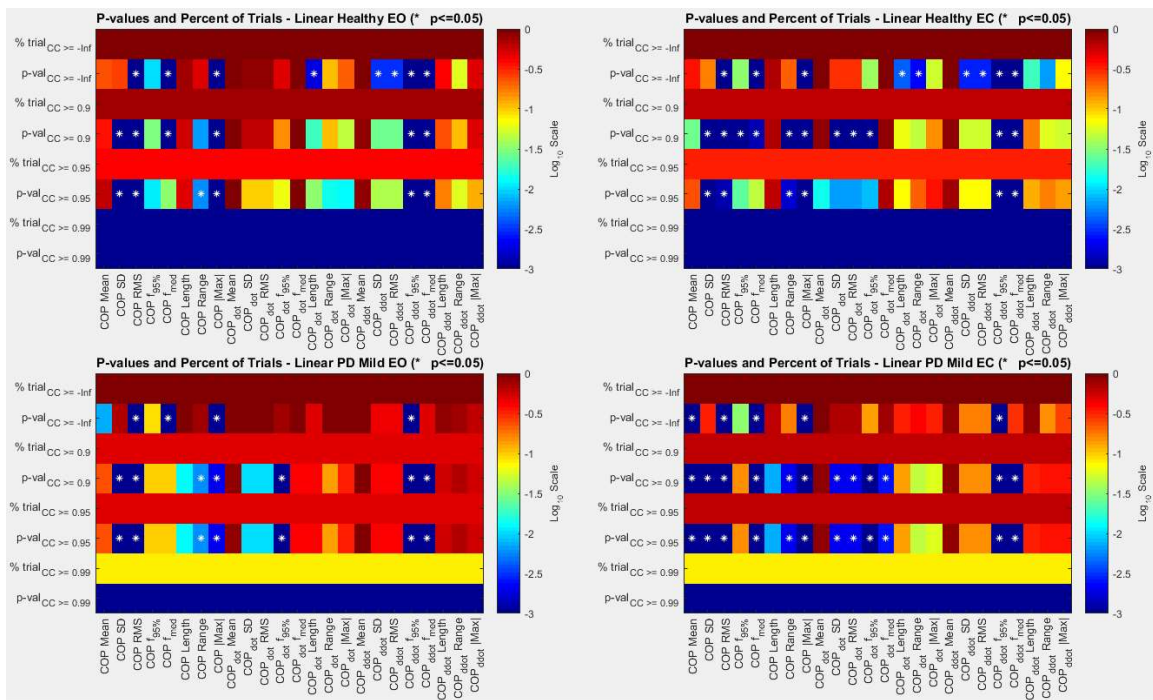


Figure 25 - PD-Mi-Study: Linear Accuracy ( $\pm 15\%$ ) for SIP ( $R_2$ ) with Zero ICs

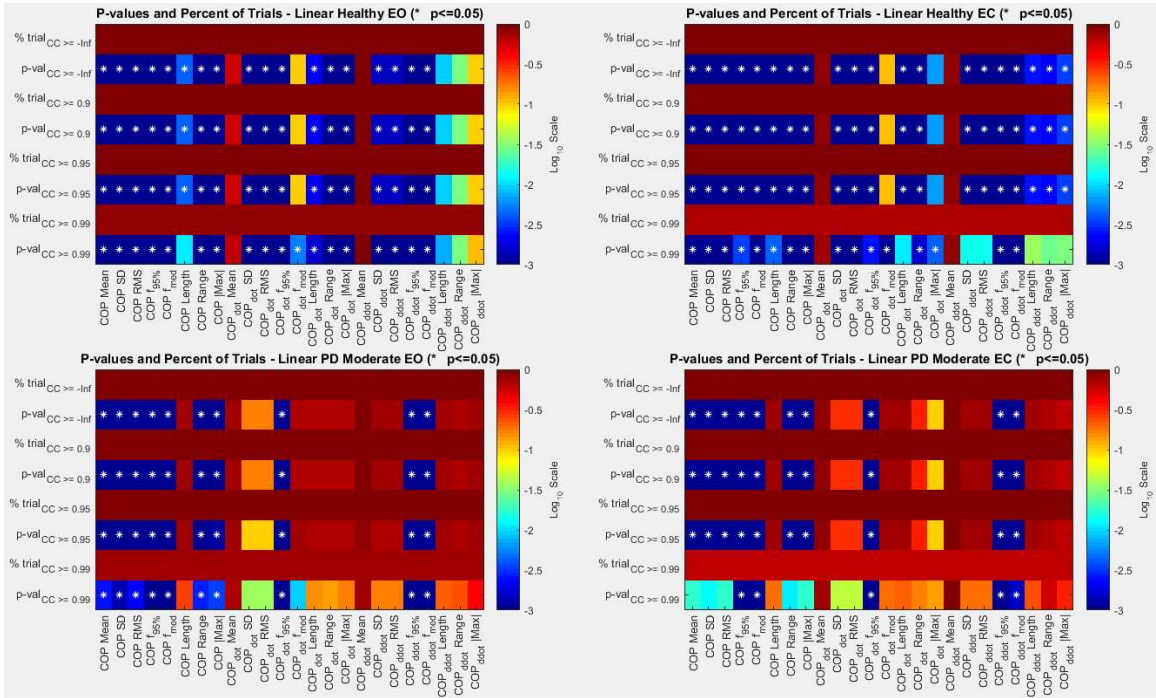


Figure 26 - PD-Mo-Study: Linear Accuracy ( $\pm 15\%$ ) for SIP ( $R_2$ ) with Optimized ICs

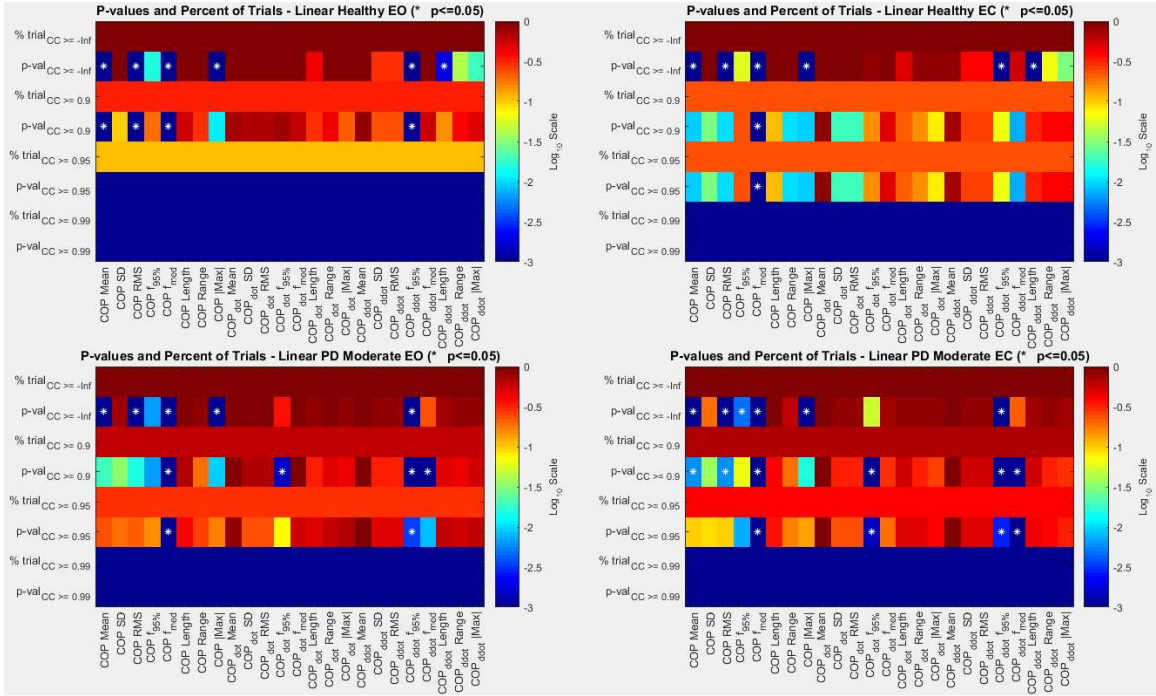


Figure 27 - PD-Mo-Study: Linear Accuracy ( $\pm 15\%$ ) for SIP ( $R_2$ ) with Zero ICs

### 3.2 SIP Nonlinear Measure Accuracy between Subjects

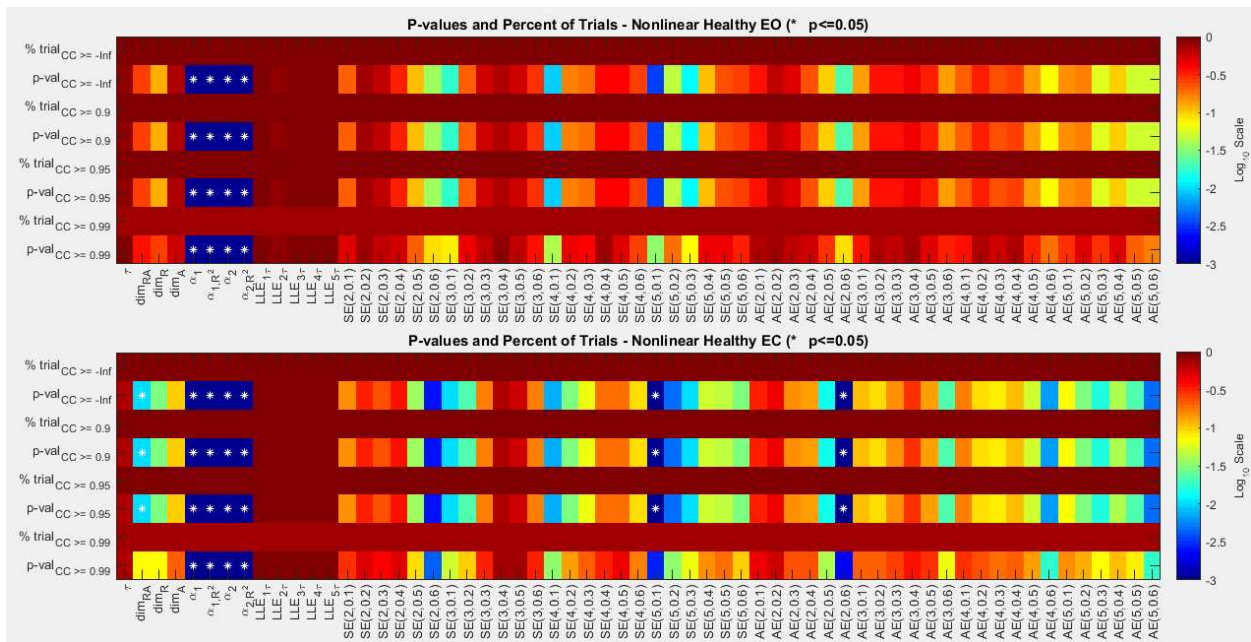


Figure 28 - PD-Mi-Study (HS): Nonlinear Accuracy ( $\pm 15\%$ ) for SIP ( $R_2$ ) with Optimized ICs

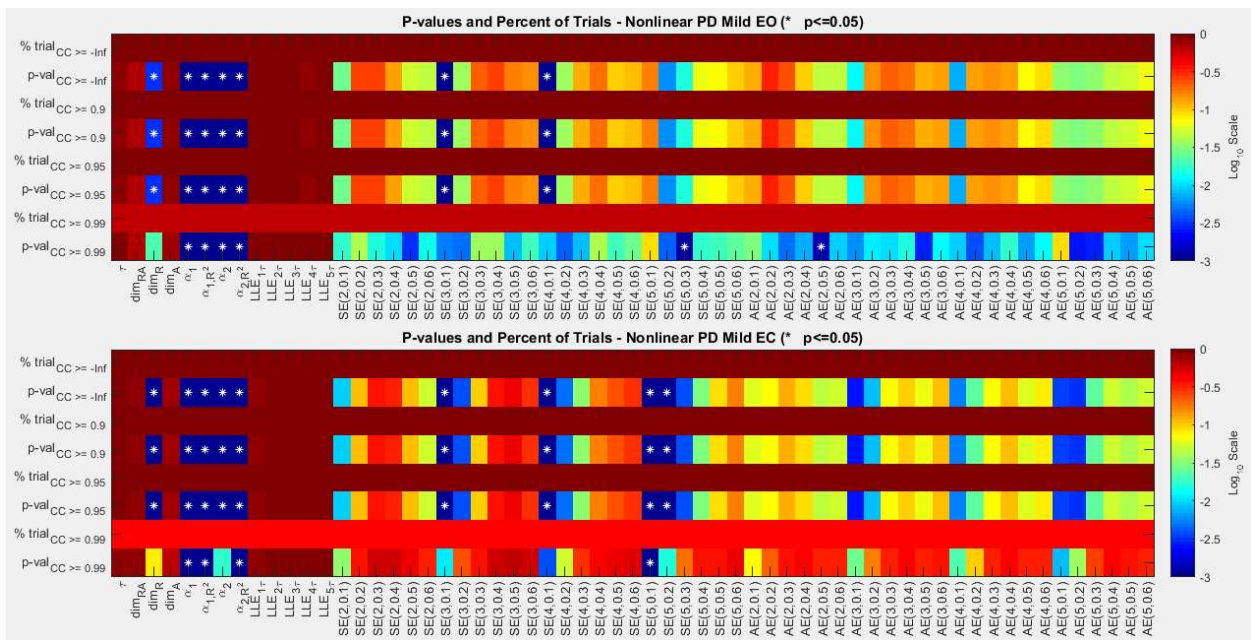


Figure 29 - PD-Mi-Study (PD-Mi): Nonlinear Accuracy ( $\pm 15\%$ ) for SIP ( $R_2$ ) with Optimized ICs

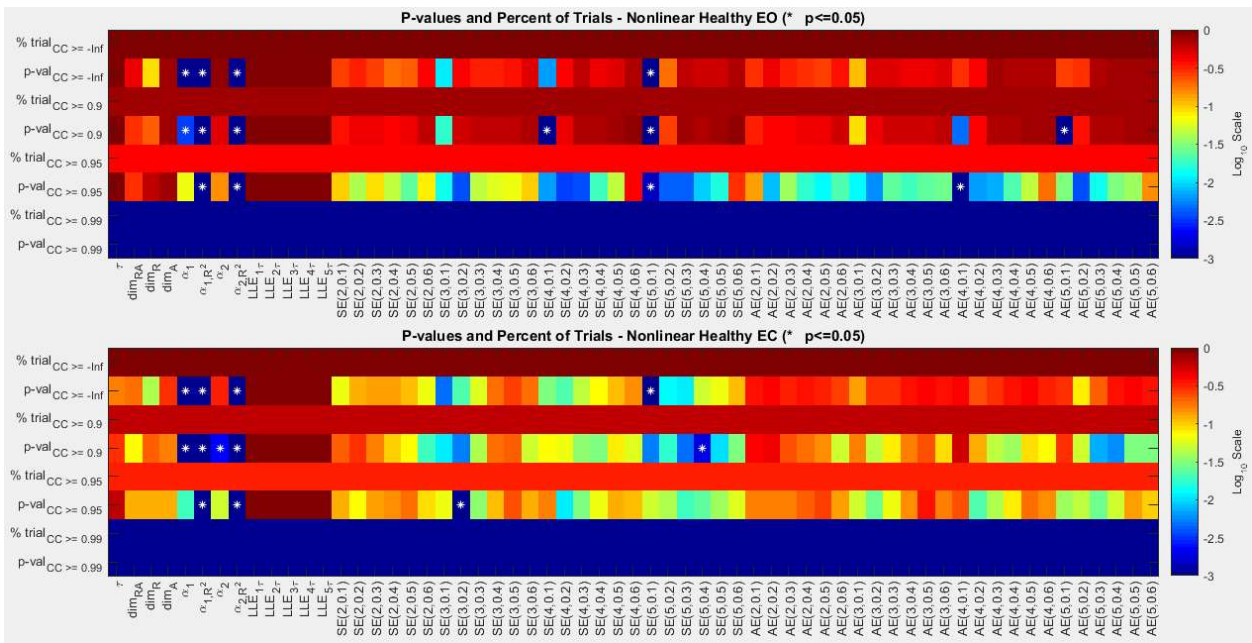


Figure 30 - PD-Mi-Study (HS): Nonlinear Accuracy ( $\pm 15\%$ ) for SIP ( $R_2$ ) with Zero ICs

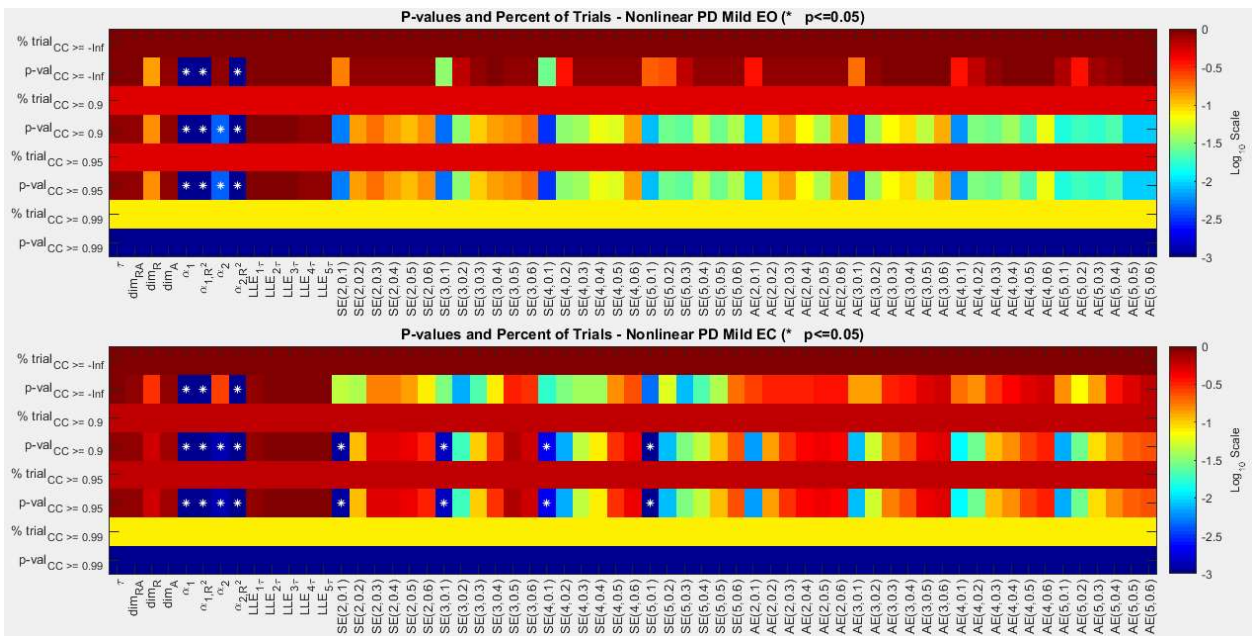


Figure 31 - PD-Mi-Study (PD-Mi): Nonlinear Accuracy ( $\pm 15\%$ ) for SIP ( $R_2$ ) with Zero ICs

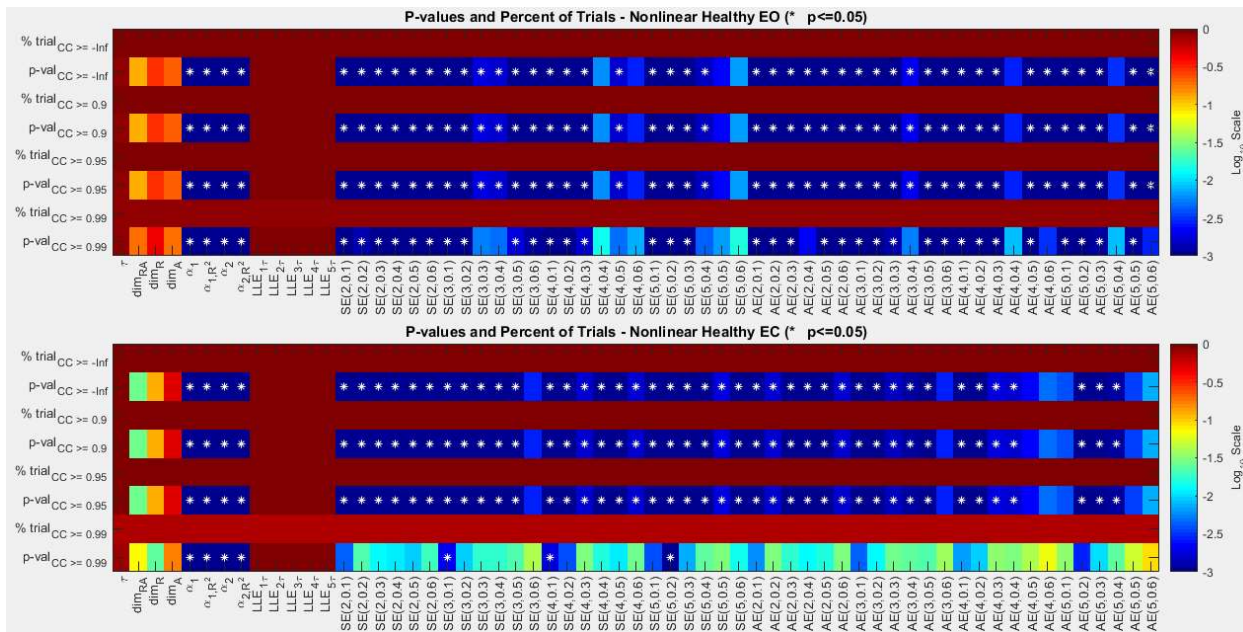


Figure 32 - PD-Mo-Study (HS): Nonlinear Accuracy ( $\pm 15\%$ ) for SIP ( $R_2$ ) with Optimized ICs

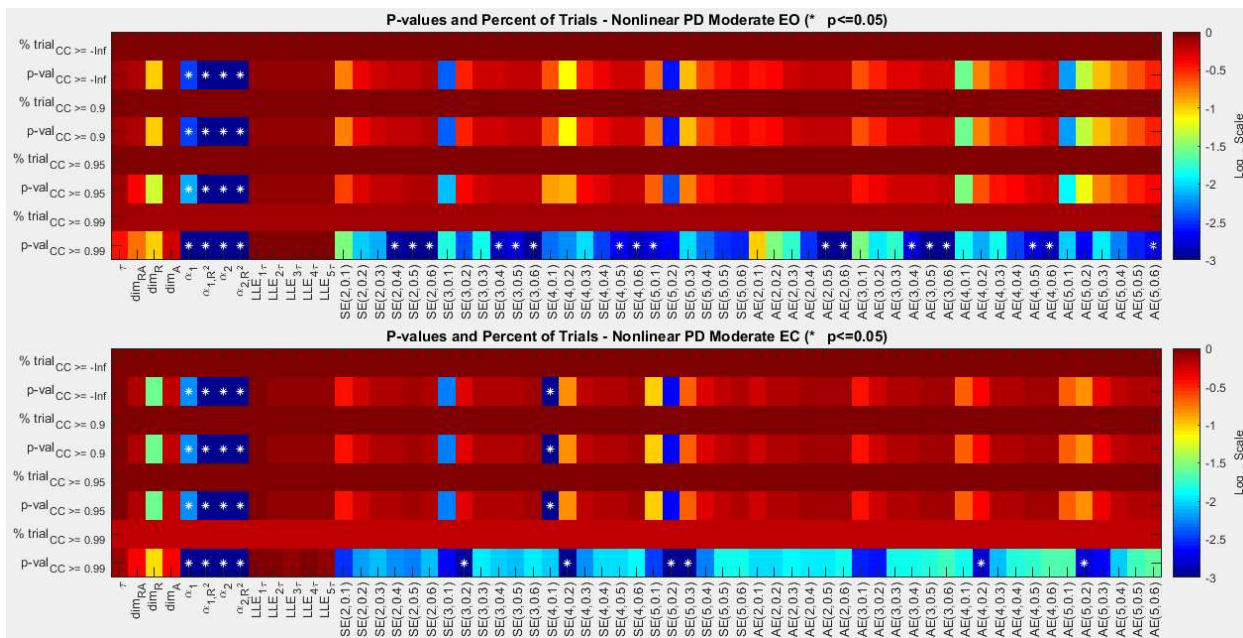


Figure 33 - PD-Mo-Study (PD-Mo): Nonlinear Accuracy ( $\pm 15\%$ ) for SIP ( $R_2$ ) with Optimized ICs

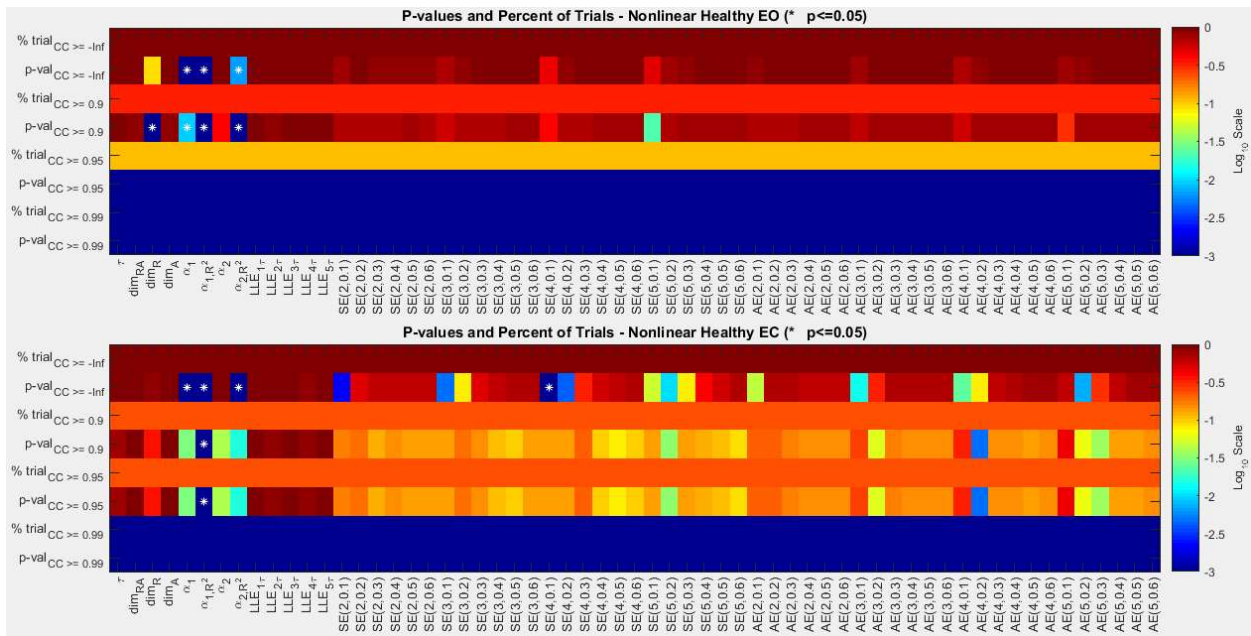


Figure 34 - PD-Mo-Study (HS): Nonlinear Accuracy ( $\pm 15\%$ ) for SIP ( $R_2$ ) with Zero ICs

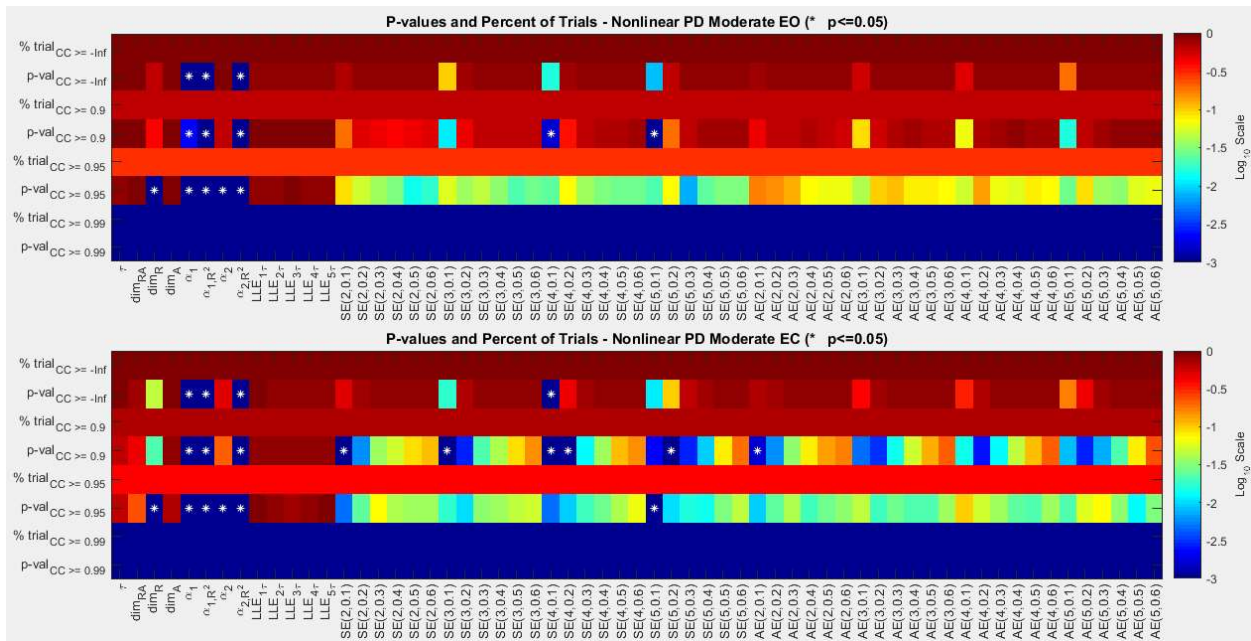


Figure 35 - PD-Mo-Study (PD-Mo): Nonlinear Accuracy ( $\pm 15\%$ ) for SIP ( $R_2$ ) with Zero ICs